FUNDAMENTAL INVESTIGATIONS OF SURFACE AND SUBSURFACE DAMAGE, AND WEAR IN DIAMOND WIRE SAWING OF SILICON

A Dissertation
Presented to
The Academic Faculty

by

Arkadeep Kumar

In Partial Fulfillment
of the Requirements for the Degree
Doctor of Philosophy

Georgia Institute of Technology
August 2018

COPYRIGHT © 2018 BY ARKADEEP KUMAR

FUNDAMENTAL INVESTIGATIONS OF SURFACE AND SUBSURFACE DAMAGE, AND WEAR IN DIAMOND WIRE SAWING OF SILICON

Approved by:

Dr. Shreyes N. Melkote, Advisor
School of Mechanical Engineering
Georgia Institute of Technology

Dr. Steven Danyluk
School of Mechanical Engineering
Georgia Institute of Technology

Dr. Richard W. Neu
School of Mechanical Engineering
Georgia Institute of Technology

Dr. Christopher Saldana
School of Mechanical Engineering
Georgia Institute of Technology

Dr. Chris Arcona
Saint-Gobain Northboro Research and
Development Center

Date Approved: May 02, 2018

This thesis is dedicated to my Ma and Baba (mother and father) Sipra and Asish Kumar,

for their love and care, encouragement and support, and everything they do.

ACKNOWLEDGEMENTS

This Ph.D. thesis/dissertation is a result of a lot of perseverance, love, and care. It is possible with many people and events, even beyond the years of Ph.D., starting with my mother Sipra Kumar and my father Asish Kumar, with their unconditional love and support, who encouraged me to pursue my Ph.D., and I am grateful to them.

I owe a lot of gratitude to my advisor Dr. Shreyes N. Melkote. For accepting me as his student, inspiring me with the pursuit of high-quality research, teaching me how to present my talks, write better, and continuing to advise on life beyond research. I admire and respect his ability to give his time and mental bandwidth for each of his grad students. It took me years to understand the father-figure in him, his efforts to make me better and ultimately the reflection of how much he cares. When he pushed me to achieve high-quality results, I thought I might fall, instead he inspired me to fly higher. I will be ever grateful for all the time he spent on me and feel blessed to have been mentored by him.

I am thankful to Dr. Steven Danyluk who generously shared his years of experience and expert advice on my research, producing valuable insights. He welcomed me into the Photovoltaic (PV) Manufacturing group. Moreover, he shared his wisdom about how to lead a life, beyond academia. My good fortune with professors continues with the rest of my committee, Dr. Rick Neu – whose courses introduced me to advanced mechanics, and Dr. Chris Saldana who shared his advice on following a career as a faculty. I must also thank other professors, who were generous with their time and advice, and open doors- Shuman Xia, Antonia Antoniou, Jonathan Colton, Suresh Sitaraman, Nazanin Bassiri, Roshan Vengazhiyil, Todd Sulchek, Ajeet Rohatgi, and many other professors.

I am thankful to Dr. Chris Arcona and Steffi Kaminski from Saint-Gobain Northboro Research and Development Center, for the support of my research over the years through their advice from challenges faced in the industry. The critical questions they raised with their experience in industry sparked ideas, which made my Ph.D. thesis better. Saint-Gobain provided even more, with materials and funding for the initial years of this research. Funding support for this research came from Silicon Solar Consortium, (SiSoC), Saint-Gobain Northboro Research, and National Science Foundation (CMMI Grant #1538293).

Parts of the work reported in this thesis were performed at the Georgia Tech Institute for Electronics and Nanotechnology (IEN), and the Material Characterization Facility (MCF) at IEN, which was a blessing, and a lifetime experience to be introduced to the world of nanotechnology. I am fortunate to have the opportunity to be trained, mentored and shared my days with the trainers at IEN and MCF- Eric Woods, Todd Walters, Rebhadebi Monikandan (Rathi), David Tavakoli, Walter Henderson, Yolande Berta and others who I might be forgetting names, but not forgetting their kindness in helping me. I am thankful to Steven Sheffield and the ME machine shop, who assisted me in building my experimental setups. Louis Boulanger, Nathan Mauldin and others who kept the spirits high at the machine shop through countless hours of iterations. The equipment support from the Precision Machining Research Consortium (PMRC) is greatly appreciated.

I am indebted to Dr. Chris Yang who mentored me in my initial days, teaching me to do experiments, and supporting me in the later years, after he moved away from our group to IEN. The other members in our PV group, Rajaguruprasath Raveendran or Guru – treated me like his younger brother, picking me up whenever I fell down, in research or

in life. Guru and his wife Swathi made me feel at home with their dinners. My officemate Kevin Skenes who welcomed me from the airport, taught me guitar, taught me how to be a gentleman, apart from the great community feeling in GTMI 413 office and PV lab. Vanessa Pogue, who is a dear friend now, sharing many conversations beyond just residual stresses in silicon as part of research. I am blessed to have found them.

I am grateful to my labmates in Dr. Melkote's research group who selflessly helped, in research and in life – Pushparghya Deb Kuila, Vinh Nguyen, Patxi Fernandez-Zelaia. I am thankful for the community of current students- Amey Vidvans, Kedar Joshi, Changxuan Zhao, and Toni Cvitanic; and years of support from our group's now alumni Dr. Andrea Marcon, Dr. Lejun Cen, David Hahn, Dr. Rui Liu, Craig Woodin, Dr. George Mathai, Dr. Lei Ma, Dr. Hao Wu. The visiting students from Italy- Alberto, Giacomo, Amarildo, and Edoardo, helped me know another culture and expand my worldview. Rebecca Ashley, for letting me discover the joy of mentoring students and enabling her to succeed. Many thanks to my lab alumni and now Professors Ramesh Singh and Sathyan Subbiah – who inspired me with their research, and volunteering work for Asha for Education. They were always available to help me with good advice. I feel very fortunate to be mentored by former lab postdoc Dr. Meisam Salahsoor, who advised me on careers and life, giving his time whenever I requested him. Siri Melkote, for being cheerful and encouraging whenever I visited her office.

I was blessed to find friends in my department and beyond, who made the graduate studies time a little more enjoyable. My grad school friends who stopped for a few minutes to talk and support every time we met – Kyle Brindley, Ara Parsekian, Christine Taylor, Vanessa Smet, Georges Pavlidis, Darshan Pahinkar, Sanzida Sultana, Mason

Chilmonczyk, Gaurav Batra, and David Torello. The awesome qualifier study groups overlapping some of them and including Patxi, Sanam, Anne, Sampath and others helped me get through quals. My grad school friends in initial years Peter Ngo, Alex Ting, Alex Shih for their friendship and welcoming me into the new culture of US universities. My friends in later years Jennifer Molnar for all the talks and discussions about careers.

For all the administrative support, I am very thankful to Glenda Johnson, Camellia Henry, Olivia Kulisz, and Dr. Wayne Whiteman at the ME office, and Latanya Buckner, Melissa Raine, David Barnes, Will Smith, Ann Lamb, Darryl Dirickson, and Kyana Giddens at GTMI. Tatianna Richardson for the support from Grad Studies, and Luis Ocasio from the Registrar's office. ME IT Support over the years from Danny Hardwar, Nick and others, for all computer related help.

I feel lucky that I got the opportunity to learn how to make persuasive presentations and written documents from Dr. David Lawrence and Dr. Kate Williams (CETL/CTL). I am grateful to Robbie Ouzts at GT Career services for her time and advice tirelessly, being available on phone to coach me before the interviews. For me to grow as a leader, and develop myself, I will be ever grateful to Stacey Doremus, my coaches Dave Williams and Monique Mills, and GT LEAD for leadership coaching.

Thanks to GT Public Speaking Club for making me a better speaker in front of people. I also discovered my love for teaching in classrooms from the ME 4215 class, and from many professors including Dr. Melkote who coached me.

For my health, I am indebted for the care I received from Stamps Health Services, to Dr. Holton who patiently heard my requests, Dr. Holbrook who was a constant support,

nurses Paula and others who treated me with care. Dr. Galante and Dr. X (Xerogeanes) who treated my ACL injury, physical therapist Charlie Ridgeway at GT Sports Medicine who ensured I came back stronger, recovering twice from injuries. GT's Stingerette and paratransit for injured students, drivers Lisa, Charles and others who ensured I reached home safe. Thanks to the excellent facilities of the CRC (Campus Recreation Center), the fields where I played soccer, the Pi mile running route to keep me healthy.

For life outside the campus, my roommates over the years, Dhwanil Shukla, Anish Mukherjee, Koustuv Saha (who also happens to be my school classmate!), Swarnava Ghosh and Vipul Thakur provided the camaraderie and the home outside of the lab, for which I am grateful. Thanks especially to Dhwanil for the long thoughtful discussions while eating food, and his company. I am very grateful to have found friends who picked me up not once, but twice, while I recovered from injuries. Thank you Geet Lahoti and Nitisha, Prasoon Suchandra, Ravi Mangal, Gaurav Agrawal, Prajwal Shivaprakash, and my roommates who took care of me like family. Thanks to Prakriti Kaini and Udaya Lakshmi who provided a feeling of home in their apartment. Thanks to the community created by Suvadeep Banerjee, Monodeep Kar, Sandeep Samal, Sourav Dutta, Anshuman Goswami, Ranadip Acharya, Arindam Khan, Souryadeep Bhattacharyya, Ananda Barua, Sabyasachi Deyati, Ushasi Roy, Deya Das, and Korak Sarkar. Ayan da and Piu di for the initial years of get-togethers and quizzes at their home. I am grateful to Shafi Motiwalla for being so welcoming to new students at Tech, and mentoring me. Over the years, I was blessed to get advice from many alumni from Jadavpur University and Georgia Tech, over long-distance communication mediums, who generously shared their time and advice for PhD and life, for which I am very thankful.

A large part of my life in Atlanta was devoted to Asha for Education Georgia Tech, the volunteers of which gave me the community and sense of belonging which I will miss. Tapomayukh Bhattacharjee for being the co-founder, believing in me and the initiative, apart from being the elder brother with advice for every situation, along with the love from Natalia. While I cannot name and thank all volunteers, thanks to Tapo da, Natalia, Dhwanil, Anish, Shashi, Mayank, Agniva and others. They believed in the initiative, made it grow, and will sustain Asha Atlanta for future. Rachit Agarwal for being the coach and inspiration for long-distance running, besides advising me about research and careers.

I want to thank my Professors throughout my undergrad at Jadavpur University, who helped me to reach where I am now – by writing letters for my grad school, and helping me find academic research internships for summers. A special place will be Indian Institute of Science (IISc) Bangalore – which convinced me that a university is the best place to live. I want to thank my teachers all along the way, who inculcated in me a love for learning- my first teachers in my parents, teachers from school, high school, and tutors. I am very grateful for the blessings from Ghosh aunty from miles away during PhD.

I am grateful to have found friends who have been rock solid support, over long-distance modes of communication enabled by the internet, my classmates from school Neha Singh, Kaustav Kundu, Nilotpal Roy, from college Suparno Bhattacharyya, Kamalika Chatterjee and Sanandita Chatterjee, Krithika Chandrasekar for writing beautifully and inspiring me, Sharmishtha Pal for support during thesis writing. There are many others with whom I am no longer in touch with, I thank them all for impacting my life to make this Ph.D. possible.

I was blessed to have a loving family both in India and in U.S., my cousins Soumya mama (Ratnanabha) and Patralika for being the support and inspiration, Mum didi (Ankita) for the caring phone calls, Trisha didi, Susanta da and Arobindo for all the laughs, Arghya dada (Arindam) and Monalisa for the support, Mithu dada for uplifting messages, Piku (Sushmit) for making me keep faith in the next generation.

Finally, I am grateful beyond measure to my parents, who sacrificed a lot, to ensure I get opportunities, without which I would not be here today. My mother Sipra left her stable job teaching Mathematics at high-school, during my initial years of growing up (she is now a high-school Mathematics teacher loved by students, which I am very glad and proud about). My father Asish made decisions in his Electrical Engineering career, to support me at critical times like my school board exams or college-entry examinations. In their words, "I would never know their love as parents, unless I become one". Ma and Baba -*You* are my world. They taught me determination, patience, perseverance, humility and kindness, and inspired me to pursue my Ph.D. degree. Their constant encouragement, supporting words and care, from miles away, are the most cherished things I am blessed with. My maternal grandparents Dida (grandmother) and Bondhu (my grandfather who I call my friend) were supportive during my studies, and always showered their blessings over phone calls from miles away. With all of you – I was never alone in this journey. I realize this acknowledgement is very long, and yet I may have missed many, whom I am thankful for. Thank you, for all that you did over the years to make me reach this point. I am blessed and fortunate to have known all of you!

TABLE OF CONTENTS

LIST OF TABLES

LIST OF FIGURES

LIST OF SYMBOLS AND ABBREVIATIONS

mono-Si	Mono-crystalline silicon
mc-Si	Multi-crystalline silicon
DWS	Diamond wire sawing
LAS	Loose abrasive slurry sawing
FIB	Focused Ion-Beam

SUMMARY

An impediment to widespread adoption of photovoltaics as an alternative to traditional energy sources is the high cost of solar cells, which use single (mono-Si) or multi (mc-Si) crystalline silicon wafers as substrates. The wafers are cut from silicon ingots using the wire sawing process, which is an expensive step in the solar cell manufacturing process. To reduce the cost of solar cells, low-cost, thin silicon wafers of superior surface quality and strength are needed. Recent industry trends indicate a shift from the traditional loose abrasive slurry (LAS) sawing to the new fixed abrasive diamond wire sawing (DWS) process for slicing silicon wafers, with higher productivity, reduced kerf-loss, thinner substrates that save material, and reduced environmental impact through the use of water-based cutting fluids. However, fundamental research to advance the scientific understanding of DWS is lacking.

This dissertation aims to develop a fundamental understanding of diamond wire sawing of crystallographically complex silicon. An open problem in DWS of silicon wafers is how the abrasive grits fixed to the core wire can be engineered to produce favorable surface and subsurface properties, which can reduce processing time and resources in addition to enhancing the mechanical strength of the solar cell substrate. Systematic experimental and analytical studies of the effects of abrasive shape are conducted on both mono and mc-Si materials. It is found that rounder abrasive shapes reduce the surface and subsurface damage in both mono and mc-Si, while the scribed surface morphology is affected only in the vicinity of the mc-Si grain and twin boundaries.

Diamond wire is an expensive consumable for silicon wafer manufacturers, and the wear of the wire affects the quality of the sawn wafers. The effect of wear of the diamond wire on the surface and subsurface damage, and on the mechanical strength of the resulting mono-crystalline silicon wafers are evaluated and compared with results for a new wire. Results show that, with increased wire wear, the wafers exhibit greater evidence of ductile removal, lower surface roughness, fewer but slightly deeper subsurface cracks, and lower average fracture strength.

Moreover, cutting multi-crystalline silicon (mc-Si) by DWS has a known limitation of higher consumption of the expensive diamond wire compared to mono-crystalline silicon. Multi-crystalline silicon is less expensive than mono-crystalline silicon and is therefore expected to enhance the affordability of solar photovoltaic energy. In spite of the advantages of DWS and the lower cost of multi-crystalline silicon, lack of fundamental knowledge of the DWS process for multi-crystalline silicon is a limiting factor for widespread practical application. Hence, systematic diamond scribing studies are conducted to find the effect of mc-Si on diamond wear. Results show that the scribing forces are higher when scribing mc-Si than when scribing mono-Si. The higher forces also correspond to a higher rate of increase in the diamond tip's radius of curvature with scribing distance, as well as higher residual stresses in the diamond (suggesting stress-induced phase transformation of diamond) compared to scribing of mono-Si.

In DWS, a water-based cutting fluid is used as a coolant and lubricant for cutting the silicon. This thesis investigates an unexplored aspect of the role of cutting fluid, namely, the effect of cutting fluid on the mode of material removal (ductile versus brittle) in diamond wire sawing of mono-crystalline silicon (mono-Si). Results show that the chemo-

mechanical effect of the cutting fluid promotes ductile mode material removal, thereby reducing the cutting damage.

The fundamental knowledge derived from this thesis will be useful in guiding future development and optimization of the DWS process to cut brittle materials, including multi-crystalline silicon for photovoltaic applications.

CHAPTER 1. INTRODUCTION

This chapter introduces the background of this dissertation on wire sawing of silicon for photovoltaic applications. The fundamentals of wire sawing processes will be discussed, followed by research objectives and approaches investigated in this study. At the end of this chapter, the outline of this dissertation will be presented.

1.1 Slicing Crystalline Silicon for Solar Cells

The sun radiates more energy every hour than we use in a year [1]. Faced with growing energy demands, shrinking reserves of conventional energy sources, and increasing environmental concerns, researchers have pursued solar energy as a viable solution. One of the most efficient ways of harnessing solar energy is using photovoltaic solar cells. Solar cells offer an optimum mix of modularity, distributed grid, and lower capital investment compared to the other renewable and clean energy sources [1]. Yet, statistics show that less than 1% of the total electricity produced in the US comes from solar cells [2], primarily due to their high cost of manufacturing compared to other sources.

Crystalline silicon (c-Si) wafers form the bulk substrate material of these solar cells. Up to 40% of the cost of silicon solar cells come from the silicon wafer substrates [3-5]. Material cost can be reduced by making and utilizing thinner wafers as substrates. However, thinner silicon wafers are more susceptible to breakage due to stresses applied during handling and processing steps used to manufacture solar cells. Yet, there has been an increase in the demand for thinner wafers in order to lower material cost. Hence, there

is a critical need to address the problem of manufacturing thin silicon wafers with *increased* mechanical strength.

Photovoltaic silicon wafers are manufactured using wire sawing processes, which slice single crystal silicon ingots or multi-crystalline silicon (mc-Si) ingots into thin wafers before they are processed into solar cells. Current high-volume manufacturing of thin (≤ 180 μm), large area (standard size 156 x 156 mm^2) silicon wafers consists primarily of the loose abrasive slurry sawing (LAS) process, which is characterized by lower productivity, environmental concerns, and greater material (kerf) loss compared to the rapidly emerging fixed abrasive diamond wire sawing (DWS) process, which promises higher cutting rates, reduced kerf-loss, thinner wafers, and reduced environmental concerns due to its use of water based cutting fluids and easier recyclability of silicon debris. While LAS utilizes a bare stainless steel wire and loose SiC particles contained in a polyethylene glycol-based cutting fluid medium to remove material, DWS uses a thin layer of diamond grits bonded to a stainless steel core wire using electroplated nickel or a resin bond and a water-based cutting fluid as coolant and lubricant (Figure 1.1). Material removal in LAS is predominantly through a three-body abrasion mechanism as opposed to a two-body abrasion mechanism in DWS. As shown in Figure 1.2, LAS follows the "rolling indentation" model, whereas DWS cuts silicon by "plastic ploughing" and "brittle chip-off" involved in a scratching process [5]. The International Technology Roadmap for Photovoltaic (ITRPV) forecasts significant growth in the use of DWS process (Figure 1.3 and Figure 1.4), due to its potential advantages over the LAS process [6]. In diamond wire sawing, the side walls of the kerf cut by the diamond wire form the final surfaces of the wafers, as shown in Figure 1.5.

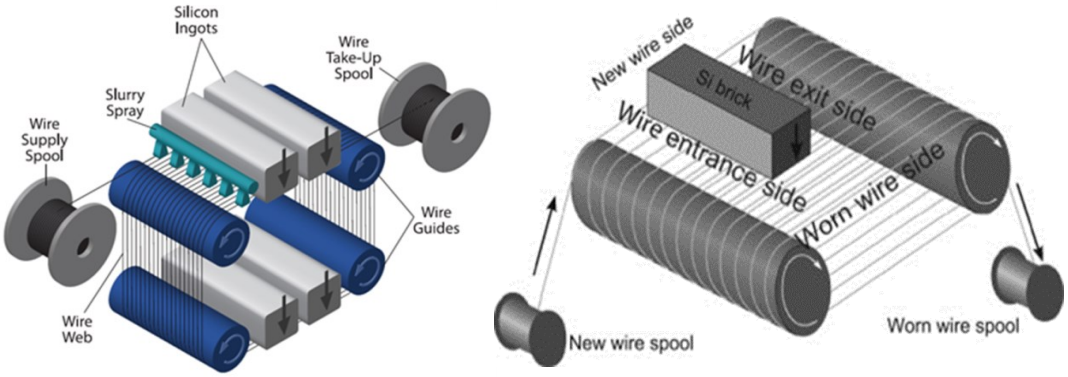

(a) (b)

Figure 1.1. (a) Loose abrasive slurry sawing process (LAS) [7], (b) Fixed abrasive diamond wire sawing (DWS) [8].

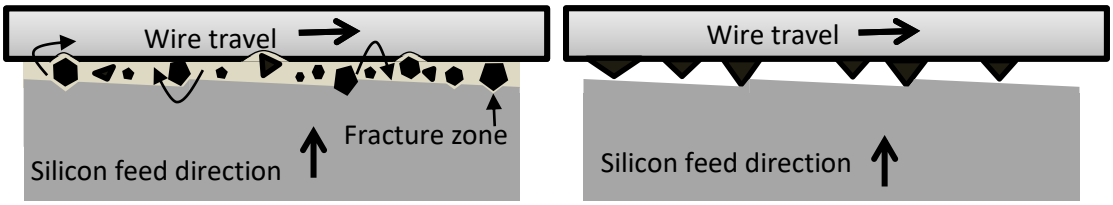

(a) (b)

Figure 1.2: (a) Rolling indenting mechanism in LAS, (b) Scratching and material removal in DWS.

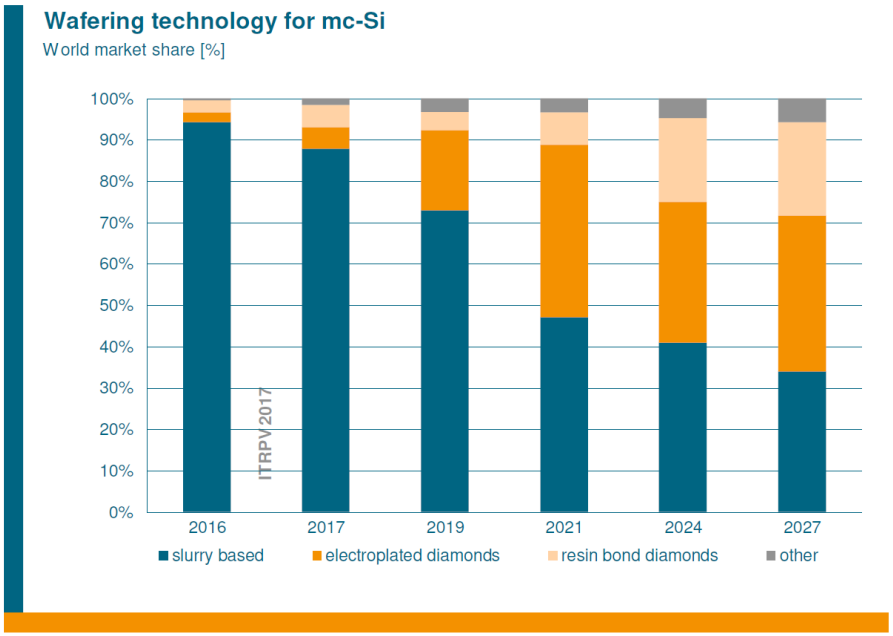

Figure 1.3: Market share of wafering technologies, with growth in diamond wire sawing (both electroplated and resin bonded diamonds) [6].

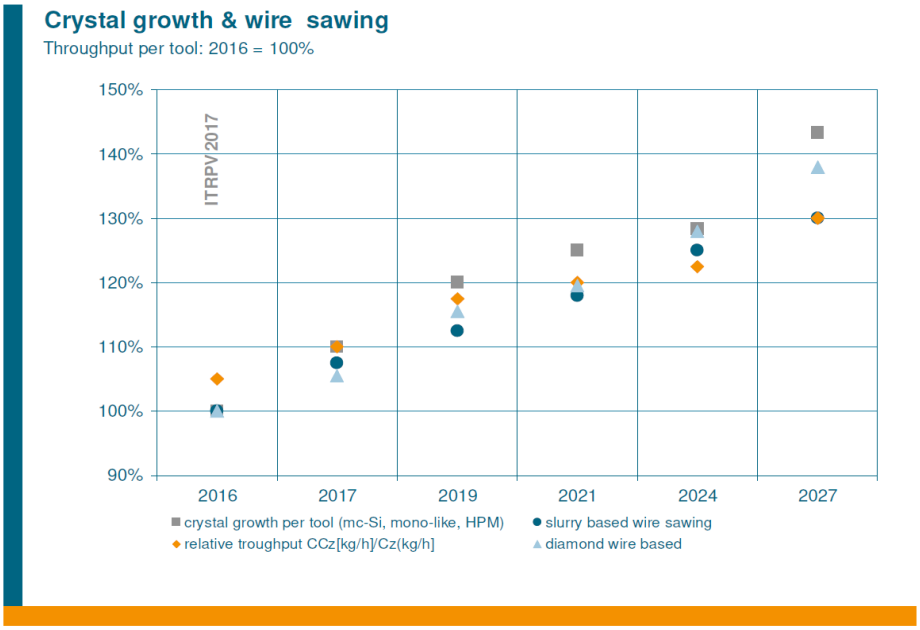

Figure 1.4: Projected trends for productivity with diamond wire sawing versus slurry based wire sawing [6].

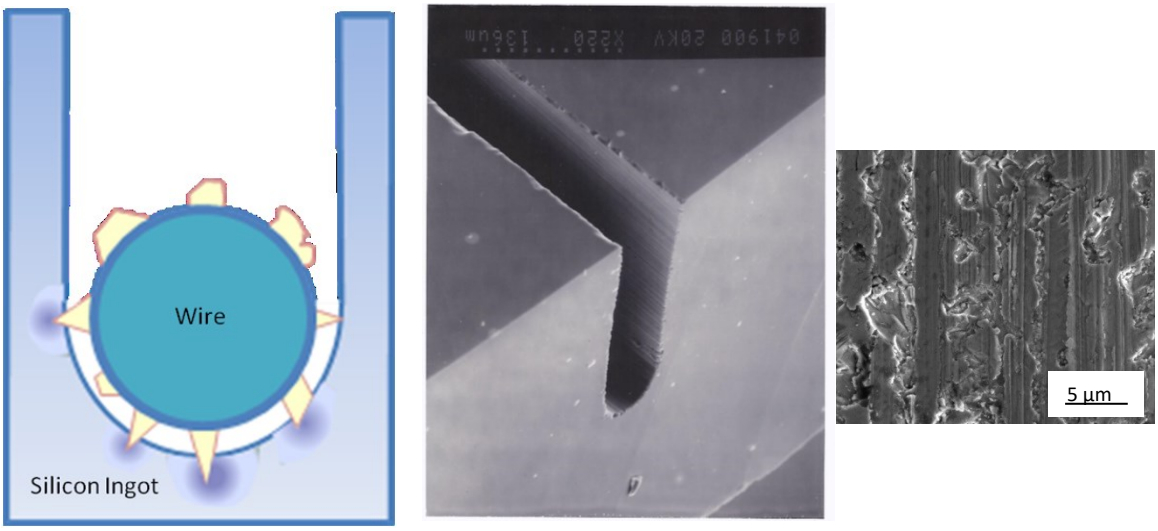

Figure 1.5: (a) Schematic showing kerf in diamond wire sawing, (b) SEM image of kerf (courtesy Dr. Steven Danyluk), (c) Side wall of the kerf forming the final surface of the sliced wafer shows scratches made by the abrasives during material removal.

1.2 Technical Challenges and Research Objectives

The fundamental understanding of the complex DWS process is limited. In particular, detailed knowledge of the effects of DWS process variables such as abrasive shape and material microstructure (e.g. mono vs mc-Si) on the material removal mode, surface and sub-surface damage, effect of the cutting fluid on the material removal mode, and wear of the diamond wire are lacking. Hence, the goal of this research is to obtain fundamental scientific understanding of the complex DWS process to enable efficient manufacturing of high quality, low-cost photovoltaic silicon wafers made from micro-structurally complex brittle crystalline silicon materials. Evidence shows that the mechanical properties, especially the strength of sliced silicon wafers, depend on the wafer

surface and subsurface condition [9]. The surfaces and sub-surfaces of as-cut wafers exhibit saw damage in the form of grooves, pits, and micro-cracks [10]. It is therefore critical that the slicing process be optimized to obtain thinner wafers with adequate mechanical strength by minimizing the surface and sub-surface damage (sub-surface cracks, pressure induced phase transformation, and dislocations) by developing a fundamental understanding of the process variables that affect the resulting wafer quality. The surface and subsurface damage in the DWS process depends on a number of process and material-related factors such as the abrasive characteristics, cutting conditions, cutting fluid, defect structures in silicon, etc.).

Silicon is known to undergo stress induced phase transformation, which causes the brittle silicon to transform from its diamond cubic structure to a meta-stable metallic phase at low depths of cut. Numerous researchers have worked on the ductile machining of silicon using diamond turning [11, 12]. However, the ductile behavior of silicon in wire sawing of wafers with reduced surface and subsurface damage is not fully understood. In particular, the following specific aspects of the DWS process on surface and subsurface damage produced are not well-understood: effect of diamond abrasive shape, cutting fluid crystal structure of the substrate silicon material, and wear of the diamond wire.

Another way of reducing material cost of solar cells is by using multi-crystalline silicon (mc-Si) material for the silicon wafer substrates, which is significantly less expensive than mono-crystalline silicon [6, 13]. The impediment to using multi-crystalline solar cells comes from reduced electrical efficiencies due to the presence of impurities and defect structures such as inclusions and increased dislocation density, specifically at the grain boundaries of mc-Si compared to mono-crystalline Si (mono-Si), which leads to

unfavorable minority carrier lifetimes [14]. However, the economic gains derived from using mc-Si are lucrative compared to using mono-Si. Hence, with the availability of large areas for solar flux capture, mc-Si is preferred over mono-Si for the solar cell substrates for utility scale solar installations [6]. Mono-Si still has applications where the area/weight of the solar cell modules is more critical, like satellites and spacecrafts. However, there are practical challenges in slicing of microstructurally complex multi-crystalline silicon by the diamond wire sawing process, such as lower manufacturing yield of wafers and higher consumption of the diamond wire during wafer slicing [15].

Thus, gaps in fundamental understanding of diamond wire sawing of crystalline silicon include the effects of the actual abrasive grit shapes on the diamond wire, effect of the microstructurally complex multi-crystalline silicon material, effect of the cutting fluid, and wear of the diamond abrasive wire. The underlying hypothesis of this thesis is *that through the fundamental understanding derived from this research, the surface and sub-surface damage in diamond wire sawing of mono-Si and microstructurally complex mc-Si can be minimized by suitably tailoring the diamond grit shape and its wear characteristics, and by engineering the chemical composition of the cutting fluid.* Hence, the following research objectives are formulated for this thesis:

1. Understand the effects of actual *abrasive grit shapes* on the surface and subsurface damage produced in scribing of mono- and multi-crystalline silicon.

2. Understand the *effect of wear* of abrasive grits on the surface quality and the mechanical integrity of sliced wafers.

3. Understand the *effect of multi-crystalline silicon* on the wear of diamond in DWS.

4. Understand the *chemo-mechanical effect* of cutting fluid in scribing silicon

1.3 Dissertation Outline

Following the introduction to the thesis presented in this chapter, Chapter 2 presents a literature review of the relevant aspects of wire sawing of silicon wafers including indentation and scribing of brittle materials, stress-induced phase transformation of silicon and ductile-brittle transition in silicon cutting, effect of defects in multi-crystalline silicon on cutting, the wear of abrasives in cutting of brittle materials, and the effect of fluids in scribing of silicon.

Chapter 3 presents a fundamental study of the effect of actual (non-idealized) abrasive grits of varying shapes fixed to the diamond wire on the surface and subsurface damage produced in scribing of both mono and multi-crystalline silicon. The effect of abrasive shape is determined by comparing the critical depth of cut, which is the depth at which the first crack appears in diamond scribing of silicon with a gradually increasing depth of cut. The effect of different abrasive shapes is validated with an analytical model from the literature. The surface and subsurface damage obtained with approximately round and sharp abrasive shapes in the diamond wire are analyzed. The effect of multi-crystalline silicon material is investigated by characterizing the surface morphology of scribes near and away from the grain boundaries. A detailed analysis and discussion of the results is presented in the chapter.

Chapter 4 presents an analysis of the effects of wear of an industrial diamond abrasive wire used to slice mono-Si wafers on the resulting surface morphology, subsurface damage, and fracture strength. The wafers sliced by the new and used sections of the

diamond wire are analyzed for surface morphology by scanning electron microscopy (SEM) and laser confocal microscopy, the subsurface damage is evaluated in an SEM after focused ion-beam sectioning, and fracture strength of the wafers is determined from biaxial flexure tests. The results indicate that with wear of the diamond wire, surface damage is reduced but subsurface damage is increased (deeper cracks), leading to a decrease in the mechanical strength of the wafers.

Chapter 5 analyzes the effect of the crystal structure (mc-Si versus mono-Si) on diamond wear produced in scribing tests. Wear of the diamond tools is monitored with increase in scribing distance, to determine the effect of mc-Si versus mono-Si on the diamond wear behavior. Diamond tip scribing of mc-Si creates higher forces, and more tool tip rounding due to wear compared to mono-Si. These results help in explaining the reason for higher wire consumption in diamond wire sawing of mc-Si compared to mono-Si.

Chapter 6 presents an analysis of the effect of cutting fluid in diamond scribing of silicon, where the chemo-mechanical effects of a water-based surfactant laden cutting fluid are shown to affect the ductile-to-brittle transition. The results are explained by the effect of the fluid on the surface charges produced in silicon (as indicated by zeta potential measurements), which influences the dislocation movement in silicon, thereby lowering the hardness of silicon and in turn promoting ductile mode material removal.

Chapter 7 summarizes the main conclusions of the thesis and their implications for the design of diamond abrasives (shape), cutting fluid medium, and microstructural composition of silicon ingots for optimization of the fixed abrasive diamond wire sawing

process for both mono and multi-crystalline silicon materials. The chapter ends with recommendations for future work in fixed abrasive diamond wire sawing of silicon and other brittle materials.

CHAPTER 2. LITERATURE REVIEW

This chapter presents the review of prior research reported in the literature on the fixed abrasive diamond wire sawing process, and related work on the associated material removal mechanisms. Specifically, the following aspects relevant to proposed work are reviewed: (i) Fixed abrasive diamond wire sawing process, (ii) Indentation and scribing of brittle materials, (iii) Phase transformation of silicon and ductile mode machining of brittle materials, (iv) Crystallographic defects and their effect on cutting performance, (v) Grit and wire wear in cutting of brittle materials, and (vi) Scribing of brittle materials in presence of fluids. Note that there are other aspects of diamond wire sawing (e.g. process dynamics) that are not covered as they are outside the scope of this dissertation's research. Based on the prior knowledge, research objectives and specific research questions are formulated for this Ph.D. dissertation.

2.1 Fixed Abrasive Wire Sawing

Wafer slicing is one of the most expensive steps in the entire manufacturing process chain of photovoltaic silicon solar cells (at about 20-25 % of the total cost) [4-6]. Hence, there is a crucial need to develop more cost-effective wafer manufacturing methods that are characterized by *higher productivity, lower kerf loss*, and the ability to produce *thinner wafers* with *superior surface quality and mechanical strength*. While the loose abrasive slurry (LAS) process utilizes loose silicon carbide (SiC) particles in a polyethylene glycol-based cutting fluid medium and a bare stainless steel wire web, the fixed abrasive diamond wire sawing (DWS) process utilizes a thin layer of diamond grits (mean size: 8-12 μm), often Ni-electroplated, on a thin (~120 μm core diameter) stainless steel wire and a water-

based cutting fluid, which makes the process environmentally safer than the LAS process [16]. Figure 2.1 shows the two processes and corresponding material removal mechanisms. Figure 2.2 shows a typical DWS machine with a silicon ingot being sliced by the diamond wire wound in parallel over rollers. The cutting action in DWS involves *two-body abrasion* as opposed to the predominantly *three-body abrasion* mechanism in the LAS process [4, 17, 18]. The DWS process is capable of higher (2 to 3X) material removal rates, lower silicon loss due to its smaller kerf, greater uniformity in wafer thickness [19], potentially less surface and sub-surface damage [16], and therefore lower wafer breakage rates and shorter texture-etch times [20]. Moreover, it permits easier recycling of costly Si particles and is therefore *more sustainable* in the long run than the LAS process [21, 22].

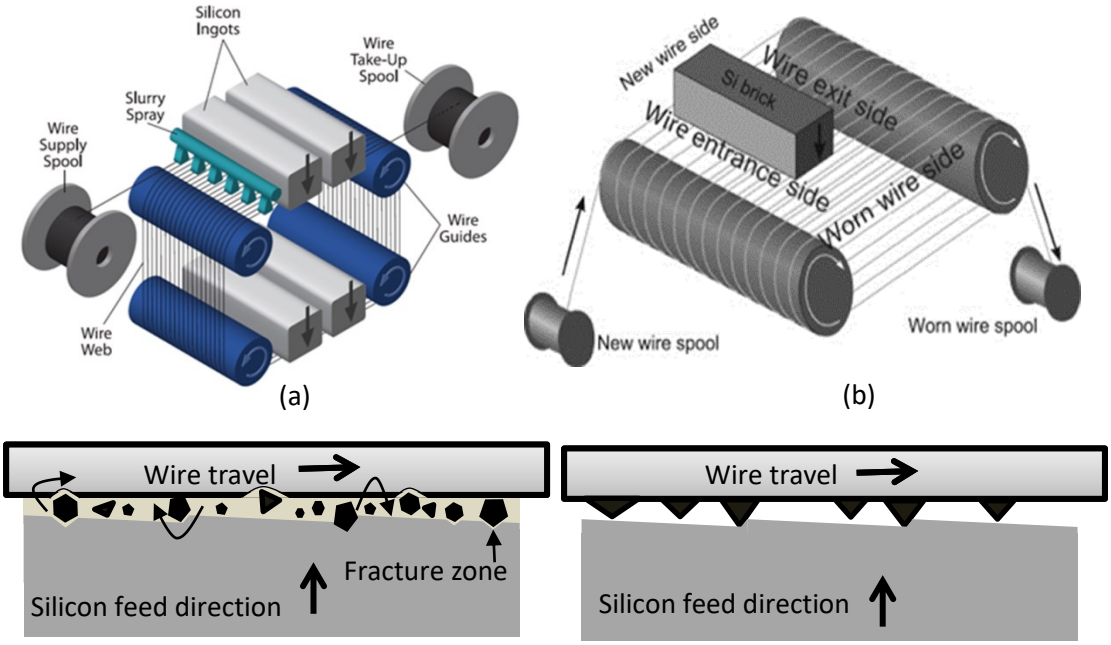

Figure 2.1: (a) Loose abrasive slurry sawing (LAS) [7], (b) Fixed abrasive diamond wire sawing (DWS) [8], and corresponding material removal mechanisms [16, 23].

Figure 2.2: Slicing of a silicon brick using fixed abrasive diamond wire sawing (Image courtesy: Saint-Gobain Northboro R&D center).

A comparison of LAS versus DWS for machining conditions and wafer production metrics is given in Table 2.1[16]. The sustainability comparison of DWS and LAS, with a

focus on the three pillars of sustainability (Environment, Society, and Economics) is given in Table 2.2 [16, 24, 25].

Table 2.1: Comparison of typical wire slicing production conditions for LAS and DWS [26].

Feature	**LAS**	**DWS**
Feed rate	0.42 mm/min	1.1 mm/min
Cutting time 156mm X 156 mm	6.8 hours	2.8 hours
Cutting time 125mm X 125 mm	5.6 hours	2.2 hours
Wafer production capacity (156 mm square)	6500 wafers/day	13800 wafers/day
Wafer production capacity (125 mm square)	7800 wafers/day	16100 wafers/day
Temperature rise	40-60° C	< 20° C

Table 2.2: Sustainability comparison of DWS and LAS processes

	Diamond Wire Sawing (DWS)	**Loose Abrasive Slurry Sawing (LAS)**
Environment	• Yields reduced kerf loss, thus saving material and preserving resources for the future. • Use of water-based cutting fluid reduces hazardous waste. • Yields smaller depth of damage, requiring fewer resources for post-processing. • Promotes adoption of clean solar energy.	• Higher kerf loss, thus more material use. • Use of polyethylene glycol (PEG) slurry increases hazardous waste. • Yields larger depth of damage, requiring more post-processing resources.
Society	• Reduced environmental damage and impact on public health. • Affordable clean energy for larger population.	• Greater environmental damage and impact on public health. • Comparatively higher cost, hence less affordable and limited impact on people.
Economics	• Higher productivity (2X-3X cutting rates). • Stronger wafers, longer lifecycle. • Reducing cost of waste treatment. • Recyclability of silicon from water-based cutting fluid is cheaper.	• Comparatively lower productivity. • Comparatively weaker wafers, leading to reduced lifecycle. • Higher cost of waste treatment. • Recyclability of silicon from slurry is costly.

However, as noted earlier, fundamental scientific understanding of the DWS process is lacking. In particular, fundamental understanding of the impact of critical process variables such as diamond grit shape and its wear on the material removal mechanism (ductile vs. brittle), cut surface morphology and subsurface damage, as a function of the c-Si microstructure (e.g. crystal orientation, grain/twin boundaries, dislocation density variations), is inadequate. This knowledge is crucial for systematic optimization and effective application of the DWS process to manufacture high quality, low-cost wafer substrates for PV and other applications. Consequently, *the proposed research seeks to investigate the micromechanical aspects of the DWS process through experimental and modeling efforts.*

2.2 Indentation and Scribing of Brittle Materials

As described previously, the material removal mechanisms are different in DWS and LAS processes. The rolling-indentation process in LAS can be fundamentally studied using the indentation response of brittle materials, which shows evidence of micro-fracture beneath the indenter [27], as seen in Figure 2.3 [19, 28]. The DWS process is more readily approximated by the scratching action of an abrasive, and hence scribing studies of brittle materials are ideal for fundamentally study of the process [29-31].

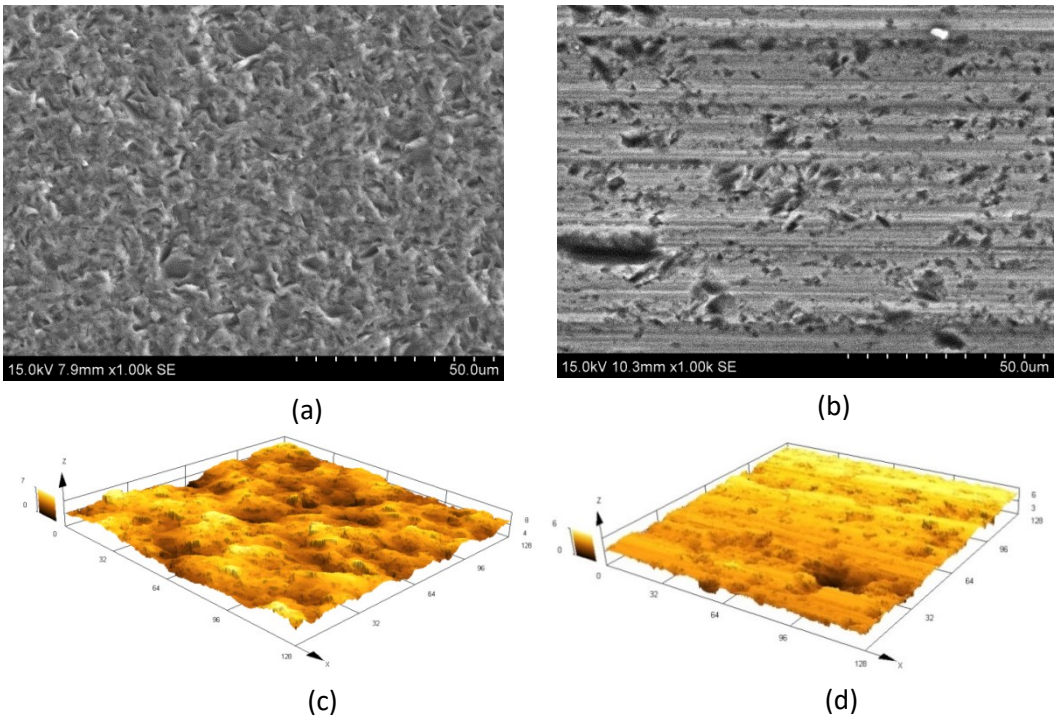

Figure 2.3: SEM images of mc-Si wafer surfaces sawn by (a) slurry and (b) diamond wire; (c) and (d) are their corresponding topographical maps obtained by confocal microscopy [28].

Indenter-based scribing of brittle materials by Lawn et al. [32] revealed the formation of a system of micro-cracks – including median and radial crack systems in the subsurface, which show that the cracks are half penny shaped and arise from the elastic and plastic residual stress fields. The work of Marshall et al. showed that lateral cracks are produced by stresses generated while unloading the indenter [33], as shown Figure 2.4. Further studies of sliding micro-indentation of brittle materials by Ahn et al. [34] and Jing et al. [35] showed that the blister stress fields produced by inelastic deformation cause lateral cracks whereas the applied forces create median cracks (shown schematically in Figure 2.5).

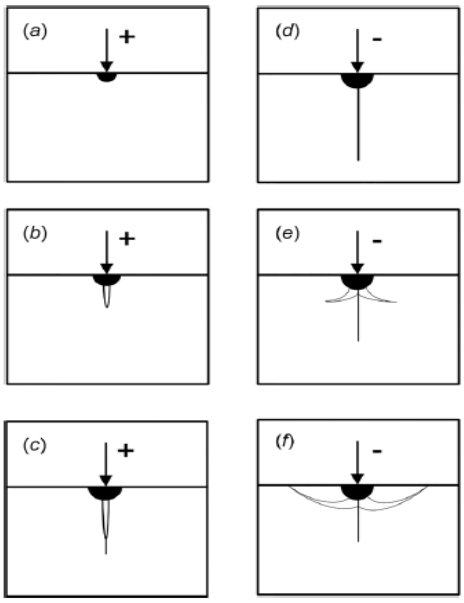

Figure 2.4: Material removal process through median/radial crack formation during loading and lateral cracks during unloading of abrasive-material interaction [27, 36].

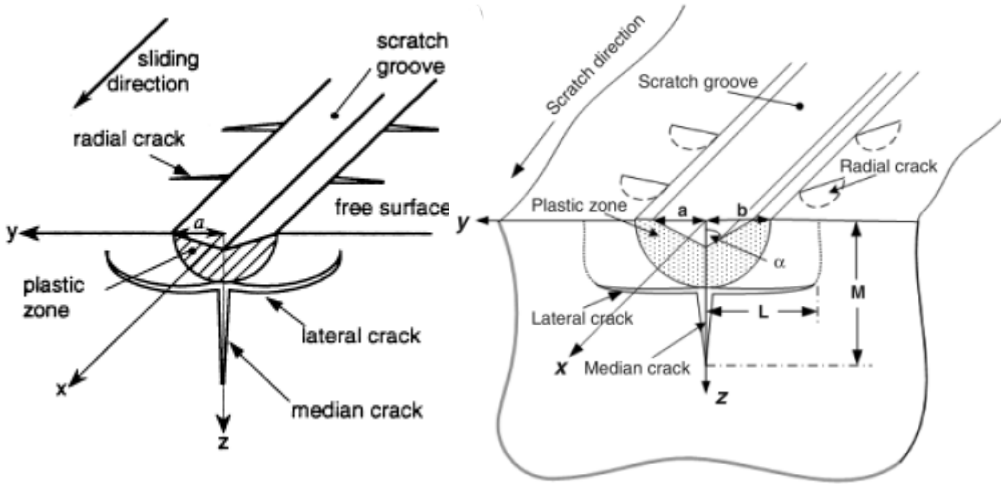

(a) (b)

Figure 2.5: Crack systems formed in sliding of sharp indenters on brittle materials, using blister stress field models (a) from reference [34] and (b) from reference [35].

Recently, the scribing of multi-crystalline silicon by indenters of idealized shape was reported by Borrero et al. [37-39] who showed that grain boundaries locally alter the nature of damage by deflecting the cracks. While prior work on indentation and scribing studies, mostly on ceramics and brittle materials, provide useful knowledge, they are not adequate to predict the cutting behavior of c-Si materials used in photovoltaic solar cells due to the presence of complex abrasive shapes, differences in the size of idealized indenters and actual diamond abrasives, and the micro-structurally complex silicon material, especially mc-Si, due to its wide distribution of crystallographic orientations and defect structures. *Hence, additional fundamental work on scribing of crystalline silicon materials with actual diamond abrasive shapes is needed.*

2.3 Ductile-to-brittle Transition in Cutting of Brittle Materials

Crystalline silicon is known to be brittle, especially at room temperature. However, it is known to undergo phase transformation and ductile mode deformation when subjected to sufficient hydrostatic pressure [40]. As shown by Bifano et al., the ductile mode cutting of silicon depends on cutting parameters (e.g. speed, feed, depth of cut) and the crystal orientation of the substrate [11, 12]. Ductile cutting of brittle optical materials has also been investigated by Nakasuji [41] and Komanduri [42, 43]. Study of nanometric cutting of silicon and ductile mode material removal of mono-Si using molecular dynamics simulation was reported by Cai et al. [44], Komanduri [45] and more recently by Goel et al. [46]. The ductile behavior of silicon is hypothesized to be due to *stress—induced phase transformation* caused by a large compressive stress immediately in front of the scribe as it pushes and removes material [47-52]. While silicon has a diamond cubic structure (Si-I) at atmospheric pressure, it transforms into a crystalline or amorphous phase when subjected

to higher pressures [53]. During cutting, Si-I transforms into a metastable metallic β-Sn phase (Si-II), which is known to be ductile. As material removal progresses and unloading occurs, Si-II transforms into amorphous Si (a-Si) at the unloading rates characteristic of wire slicing [54-59]. The phase transformations of silicon are depicted schematically in Figure 2.6. Raman spectroscopy has shown that scratch marks on silicon wafers mostly consist of a-Si [60], as shown in Figure 2.7. This phase transformation is accompanied by ~20% volume change [40] thus affecting the Si deformation and removal processes and subsequent residual stresses produced in the surface layers.

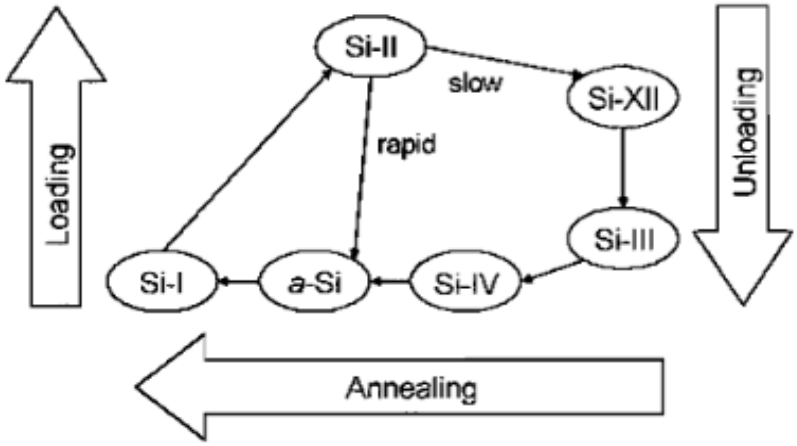

Figure 2.6: Schematic representation of the phase transformations occurring in silicon under loading, unloading, and heat treatment [58]

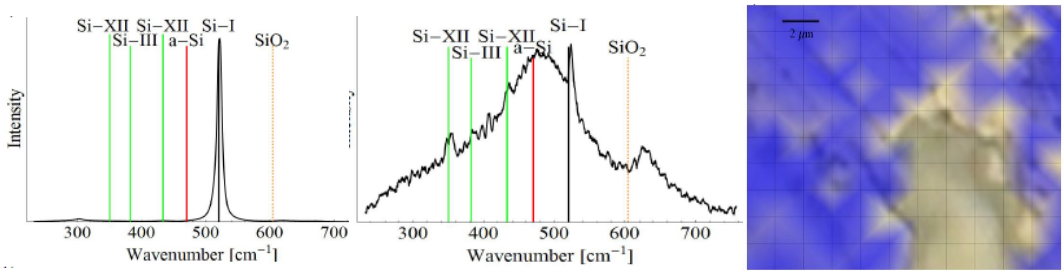

(a) (b) (c)

Figure 2.7: Raman spectra of (a) chipped regions showing crystalline silicon, (b) inside the grooves show amorphous silicon, and (c) amorphous silicon superimposed on the optical micrograph of diamond sawn surface of silicon [60].

The effect of tool parameters like radius of curvature of the tool, and depth of cut is schematically shown in Figure 2.8. The critical depth for ductile-to-brittle transition in nano-scratching of mono-crystalline silicon using idealized indenter shapes was reported in [61] and is reproduced in Figure 2.9. For silicon, Budnitzki and Kuna presented a new phenomenological constitutive law developed using a thermo-mechanical framework [62]. This model captures both Si-I to Si-II phase transition upon compression and the Si-II to a-Si transition (most relevant to DWS) upon rapid decompression. Budnitzki and Kuna also compared the depth of transformed zone reported in multiple studies and found it to be in the range of 1-2 μm, as shown in Figure 2.10. *With the help of available data for silicon phase transformation, the present thesis seeks to identify the abrasive parameters (i.e shape) that yield favorable stress conditions for ductile material removal during diamond wire sawing.*

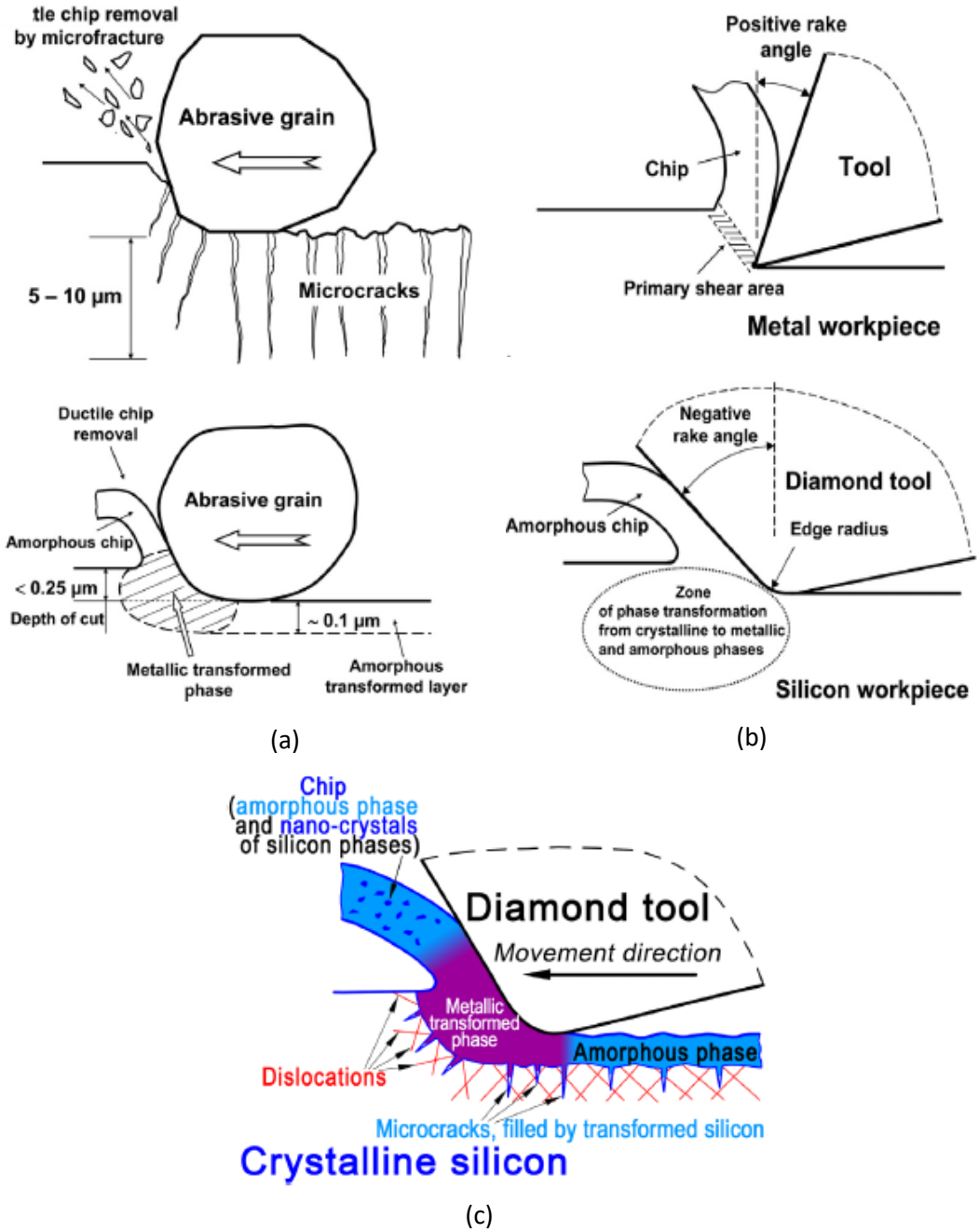

Figure 2.8: (a) Cutting silicon in brittle and ductile modes with abrasive grain, (b) effect of the tool rake angle on phase transformation of silicon, (c) mechanism of stress induced phase transformation [52].

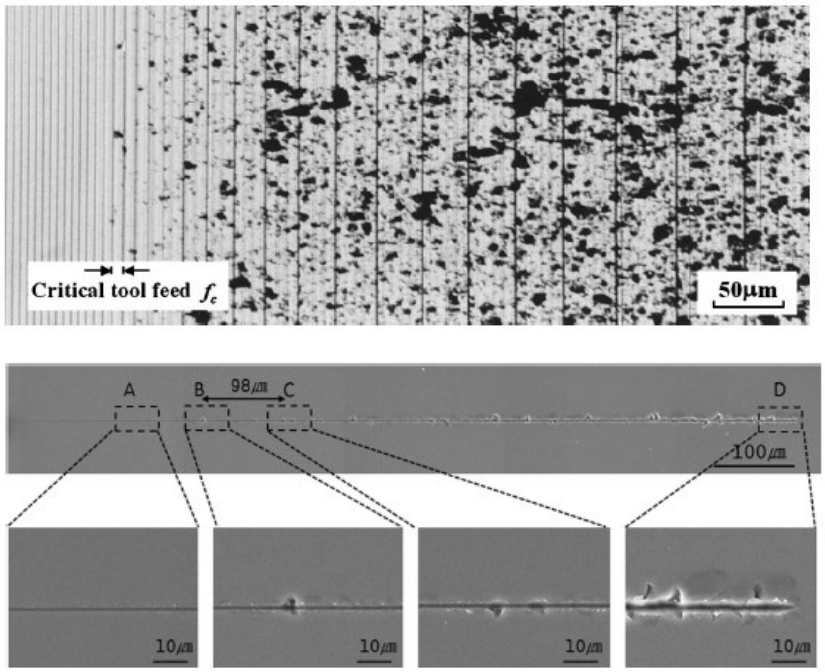

.

Figure 2.9: Ductile-to-brittle transition in turning of silicon in ultraprecision turning [63], and in nano-scratch testing of single crystal silicon with increasing thrust force [61].

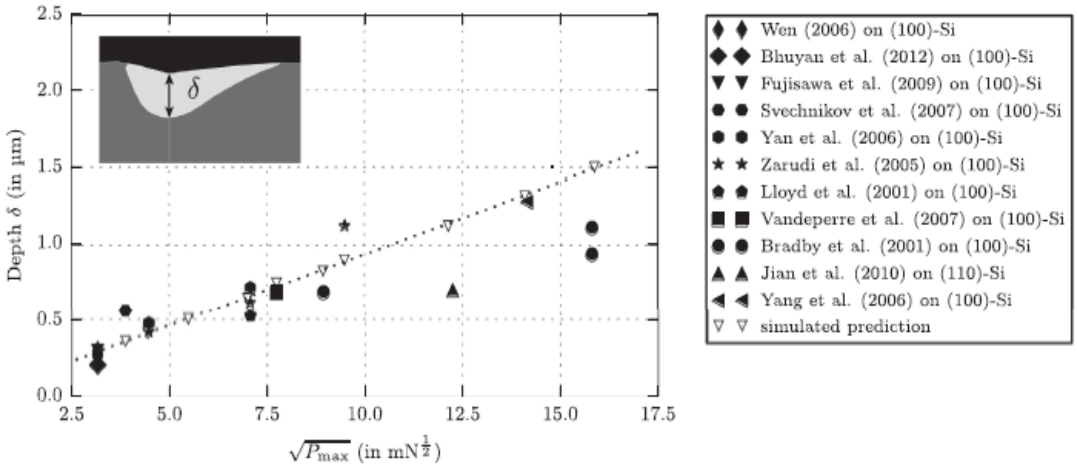

Figure 2.10: The depth of transformed layer in fundamental indentation experiments and TEM observations, as well as in numerical simulations [64].

2.4 Crystallographic Orientation and Defects in mc-Si and Their Effect on Cutting

Experiments have shown that crystallographic orientation of the substrate material impacts the surface roughness and cutting characteristics [31, 65]. As shown by Shibata et al. [50], ductile mode cutting of mono-Si in diamond turning depends on *crystallographic orientation* of the crystal, as shown in Figure 2.11. Crystallographic orientation of mono-crystalline silicon affects the crack patterns as reported by Leu and Scattergood (see Figure 2.12) [31].

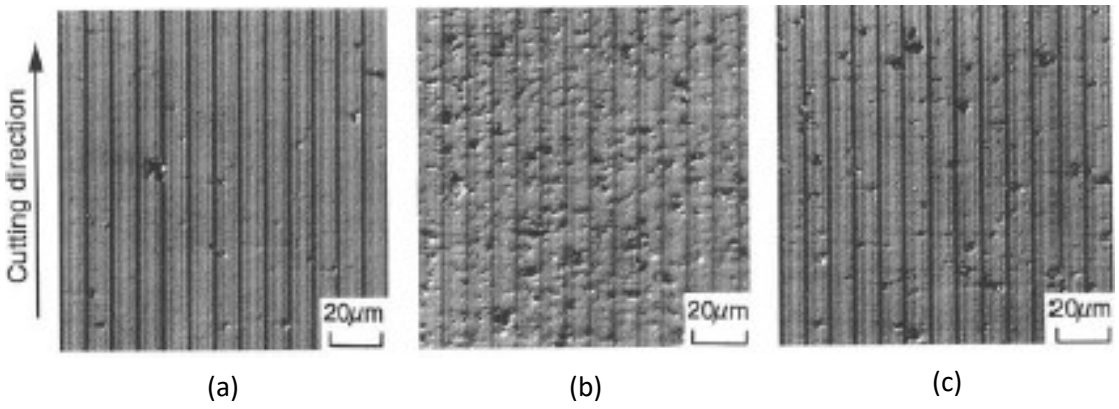

Figure 2.11: Surface morphology showing less pitting damage when turning was carried along [110] direction (for (a)) versus other cutting directions (b and c) [50].

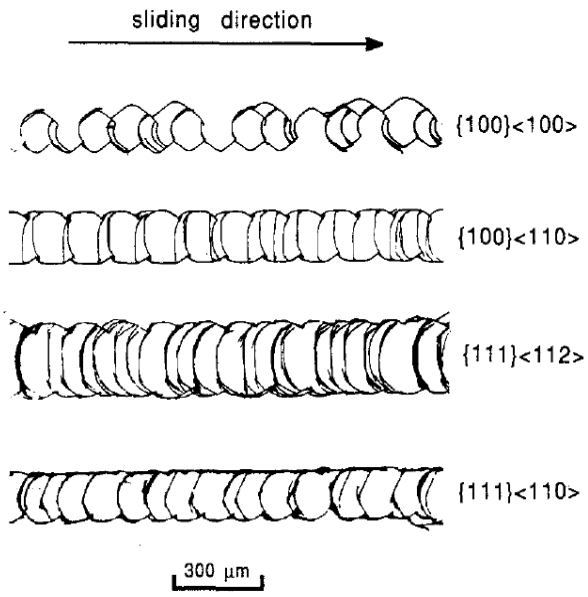

Figure 2.12: Crack patterns in different sliding and workpiece crystallographic directions for single crystal silicon [31].

Compared to single crystal silicon material, mc-Si material is cheaper [6, 13, 66-68] and therefore finds significant use in PV solar cells. However, recent trends in PV wafer manufacturing show considerable difficulty in using the DWS process for mc-Si wafer sawing. Photovoltaic mc-Si is characterized by a number of crystallographic defects such as grain and twin boundaries, dislocations, hard precipitates and other impurities [13, 14], which can significantly alter the cutting characteristics. However, the effects of such crystallographic defects in mc-Si on the cut surface morphology and subsurface damage are not fully understood. Prior work has shown that a correlation exists between the dislocation density and fracture toughness in quasi mono-Si or mono-like materials (a special type of mc-Si material), which can cause the cutting characteristics to be different in different regions of a single grain [69, 70]. Other work has investigated the effect of

carbide and nitride inclusions on the cutting characteristics of mc-Si material [71], as shown in Figure 2.13 and Figure 2.14. However, given that a mc-Si wafer has a large distribution of grain orientations with varying defect densities, *more comprehensive studies of the effect of crystal orientation and defects such as grain and twin boundaries are needed. The present thesis therefore aims to fulfill this need.*

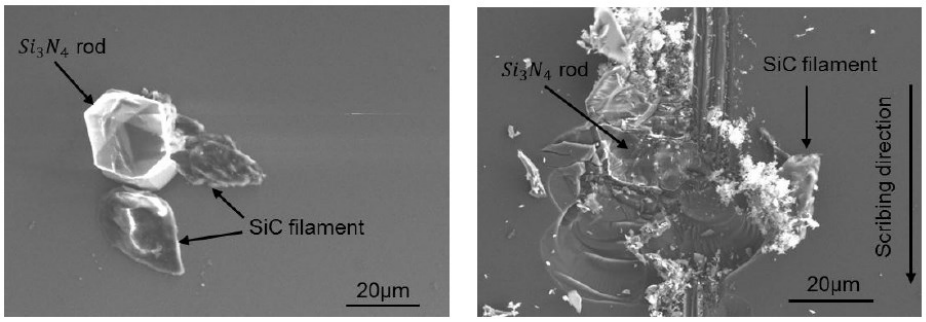

(a) (b)

Figure 2.13: SEM images of silicon nitride (rod) and silicon carbide (filament) inclusions (a) before and (b) after scribing with diamond indenters [71].

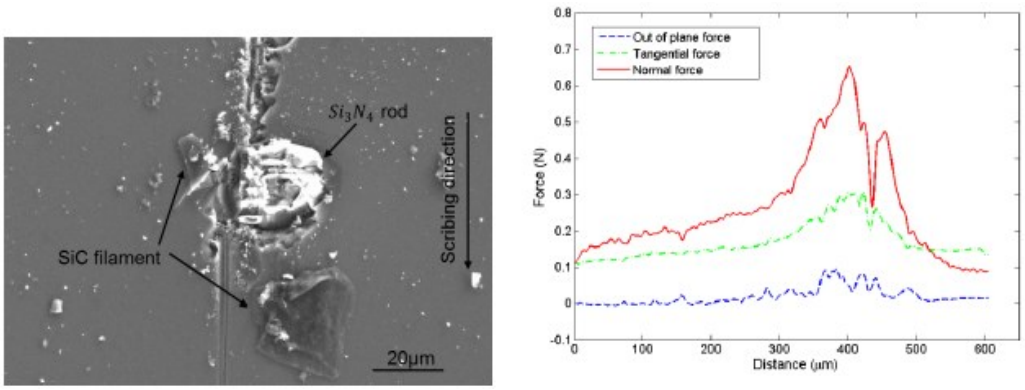

(a) (b)

Figure 2.14: Scribing through silicon nitride rod and the corresponding increase in the scribing force [71].

2.5 Wear of Abrasive Grit and Diamond Wire in Cutting of Brittle Materials

An advantage of DWS over LAS is related to differences in the wear characteristics of the wire. LAS involves three-body abrasion [4, 17, 72] involving the steel wire, the SiC grits, and silicon, leading to wear of the wire core. In comparison, DWS involves material removal by two-body abrasion where the core metal wire is less likely to be worn. Other multi-wire sawing processes involve abrasive based electrochemical methods [73], and resinous diamond wire [74]. In a previous study, electroplated diamond wire manufactured by felt brushes showed better wear resistance [75]. The phenomenon of diamond wire break-in during initiation of cutting and its effect on process performance were studied [76]. Based on the wire sawing conditions used, researchers have shown a reduction in the diamond density with increase in contact length [77], and lifetime estimation were also reported [78]. High stresses in cutting of brittle materials by DWS have been shown to induce graphitization of the diamond abrasives [79], as shown in Figure 2.15. Other studies of cutting single crystal silicon with diamond tools showed tool wear to influence the nanoscale ductile cutting behavior of silicon [80]. The effect of diamond tool wear, especially groove wear, was found to be significant on the nanoscale ductile cutting of silicon [80, 81].

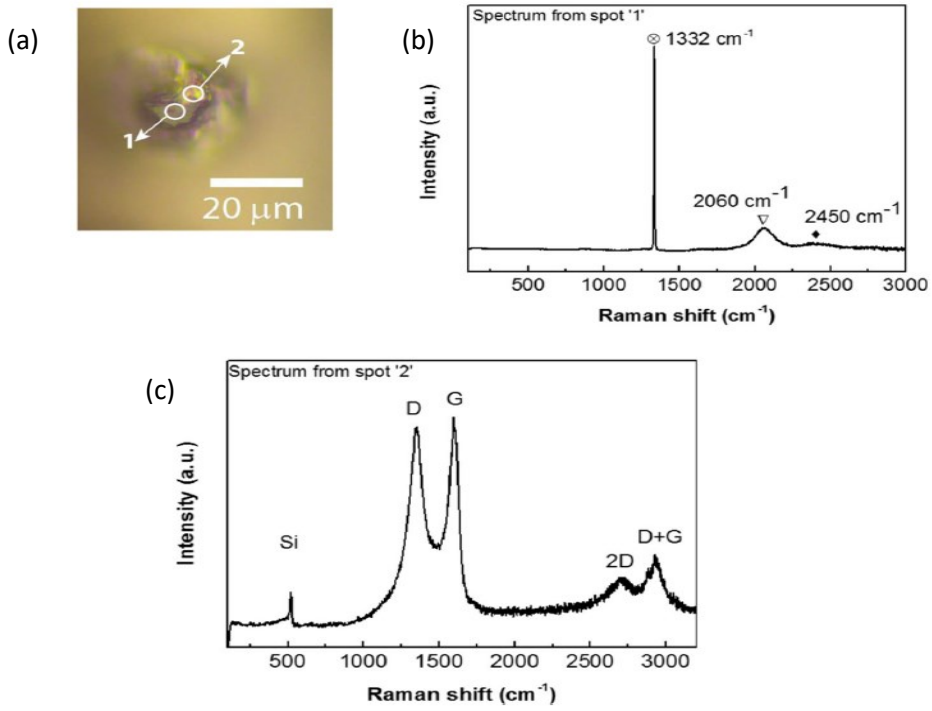

Figure 2.15: (a) Confocal microscopy of the diamond abrasive taken from a fixed abrasive wire used to cut mono-crystalline silicon ingot. (b) Raman spectrum from location 1 shows diamond peak at 1332 cm^{-1}, (c) Raman spectrum from location 2 showing the graphitic peak (marked with G) [79].

Wire dynamics and spooling of the wire can also scratch the electroplated nickel coating, which can be prevented by recently developed wire spooling solutions [82]. Wear of diamond during die separation of microelectronics MEMS devices has been also reported [83], as shown in Figure 2.16. Tool wear mechanisms in diamond turning of silicon consists of abrasive wear, adhesive wear, and micro-chipping [84], as shown in Figure 2.17.

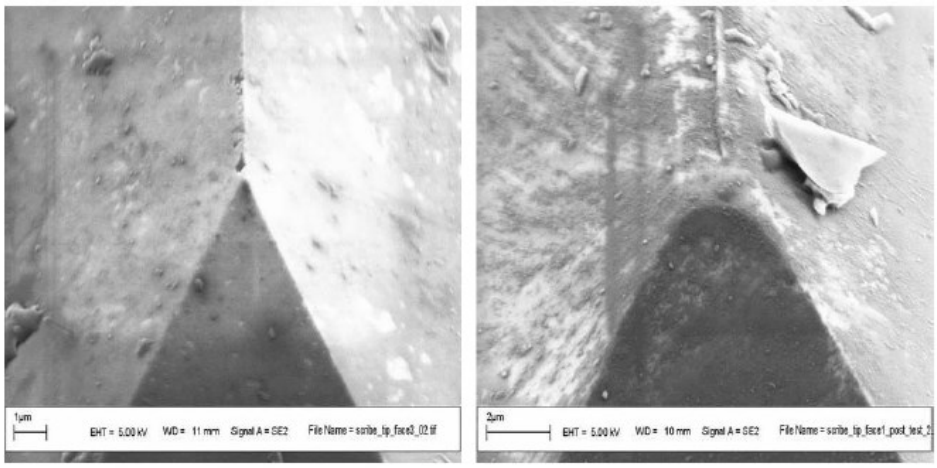

(a) (b)

Figure 2.16: Wear of the tip of a scriber used for die separation of MEMS devices, (a) unused scriber tip, (b) after 56 m of wear on mono-crystalline silicon [83].

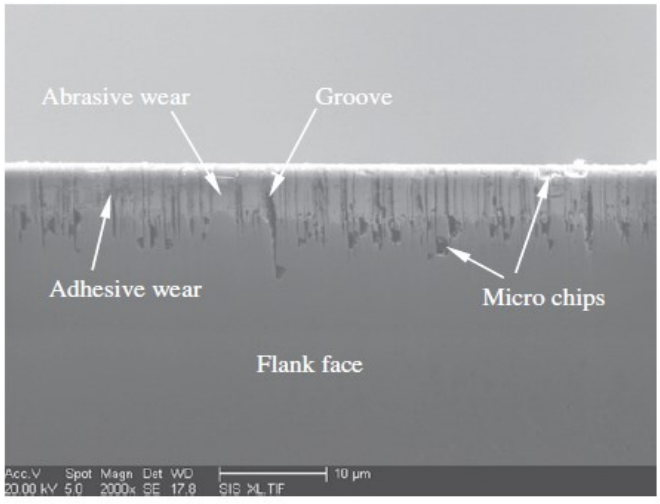

Figure 2.17: Wear on the flank face of diamond tool in precision turning of silicon [84].

Studies of single crystal diamond tool wear in machining (turning) of semiconductor grade mono-Si material show that gradual wear of the single crystal diamond tool occurs in ductile mode cutting while micro-chipping of the diamond occurs in brittle mode cutting [85], as shown in Figure 2.18. The crystallographic orientation of single crystal diamond tools is known to influence the wear of diamond tools, as seen in prior studies of diamond turning [86], and in scratching with diamond tools of specific crystallographic orientations [87]. However, the crystal orientations of diamond grits in a fixed abrasive diamond wire are not controlled, especially since the grits are produced by milling of natural or synthetic diamond. Molecular Dynamics (MD) simulations of scratching of a softer material such as silica have shown the wear of diamond to be due to the breaking of C-C bonds [88], which is attributed to mechano-chemical mechanisms of wear [89]. Wear of a diamond AFM tip when sliding on softer silicon has been reported [90]. In nanoscale cutting of silicon wafer by diamond turning, XPS analysis of the cut grooves revealed the formation of silicon carbide and diamond-like carbon particles with corresponding scratching and grooving wear of the diamond tool [84]. MD simulations of single point diamond turning of silicon also suggested the formation of silicon carbide [91]. However, Raman spectroscopy of abrasive grits used in the diamond wire sawing of silicon have not shown any evidence of silicon carbide formation [79].

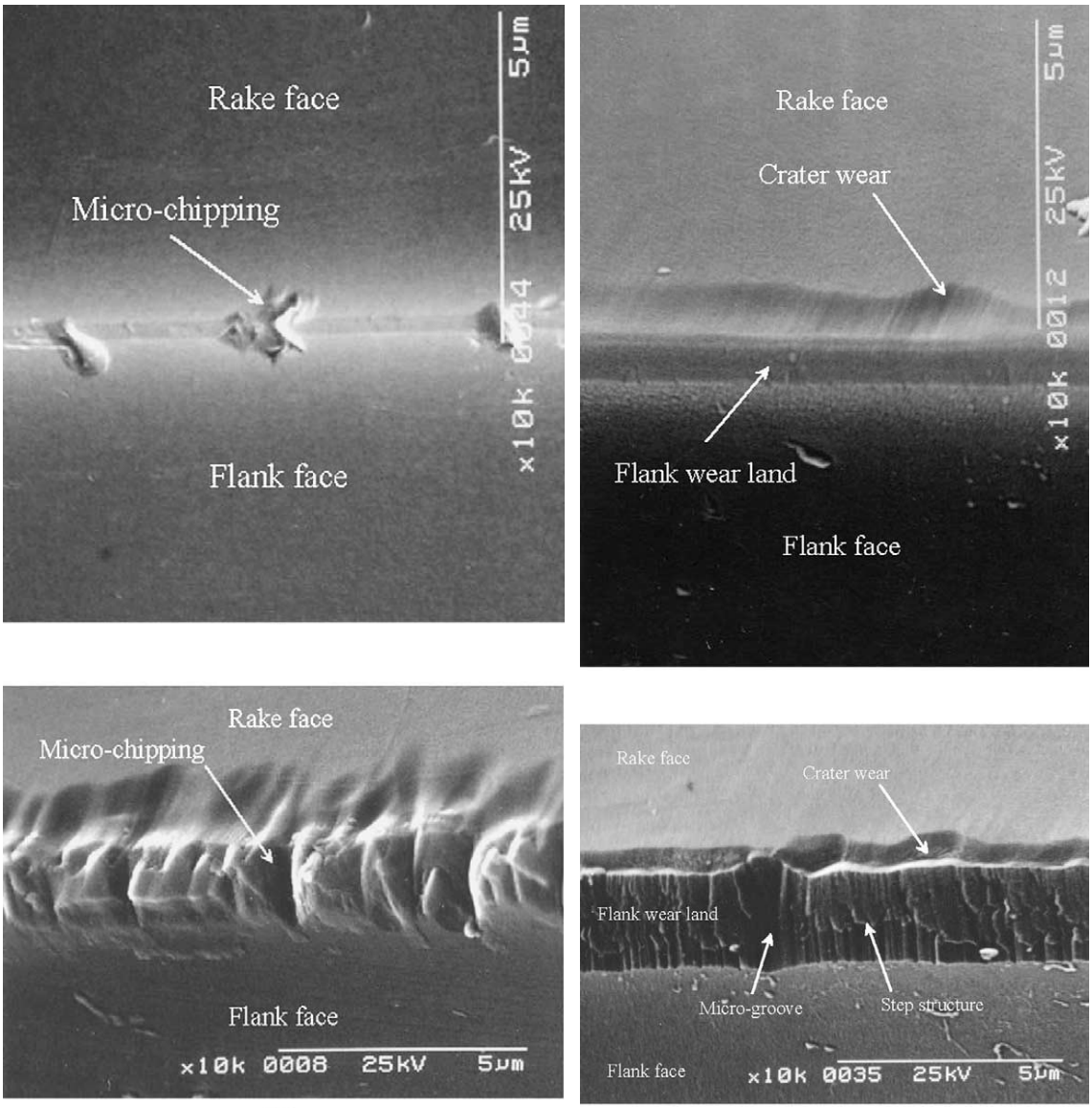

(a) (b)

Figure 2.18: (a) SEM of cutting edge after brittle mode turning of mono-silicon by diamond tool for 1.27 km (top) and 7.62 km (bottom) showing microchipping on the rake and flank faces, (b) Cutting edge after ductile mode turning of mono-silicon after 1.27 km (top) and 7.62 km (bottom), showing crater wear and flank wear land [85].

However, there is limited work on the wear behavior, mechanism, and characterization of diamond wires used in DWS and more importantly, their effect on the cut surface and sub-surface damage. On the other hand, studies of the LAS process have found more non-uniformity in wafer thickness with wear of SiC grits [92]. In the LAS process, with usage and wear, rounder and smaller grits tend to produce lower surface roughness [93]. In addition, the SiC grit size distribution was found to have a greater effect on the cutting characteristics than the grit shape [94]. Another recent study of the LAS process has shown that a bare steel wire with high ductility exhibits better wear resistance and minimizes wire breakage during the wafer slicing process [95]. Tensile tests of new and used wires show that the slicing force decreases with decreasing wire diameter [96]. Studies of the evolution of grit size in LAS [97] have shown that the grit size decreases while its circularity increases with cutting duration. While it is clear that detailed studies of the wear characteristics of the abrasive and wire in the LAS process have been conducted, scientific studies of diamond grit wear in the DWS process are lacking. Moreover, practical experience reported by wafer manufacturers suggests that wear of diamond wire has a significant effect on the cut surface and sub-surface damage. Manufacturers also report that the problem of wear is more acute (wire breakage and loss of productivity) while using DWS for mc-Si [15]. *Hence, detailed studies of diamond grit/wire wear and its impact on the cut surface morphology and sub-surface damage are needed to provide the scientific basis for diamond wire optimization. Moreover, scientific knowledge of why there is higher consumption of the diamond wire when cutting mc-Si versus mono-Si is lacking. The present thesis seeks to address these needs.*

2.6 Scribing of Brittle Materials in the Presence of Fluids

In DWS, a water-based cutting fluid is used primarily as a coolant for cutting the silicon ingot with 8-20 μm average diameter diamond abrasives attached to a high carbon steel wire with nickel coating. Fluids are known to influence the mechanical properties of solids they are in contact with. Prior work investigated the effects of ethanol, acetone, and deionized water in constant-depth scribing of monocrystalline (111) silicon [98-101], as shown in Figure 2.19.

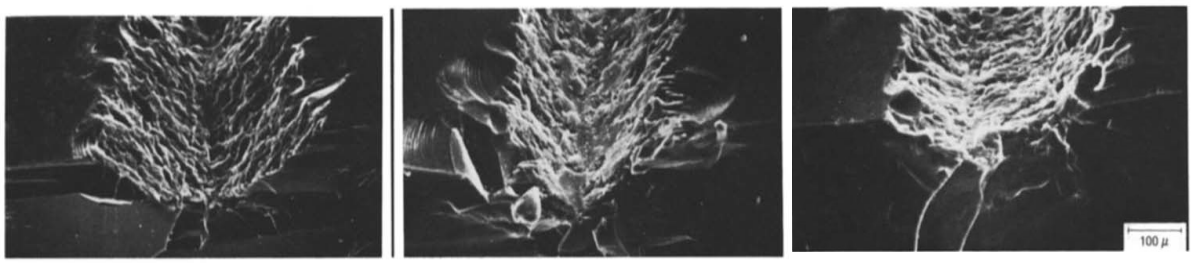

(a) (b) (c)

Figure 2.19: Scribe morphology of mono-silicon scribed in presence of (a) ethanol, (b) deionized water, and (c) acetone [100].

Various theories have been proposed to explain this "chemo-mechanical effect". Research on chemo-mechanical effects dates back to the 1920s when Rebinder's theory of reduction in the hardness of solids due to adsorbed chemical species was proposed [102]. Later, Westwood [103, 104] found the hardness of a solid and the zeta potential of the fluid in contact with the solid to be correlated. Zeta potential is the electrostatic potential between the Stern layer of the double layer at the liquid-solid interface and the bulk solution [105] (schematic in Figure 2.20).

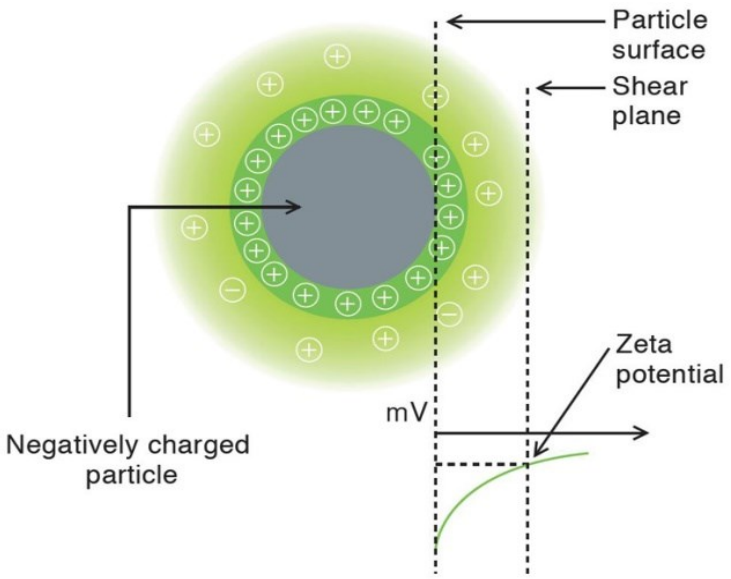

Figure 2.20: Zeta potential is the electrostatic potential between the Stern layer of the double layer at the liquid-solid interface and the bulk solution (image from Horiba scientific instruments).

Westwood showed that a zero zeta potential corresponds to the maximum hardness of very brittle non-metals [103]. Yost and Williams [105] found that when intrinsic and doped (*n*- and *p*-type) silicon are exposed to NaCl and $Na_4P_2O_7$, the minimum hardness is correlated with the most negative value of zeta potential. Yost and Williams explained that the change in hardness with zeta potential is due to the surface charges, which affect the near-surface mobility of dislocations. This explanation is based on prior work where charges produced by electronic doping influenced the dislocation velocities [106] and dislocation kink formation [107]. In another study, Westbrook and Gilman [108] reported softening of silicon by 60% during indentation in the presence of a small potential between the silicon surface and the indenter. *Based on the prior work on chemo-mechanical effects,*

we investigate the effect of cutting fluids used in diamond wire sawing, on the mode of material removal (ductile vs. brittle) by scribing experiments.

2.7 Summary

It is clear from the review of prior work that fundamental understanding of the DWS process, specifically several aspects of the grit-material interaction process, is critical for its systematic optimization and effective application to the cutting of microstructurally-complex *c-Si* materials used as substrate materials in PV solar cells. Specifically, the following aspects of the process need further work.

- The effects of *actual* abrasive grit shapes in industrial grade fixed abrasive diamond wire on the surface and subsurface damage of silicon wafers have not been investigated.
- The effects of grains and twin boundaries during cutting of multi-crystalline silicon on the surface and subsurface damage of the wafers have not been adequately investigated.
- Knowledge of the effect of wear of the diamond wire on the surface and subsurface damage of the sliced silicon wafers is lacking.
- An understanding of why there is higher wire consumption of the expensive fixed abrasive diamond wire while cutting multi-crystalline silicon versus mono-crystalline silicon is lacking.
- The effect of cutting fluid on the mode of material removal (ductile versus brittle) in slicing of silicon has not been adequately investigated.

Therefore, the rest of the thesis describes work aimed at fundamental understanding of the effects of the abrasive parameters (i.e. shape) and cutting fluid on ductile mode material

removal in scribing of silicon, effects of grains and twin boundaries of multi-crystalline silicon on diamond scribing, the effect of wear of diamond wire on the surface and subsurface damage of sliced wafers, and the cause of diamond abrasive wear when cutting multi-crystalline silicon.

CHAPTER 3. EFFECT OF GRIT SHAPE AND CRYSTAL STRUCTURE ON DAMAGE IN DIAMOND WIRE SCRIBING OF SILICON

This chapter investigates the effect of the abrasive grit shape and grain/twin boundaries in multi-crystalline silicon material on the surface and subsurface damage in scribing with the diamond wire. Fundamental understanding of the fixed abrasive slicing of photovoltaic silicon wafers is crucial for producing low-cost wafers with superior surface quality and mechanical strength. With the goal of understanding the diamond wire sawing process, this chapter investigates the scribing of mono- and multi-crystalline silicon by the abrasive grits in an actual diamond wire. Specifically, the effects of grit shape and silicon crystal structure on the resulting surface morphology, subsurface damage, and the critical depth of cut at which ductile-to-brittle transition occurs are investigated.

3.1 Introduction

An impediment to widespread adoption of photovoltaics as an alternative to traditional energy sources is the high cost of solar cells, which use single (mono-) or poly (multi-) crystalline silicon wafers as substrates. The wafers are cut from silicon ingots using wire sawing, which is an expensive step in the solar cell manufacturing process. Hence, low-cost, thin wafers with superior surface quality and strength are needed. Recent industry trends indicate a shift from loose abrasive slurry (LAS) to fixed abrasive diamond wire sawing (DWS) [3]. The slicing action in LAS consists of a three-body abrasion [4, 17]

mechanism in contrast to two-body abrasion in DWS, which cuts silicon by a combination of ductile cutting and brittle fracture [10, 109]. Consequently, scribing can be used to understand the fundamentals of DWS. Previous work investigated DWS through scribing with idealized indenters [110]. However, the shapes of diamond grits used in DWS differ significantly from the shapes of idealized indenters. Hence, in this chapter, the effect of *actual diamond grits* on the surface and subsurface damage produced in scribing of mono- and multi-crystalline silicon (mc-Si) materials is investigated. This is achieved by scribing with a small section of an actual diamond wire. By correlating the resulting scribed surface and subsurface characteristics with the individual grits producing them, a basic understanding of the effects of actual grit shapes in DWS can be obtained. Ideally, a diamond wire with a narrow distribution of known grit shapes is desirable for such an experiment. However, actual diamond wires are characterized by millions of grits with randomized shapes. Consequently, this chapter analyzes the scribed surface and subsurface damage in mono- and mc-Si produced by a *sample of grits* contained in a section of commercially available diamond wire, which is selected without bias. The knowledge derived from the scribing analysis is expected to aid in developing recommendations for grit shape control during the design and manufacture of diamond wires.

Although silicon is brittle, it undergoes ductile deformation in the presence of sufficient hydrostatic pressure [40]. A number of studies have reported the ductile cutting of silicon [11, 55, 111]. The ductile behavior of silicon is attributed to stress-induced phase transformation caused by the large compressive stresses generated in front of the scriber [47, 50, 57, 109]. Ductile removal of silicon during DWS could produce less micro-cracks, thereby enhancing the fracture strength of the wafer. Moreover, reduced saw damage of

wafers can minimize the need for saw damage etching. Motivated by these considerations, the effects of grit shape and crystal structure on the scribing depth at which ductile-to-brittle transition occurs are investigated.

Compared to mono-Si, mc-Si is cheaper [13] and is widely used to produce low-cost solar cells. However, mc-Si wafering using DWS faces many challenges due to crystallographic defects such as grain/twin boundaries, dislocations, precipitates, and impurities [14]. Dislocation density variation is correlated with variation in the fracture toughness, which affects the cutting characteristics [69, 70]. Cutting is also affected by carbide and nitride inclusions [71]. In this chapter, the effects of crystallographic defects in mc-Si such as grain/twin boundaries on the scribed surface morphology are also investigated.

3.2 Experiments

3.2.1 Diamond Wire Scribing

Scribing experiments were conducted using a small section of wire cut from a commercially available electroplated diamond wire (PV 130124, 120 μm core diameter) (Figure 3.1a). Imaging analysis of approximately 50 exposed diamond grits on the wire showed that the grit size follows a normal distribution with an average diameter of 8.5 μm and a standard deviation of 2.6 μm. The aspect ratio of the grits was determined to be 0.76. Substrate materials used for scribing consisted of 10mm x 10mm x 25mm blocks of mono- and mc-Si. The surfaces of the blocks were ground, lapped and polished to a mirror finish. The wire was tensioned on a fixture by two screws (Figure 3.1b) and mounted on the scribing setup (Figure 3.1c).

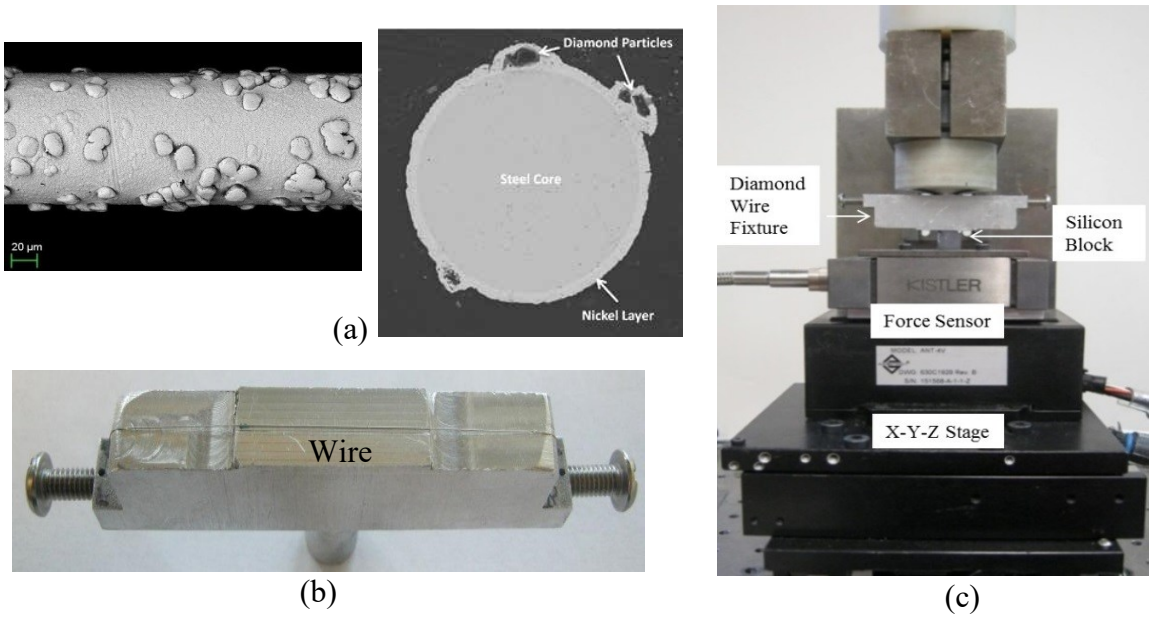

Figure 3.1: (a) SEM image of diamond wire (representative cross-section from [18]), (b) wire in scribing fixture and (c) wire scribing setup.

The silicon block was mounted on a flat baseplate fixed to a three-component piezoelectric force dynamometer (Kistler 9256C), which was rigidly mounted on computer-controlled stacked X-Y-Z motion stages (Aerotech ANT-4V). The dynamometer detected the contact between the grits and silicon just prior to scribing and also measured the scribing forces. Scribing direction was always perpendicular to the wire length, thereby isolating the cutting action of individual grits. Actual wire sawing involves material removal along the length of the wire as the wire is arranged in multiple loops that form a wire web [4]. X-ray diffraction (Panalytical X'Pert XRD) was used to determine the crystallographic orientations of both the mono- and mc-Si substrates. From XRD measurements on the mono-Si, the crystallographic orientation of the scribed plane and the scribing direction were (100) and [110], respectively. For mc-Si, scribing was limited to a

twinned grain of (311) orientation and to scribing across a grain boundary delineating two grains with (111) and (331) crystal orientations. The scribing speed used in all experiments was 100 mm/min. The effect of scribing speed is assumed to be negligible [112].

The critical depth of cut is defined as the depth corresponding to the onset of the first crack and where the material removal mode changes from ductile to brittle. A larger value of critical depth of cut indicates that ductile removal can be obtained at higher depths of cut. In order to determine the critical depth of cut, scribing tests with gradually increasing depth of cut (0 to 5μm over a 5mm length) were performed using displacement control.

Since protrusion of grits on a diamond wire is non-uniform and because the fresh wire is coated with electroplated nickel as bonding agent to fix the diamond to the steel wire, a few trial scribes were made to expose the grits. The representative cross-section of the wire (from [18]) is shown in Figure 3.1. SEM imaging (Hitachi S-3700N and SU8230) revealed the exposed grits involved in the scribing action. Careful analysis of the scribes and the location of the exposed grits on the wire in each test enabled the association of a specific grit with a particular scribe. Note that the grit density of the wire section used was low enough to minimize multiple grit interactions with the same region of the silicon sample. Each experiment for a particular grit shape and material combination was repeated three times. The replications showed that surface features produced by a particular grit shape were repeatable. The resulting scribed surface morphologies were imaged in an optical microscope (Leica DMRM) and in the SEM. Scribes produced by four grits with distinct shapes were selected for analysis aimed at understanding the effect of grit shape on scribe morphology. We performed confocal microscopy (Olympus LEXT) of the

grooves at the location of ductile-to-brittle transition to obtain the critical depth of cut. Cross-sectional profiles obtained from confocal microscopy of the ductile portion of the scribes correlated well with the SEM images of the corresponding grits. Given the higher hardness of diamond compared to silicon, we assume that the grit shape did not change significantly with repeated scribing.

3.2.2 Subsurface Damage

To evaluate subsurface damage, we used a focused ion beam (FIB) method (Figure 3.2). A gallium source FIB (FEI NOVA) was used to cut sections perpendicular to the scribes. First, a high-energy beam (7nA, 30KV) was used to make a rough cut. Next, a low-energy beam (30KV, 1nA) polished the rough cut surface to minimize FIB induced damage. This procedure was used for both mono- and mc-Si samples. Since the grooves analyzed for subsurface damage were produced by a gradually increasing depth of cut, each scribe was characterized by a ductile-to-brittle transition zone whose location was governed by the critical depth of cut for a particular grit shape-material combination. To make FIB cuts, we selected two regions along the groove. The region before the ductile-to-brittle transition (zone A) and the region after the transition (zone B), are shown schematically (Figure 3.3).

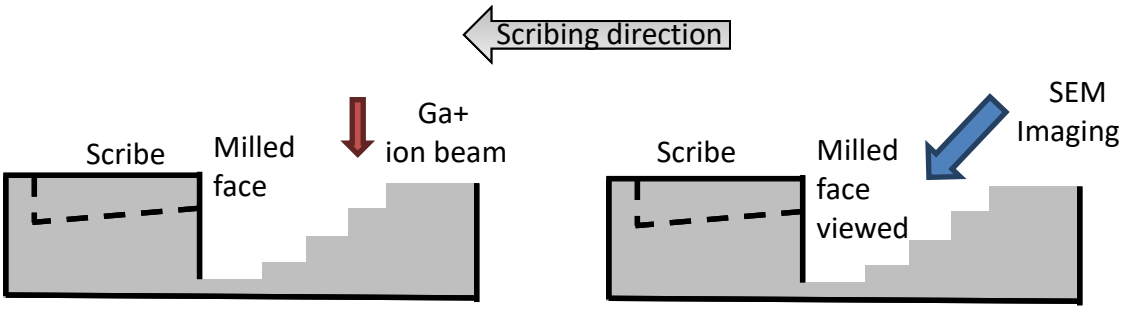

Figure 3.2: FIB procedure for subsurface damage evaluation.

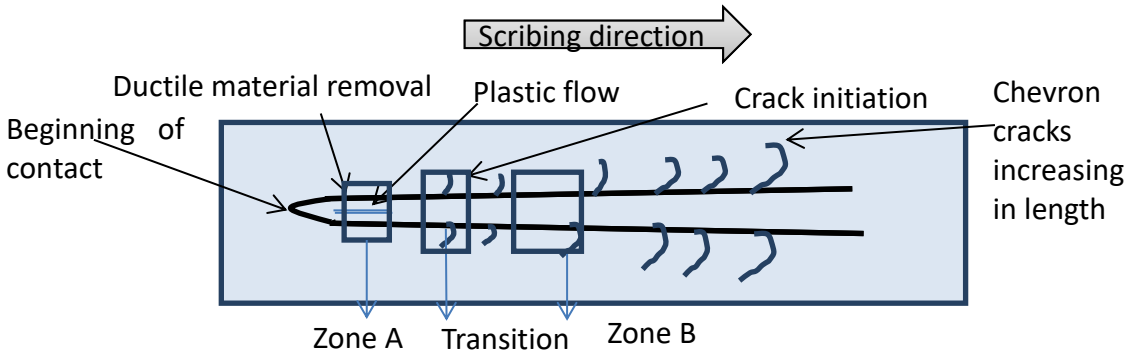

Figure 3.3: Schematic plan view of scribe morphology and locations for FIB cuts. Scribing direction is from left to right.

3.3 Results and Discussion

3.3.1 Effect of Grit Shape and Material

The exposed diamond grits selected for analysis are shown in Figure 3.4. Grit 1 has a pointed contour while grit 2 has a more rounded contour with multiple small protrusions. The grit shapes can be approximately assessed from the cross-sectional optical profiles of the ductile regions of the grooves, which contain the imprint of the grit contours.

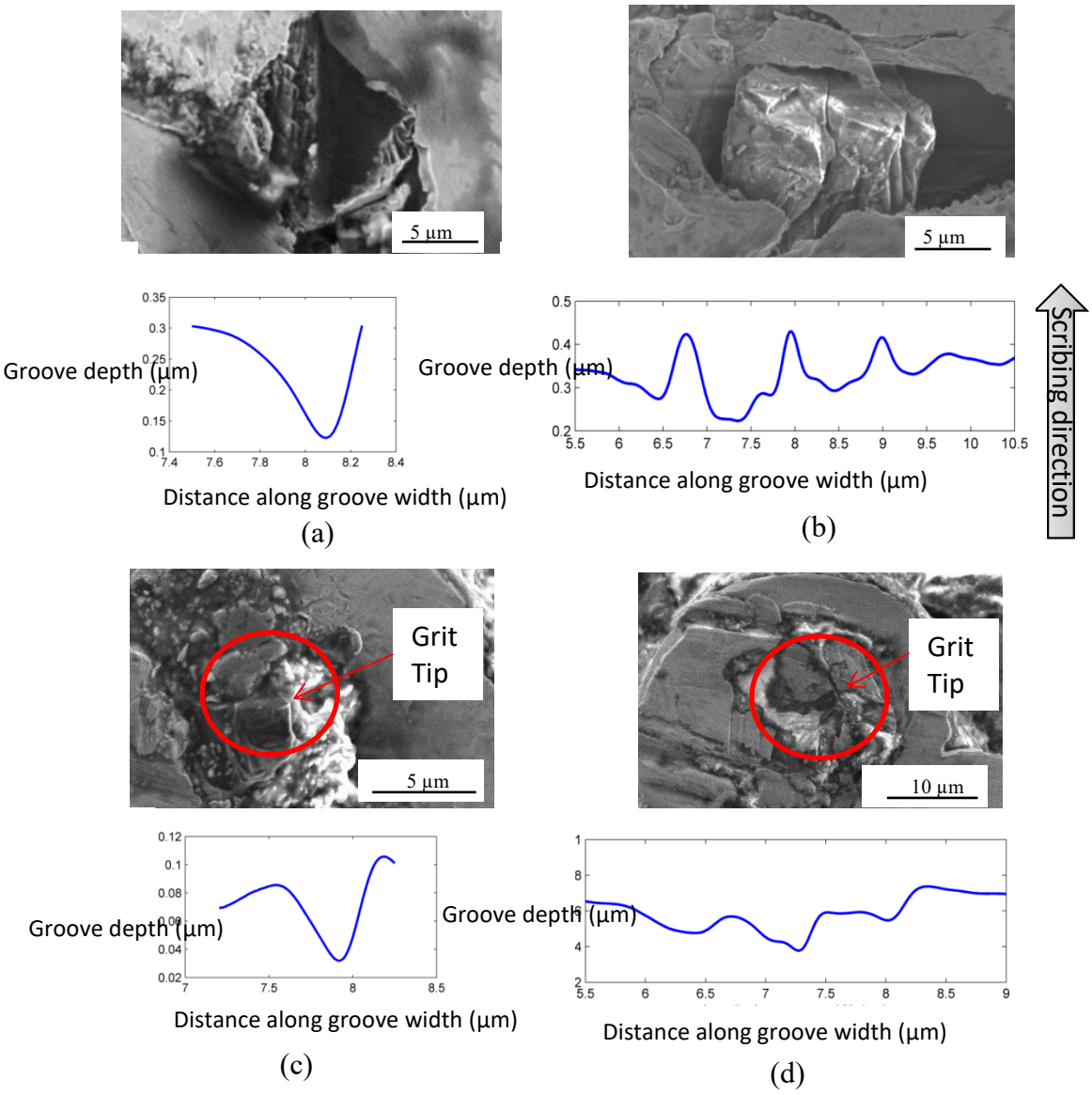

Figure 3.4: SEM images of (a) grit 1, (b) grit 2, (c) grit 3, and (d) grit 4. Cross-sectional profiles of the ductile portions of the grooves, which represent the grit contours, are shown below each grit image.

As seen in Figure 3.5, the scribe morphologies produced by grits 1 and 2 in the mono- and mc-Si samples differ considerably. At the beginning, each scribe exhibited completely ductile behavior, with cracks appearing at the ductile-to-brittle transition as the scribing depth gradually increased. We attribute the differences in morphology to the difference in grit shapes, specifically from sharp to a more rounded grit with multiple edges. Prior work [30] showed that various types of cracks are generated by indenters with different idealized shapes. Sharp indenters were shown to produce chevron cracks on the surface, and a system of lateral and median subsurface cracks. Spherical indenters produced partial cone cracks [31, 113, 114] with semicircular, horseshoe-like patterns contained within the grooves. Approximating grits 1 and 2 with the closest idealized indenter shapes, namely sharp and round, the corresponding scribe morphologies are comparable to those reported for the idealized shapes [30]. Grit 1 produced chevron or radial cracks in both mono-Si and mc-Si with brittle chip-out on one side of the groove. In contrast, grit 2 produced horseshoe-like cracks, which were confined to the groove in both mono- and mc-Si. The damage caused by grit 2 resembles the cracks produced by the sliding of a spherical indenter on (100) silicon in the <110> direction, as shown in prior work [115]. Thus, for a given grit shape, the scribed surface morphologies were similar in both materials.

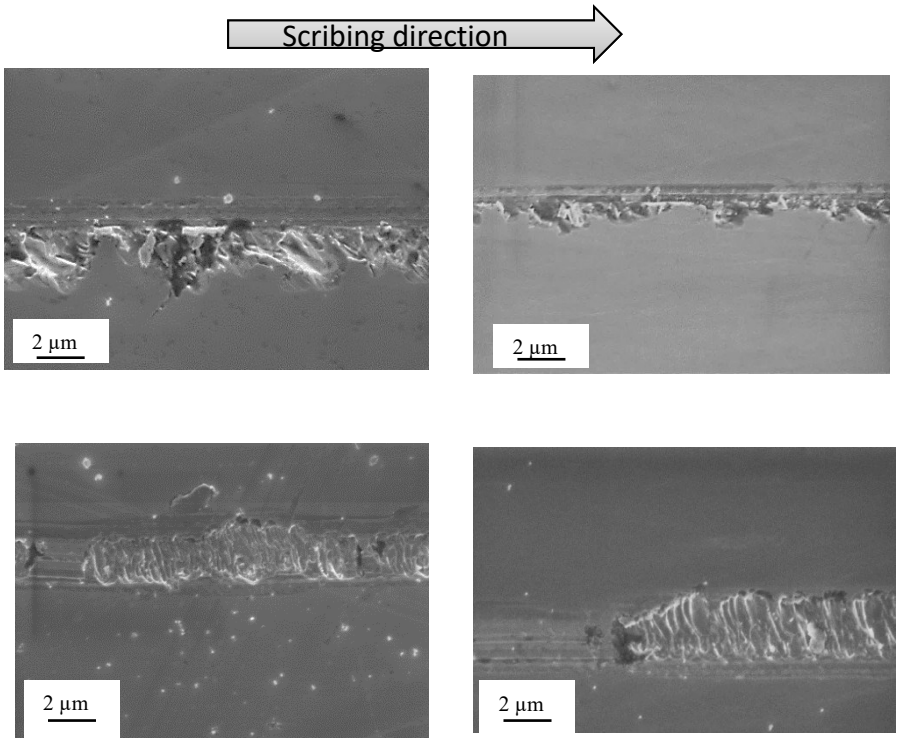

Figure 3.5: SEM of scribes for grit 1 (top row) and grit 2 (bottom row); mono-Si (left) and mc-Si (right). Scribing direction is from left to right.

Figure 3.4(c) and Figure 3.4(d) show grit 3 is essentially a triangular pyramid with a pointed tip and cutting edges, whereas grit 4 is approximately blunt. Figure 3.6 shows the morphologies of the scribes produced by grits 3 and 4 in mono- and mc-Si, respectively. Grit 3 produced chevron-type radial cracks emanating from one edge of the groove. Grit 4 mostly caused radial cracks on one side of the groove that chipped out, possibly after the radial cracks combined with lateral cracks. Similar to grit 1 and grit 2, the scribed morphologies produced by grits 3 and 4 were influenced more by the grit shape than by the material. The comparatively round grit 4 produced a wider groove than grit 3, which is sharper.

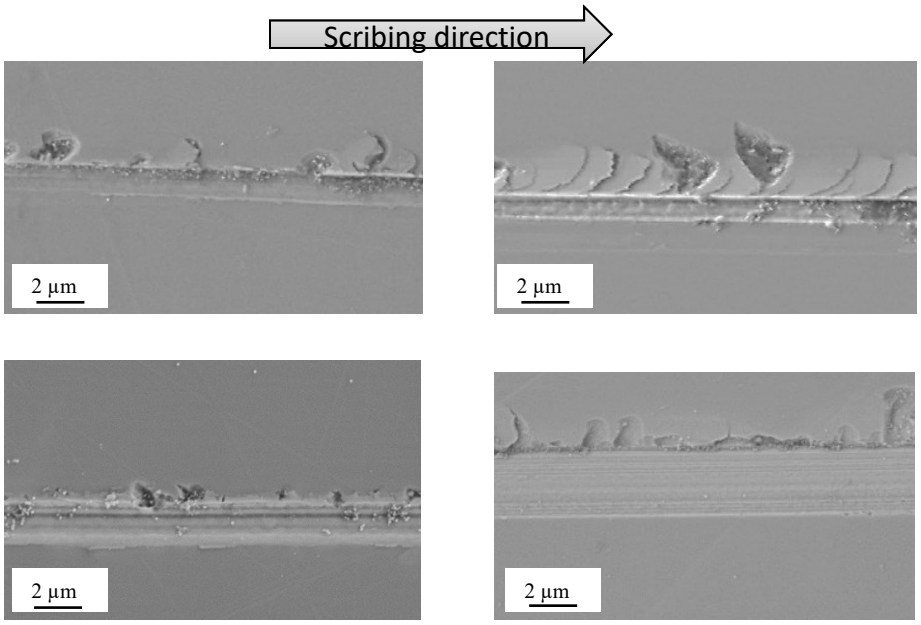

Figure 3.6: SEM of scribes for grit 3 (top row) and grit 4 (bottom row); mono-Si (left) and mc-Si (right). Scribing direction is from left to right.

The scribe depth at which the first crack appeared was designated the critical depth of cut. Figure 3.7 shows that the critical depth of cut varies with grit shape, which affects the stress state. Brittle fracture occurs when the tensile stress reaches the fracture strength of silicon. However, the same material (for example, mono-Si) can reach the critical stress value at different depths of cut depending on the grit shape. The difference in stresses due to grit shape variation is discussed next.

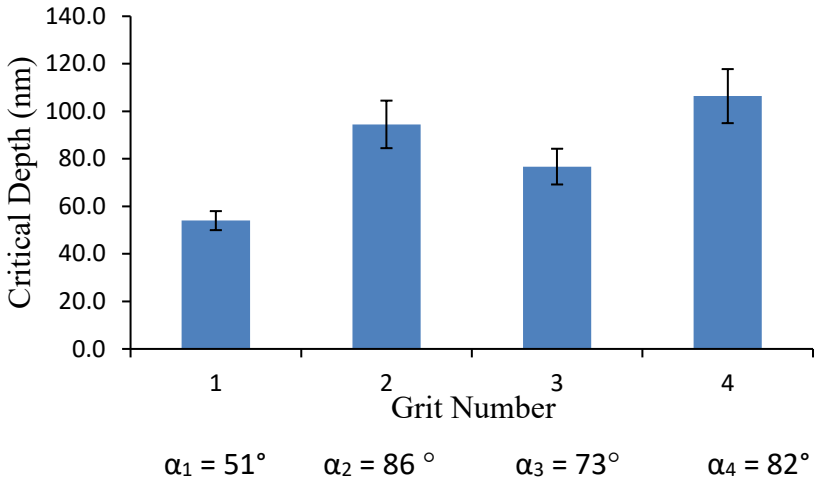

Figure 3.7: Critical depth of cut versus grit shape in mono-Si; α_i refers to the semi-apex angle of grit *i* – it is estimated from the groove cross sectional profile via curve fitting

Prior work explains crack formation due to elasto-plastic behavior of brittle materials when scribing with idealized diamond indenters [32-34]. We use the sliding blister field model of Jing et al. [35], which describes the Boussinesq and Cerruti elastic stress fields and the residual stress field due to plastic deformation. The scratch induced blister field stress depends on the material properties and a grit geometry related factor, which is given by the co-tangent of the semi-apex angle α. The semi-apex angles corresponding to the sampled grit shapes discussed in the current chapter were estimated by curve fitting the 2D cross sectional profiles of the scribes produced by the grits. It can be seen from Figure 3.7 that rounder grits have larger values of α (and smaller values of cot α) and sharper grits have smaller values of α (and larger values of cot α). Keeping all other variables constant, it can be shown from the sliding blister field model that grits with larger α produce lower stresses while grits with smaller α produce higher stresses. This analysis supports the current experimental findings of higher critical depths of cut for

rounder grits (those with larger semi-apex angles) and smaller critical depths of cut for sharper grits (those with smaller semi-apex angles While the stresses depend on the co-tangent of the semi-apex angle, the change in critical depth of cut is not linearly related to cot α because of the effects of other factors such as the increase in area of contact with scribing depth and the anisotropy of silicon.

3.3.2 Effect of Twin and Grain Boundaries

The mc-Si blocks scribed using grits 1 and 2 were etched for 1.5 minutes with 45% by vol. Potassium Hydroxide (KOH) at 55ºC and then rinsed in D.I. water in order to reveal the twin or grain boundaries (GBs) interacting with the scribes. Figure 3.8 shows that the XRD peaks across the boundary have (311) crystallographic orientations, but shifted peaks (approx. 0.6-0.7° shift) indicate that it is a low-angle twin boundary. SEM images show the difference in the brightness contrast on either side of the twin boundary (Figure 3.9).

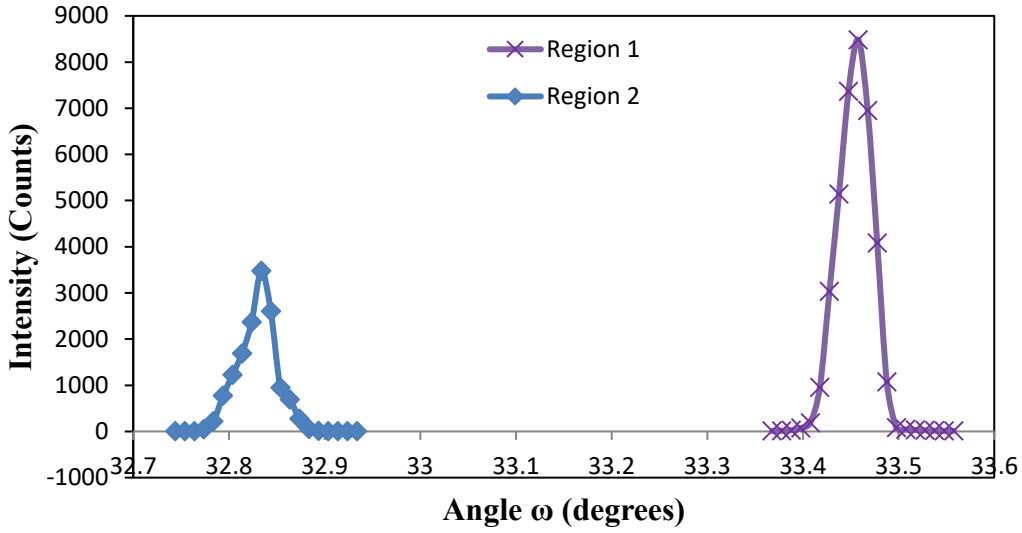

Figure 3.8: XRD for mc-Si regions separated by a twin boundary across which scribing was done.

SEM of the scribed surface reveal changes in the frequency of the chevron-type-radial cracks emanating from the edge of the scribe as it crosses the twin boundary. Specifically, in Figure 3.9, the left (311) grain exhibits more frequent cracks than the right (311). The upper scribe in the figure shows 0.575 cracks/μm to the left of the twin boundary and 0.08 cracks/μm to the right of the twin boundary. The lower scribe shows 0.563 cracks /μm to the left of the twin boundary and 0.22 cracks/μm to the right of the twin boundary. The observed variation in cracking frequency across the twin boundary is attributed to a combination of variation in the local mechanical properties of silicon (e.g. fracture toughness) across the twin boundary [69, 70] *and* dynamic effects associated with scribing across a discontinuity (twin boundary).

We used Vickers micro-hardness indentation technique [116] to determine the fracture toughness. We made 20 indentations on each side of the grain/twin boundary in

the vicinity of the scribe. A 300 gf load was applied for a 15 s duration. Fracture toughness (K_{Ic}) was calculated as [116]:

$$K_{Ic} = 0.129 \left(\frac{c}{a}\right)^{\frac{-3}{2}} \left(\frac{\varphi E}{H}\right)^{\frac{2}{5}} \left(\frac{H a^{\frac{1}{2}}}{\varphi}\right)$$

where φ = constraint factor (~3), E = Young's modulus (GPa), H = Hardness (GPa), a = indent size (μm), and c = crack length (μm).

Using E = 153 GPa for (311) silicon [117], the fracture toughness was found to be 1.03 ± 0.03 MPa √m in Region 1 and 1.21 ± 0.05 MPa √m in Region 2 (see Figure 3.9). Note that the difference in fracture toughness in the two regions is statistically significant at a 95% confidence level. These measurements confirm that Region 1 has a lower threshold for cracking, and hence it exhibits more cracks (see lower edge of scribe) compared to Region 2, which has a higher threshold for cracking and is therefore characterized by fewer cracks. These observations suggest that microstructural defects such as twins can influence the cutting behavior and the resulting surface morphology.

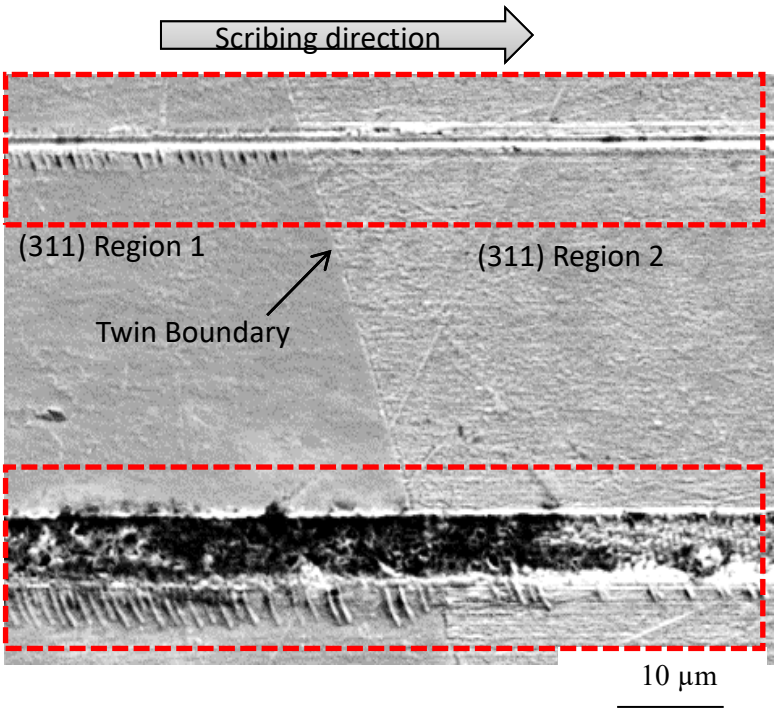

Figure 3.9: SEM of scribe across twin boundary for indicates higher frequency of cracks in (311) to the left of the twin boundary compared to the right.

The results of the effect of twin boundaries prompted another scribing experiment to determine the effect of GBs. A new mc-Si block was first etched to reveal GBs. XRD revealed grain orientations on either side of a selected GB to be (111) and (331). We scribed at a constant programmed depth of 250±40 nm, which is larger than the critical depth of cut, in order to compare the morphology of brittle fracture on either side of the grain boundary. Figure 3.10 shows the scribes across this GB produced by grits 1 and 2.

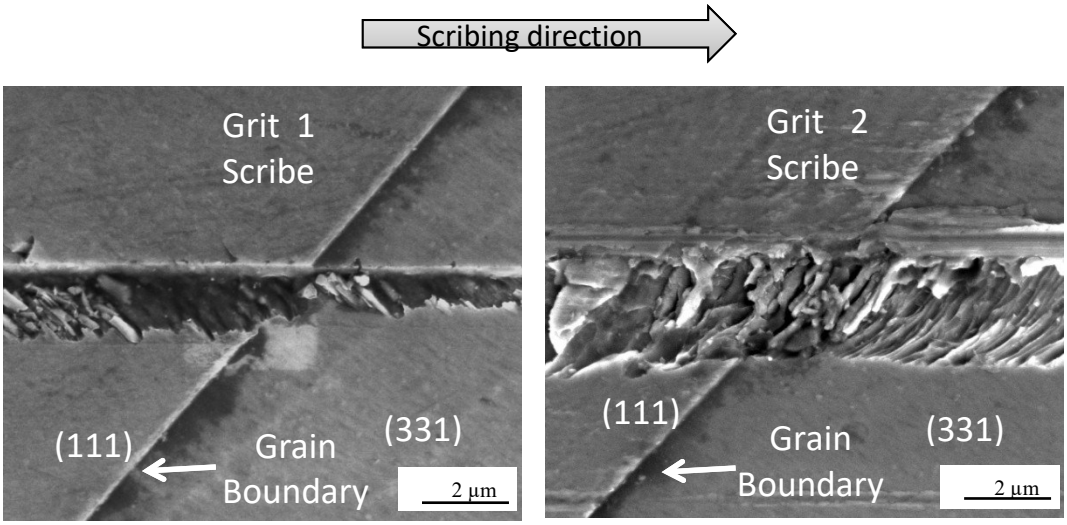

Figure 3.10: SEM of scribe across grain boundary for grits 1 and 2.

Surface cracking behavior changed distinctly as the scribe crossed the GB. For grit 1, chipping was more in the (111) grain than in the (331) grain, which changed the groove width. For grit 2, ridge-like features were observed inside the groove and were more closely spaced in the (331) grain than in the (111) grain; the cracking frequency changed from 0.5 cracks/µm to the left of the grain boundary to 1.2 cracks/µm to the right of the grain boundary. However, away from the GB and in the interior of the grains, the scribe morphology was found to be independent of crystal orientation and more dependent on the grit shape. This agrees with recent findings of Borrero-Lopez et al. [37] who showed that the damage mode in scratching of mc-Si is independent of grain orientation and suggested that GBs may locally change the nature of cracking already initiated, possibly due to deflection of subsurface cracks. SEM imaging was done at 250µm, 500µm and 1000µm distances from the GB on either side. It was found that at a distance of ~1000µm from the grain boundary (right-most images in top and bottom rows in Figure 3.11), the scribe

morphology was different from that observed near the GB, but similar in both grains for a given grit shape (grit 2). We observed similar results for the scribes produced by grit 1. Hence, away from the GB, the effect of grit shape on the scribe morphology appeared to be greater than the effect of grain orientation. A possible explanation for this observation is the variation in the local mechanical properties such as fracture toughness near the GB, which is generally characterized by a higher dislocation density than the grain interior [70]. Vickers indentation based fracture toughness measurements on either side of the grain boundary showed that K_{Ic} = 1.51 ± 0.06 MPa √m in the (111) grain and 1.21 ± 0.05 MPa √m in the (331) grain, with the difference being statistically significant at a 95% confidence level. We used E = 188 MPa for (111) and E = 174 MPa for (331) Si, respectively [117]. As seen in Figure 3.10, cracks are less frequent on the (111) side, which has a higher K_{Ic} value and therefore a higher threshold for cracking, whereas cracks are more frequent in the (331) side, which has a lower K_{Ic}. The seemingly small differences in fracture toughness values for different crystallographic orientations are known to be associated with significant differences in the fracture characteristics [118-121]. In addition to the difference in fracture toughness, other factors such as dynamic effects associated with crossing a GB discontinuity may also play a role in explaining the observations. Our results suggest that the grain boundary modifies the cracking frequency to a lesser extent than the twin boundary. However, further work is necessary before this finding can be generalized to all grain and twin boundaries in silicon. The effect of the variations in cracking frequency across the grain and twin boundaries on the fracture strength of mc-Si wafers needs further investigation. While mc-Si is known to be weaker than mono-Si, the contribution of

cutting-induced damage, such as surface cracks, on the fracture strength of mc-Si is not fully understood.

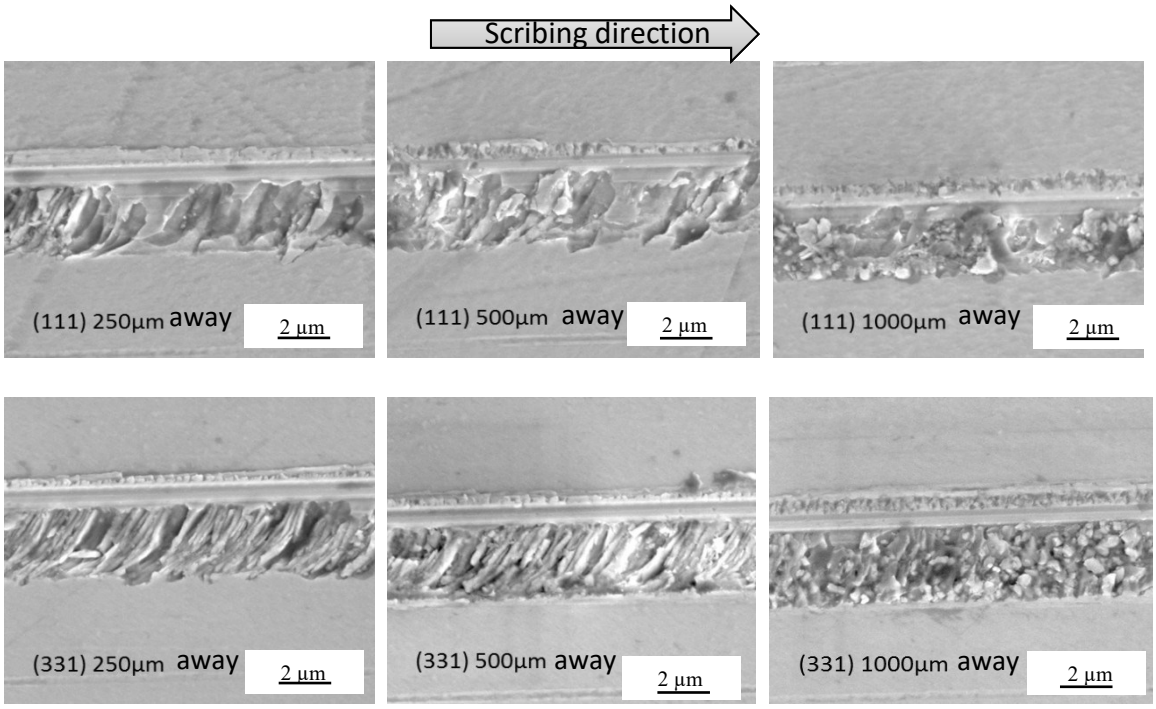

Figure 3.11: For grit 2, scribe morphology away from the grain boundary at 250 µm, 500 µm, and 1000 µm, respectively: for (111) grain (top row) and (331) grain (bottom row).

3.3.3 Subsurface Damage

We performed FIB on scribes by grits 1 and 2 since they had distinctly different shapes, expecting differences in subsurface damage. For both mono- and mc-Si, we did not observe any subsurface damage for grits 1 and 2 in the ductile zone, which was expected as silicon in ductile cutting is plastically deformed without fracture. In the brittle fracture

region, for mono-Si, just after transition from ductile-to-brittle behavior, we observed subsurface cracks for grit 1 (Figure 3.12), lateral cracks that curved upward from the groove bottom, but none for grit 2. A possible reason is that the shape of grit 2 promoted shallow surface cracks within the groove for mono-Si, and no subsurface cracks of discernible length remained. We made 3-5 FIB cuts to confirm repeatability and each cut yielded similar subsurface features.

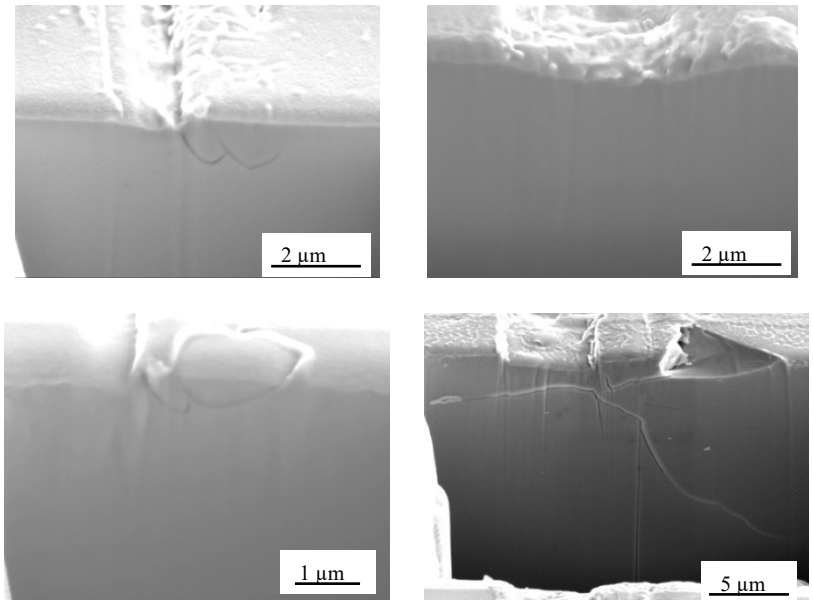

Figure 3.12: Subsurface damage in mono-Si (top row), and multi-Si (bottom row) in the brittle regime for grit 1 (left) and 2 (right).

Scribes made by grit 1 in mc-Si in the brittle region exhibited lateral cracks that branched out from the groove bottom (Figure 3.12). Subsurface crack characteristics for mono and mc-Si are similar for grit 1 with average damage depth of 1.5-2µm. Scribes made by grit 2 in mc-Si in the brittle region showed a complex crack system with average depth

of 5-7 μm, consisting of lateral cracks from either side of the groove and a median crack at an angle to the vertical. The lateral cracks curved towards the top surface and combined with surface cracks, ultimately causing chip-out (Figure 3.12). The median crack was tilted from the vertical due to the non-regular grit shape compared to an idealized-shape indenter. The curling up of cracks for both grit shapes followed the shape of the lateral cracks discussed by Lawn and Swain [27, 29] and Marshall [33], generated during unloading behind the sliding indenter.

Comparing subsurface damage for grit 2 in mono-Si and mc-Si, we observed that crack initiation and propagation were easier in mc-Si than in mono-Si, leading to a larger damage depth. In mono-Si, fewer sites for crack nucleation are present [122], and therefore complex crack systems did not form. Since mc-Si typically has more defects, which can serve as crack nucleation sites, a system of longer cracks formed. Since mono-Si has fewer defect initiation sites, larger tensile stresses would be required to initiate subsurface cracks. Therefore, it is possible that the stress imposed by grit 2 in mono-Si is insufficient to initiate fracture, whereas it may be enough to initiate cracks in mc-Si. Hence, the absence of cracks in mono-Si and the presence of cracks in mc-Si for grit 2 appear to be the result of a combination of factors including the stress state produced by a specific grit shape and differences in material strength. The locations in mc-Si where grits 1 and 2 produce cracks are different and very likely have different defect densities. Thus, even though grit 2 is more round than grit 1, it produces longer cracks in mc-Si.

These observations point toward the potential for engineering grit shapes for slicing of both mono and mc-Si, which can lead to an improved fixed abrasive wire sawing process. In general, at moderate loads, damage can be reduced by employing rounder grits

and ensuring that a sufficient number of them are actively engaged in the cutting process. Given the large number of randomly oriented Si grains present in the multi-crystalline silicon sample, specifying a favorable grain orientation is difficult. The diamond wire can be optimized to be made up of a higher percentage of grits of a certain shape that create a desired system of cracks. For wafering silicon, grits at the kerf bottom can have shapes that promote the formation of median cracks, which would speed up the wafer cutting process. Simultaneously, the grit shape at kerf bottom should be such that it inhibits the formation of long lateral cracks, which become median cracks for wafer surfaces, and cause fracture in Mode I. For kerf sides, grit shape should inhibit lateral cracks thereby reducing material loss from the resulting wafer due to chipping and subsurface damage, and eliminating surface radial-chevron and median cracks that cause surface micro-cracks, which are generally removed by chemical etching. Minimizing micro-cracks can reduce both time and resources required to remove saw damage. Through engineered grits, stronger silicon wafers with smaller micro-cracks can be produced, leading to lower wafer production costs, and in turn lower cost of solar cells.

3.4 Conclusions

Scribing with diamond wire on silicon demonstrated the fundamental effect of shape of actual grits and crystal orientation. The results showed that grit shape significantly affected scribe morphology. While the sharper grit produced radial-chevron cracks, the rounder grit produced horseshoe-like cracks inside the groove. The critical depths of cut differed in the same material as a result of the differences in stress states produced by the different grit shapes. Qualitatively, the same grit shape produced scribes of similar surface morphology in both mono and mc-Si.

In mc-Si, scribing across twin boundaries exhibited differences in cracking frequency. The scribe morphology across GBs changed near the boundary. However, away from the GBs, scribe morphology was more dependent on the grit shape than on crystallographic orientation.

Subsurface damage depended on grit shape and material combination. For both mono-Si and mc-Si, grits 1 and 2 showed no subsurface cracks in the ductile region, which was expected, because of stress-induced plasticity and ductile material removal. In the brittle regime, for grit 1, similar subsurface cracking (lateral) was observed in mono- and mc-Si; for grit 2, no subsurface damage was found in mono-Si, whereas a complex system of angled median and lateral cracks formed in mc-Si. This result was attributed to more defect sites in mc-Si, which enable subsurface cracks to initiate easily at lower stress levels.

CHAPTER 4. EFFECT OF WEAR OF DIAMOND WIRE ON SURFACE MORPHOLOGY, ROUGHNESS AND SUBSURFACE DAMAGE OF SILICON WAFERS

Wear of fixed abrasive diamond wire affects the quality of sliced silicon wafers, necessitating replacement of the costly wire. This chapter analyzes the effect of wire wear on the surface morphology, roughness, and subsurface damage of as-cut single crystal silicon wafers. Scanning electron microscopy, Raman spectroscopy, confocal microscopy, focused ion beam machining (FIB), and biaxial flexure are used to evaluate the surface morphology, areal surface roughness, and subsurface damage (cracks).

4.1 Introduction

Silicon wafers for photovoltaic solar cells are manufactured by wire sawing processes, which slice mono-crystalline silicon ingots produced by the Czochralski (Cz) process or multi-crystalline silicon produced by the casting process. In recent years, there has been a shift from loose abrasive slurry wire sawing (LAS) to fixed abrasive diamond wire sawing (DWS), a trend that is forecast to grow [3]. While LAS involves cutting silicon by the abrasive action of loose silicon carbide (SiC) particles in a polyethylene glycol based slurry poured onto a stainless steel wire web, DWS uses diamond grits fixed to the steel wire with electroplated nickel or resin as the bonding agent, and a water based cutting fluid. DWS is advantageous over LAS as it provides increased material removal rate and lower silicon loss due to a smaller kerf. LAS involves three-body abrasion [4, 17, 72] of the wire,

SiC grit, and silicon, leading to wear of the wire core. In comparison, DWS involves material removal by a two-body abrasion mechanism where the core metal wire is less likely to be worn. Other multi-wire sawing processes involve abrasive based electrochemical methods [73], and resinous diamond wire [74]. In a previous study, electroplated diamond wire manufactured by felt brushes showed better wear resistance [75]. The phenomenon of diamond wire break-in during initiation of cutting and its effect on process performance has been studied recently [76]. Related work on the prediction of diamond wire wear [77] and lifetime estimation has been also reported [78]. High stresses in cutting brittle materials by diamond wire has been shown to induce graphitization of the diamond abrasives [79]. Other studies of cutting single crystal silicon with diamond tools have shown tool wear to influence the nanoscale ductile cutting behaviour of silicon [80]. In particular, groove wear in nanometric cutting was found to be significant [81, 123, 124]. Diamond tool wear is also known to be affected by its crystallographic orientation [86].While only indirectly related to diamond wire sawing, ductile material removal mechanisms active during abrasive and chemical mechanical polishing (CMP) of silicon wafers have been studied extensively [42, 72, 125-128]. Micro-contact modelling approaches have been used to study wear in CMP [129].

For DWS to be a commercially viable alternative to slurry sawing, DWS has to produce silicon wafers with the required mechanical integrity and strength without increasing cost. Mechanical properties of sliced silicon wafers depend on the wafer surface and subsurface condition [10, 130]. The surfaces of as-cut wafers have saw damage in the form of grooves, pits, and micro-cracks [10, 131-133]. To reduce the cost of saw damage removal, wafers with minimal surface and subsurface damage are needed. The surface and

subsurface damage depend on the condition of the diamond grits. The diamond grits undergo wear due to the high speed sliding contact of the wire with silicon. Thus, the surface and subsurface conditions of as-cut silicon wafers depend on wear of the diamond wire. This chapter investigates the effects of diamond wire wear on the surface morphology, surface roughness, and subsurface damage of full-size silicon wafers.

4.2 Experimental Details

Mono-crystalline silicon wafers of (100) crystal orientation, and 125 mm X 125 mm size and 195-200 μm thickness were cut in a reciprocating multi-wire saw using the slicing conditions listed in Table 4.1. As shown schematically in Figure 4.1 [8], the new wire spool feeds unused diamond wire into the wire web, which consists of a wire wound in parallel over rollers. The silicon brick is fed into the wire web, thus slicing it into multiple thin wafers. The used wire is taken up by the worn wire spool on the other side.

Table 4.1: Wafer slicing conditions

Parameter	**Condition**
Workpiece	(100) mono-crystalline silicon cut into 700 wafers
Wire	Ni-electroplated diamond wire with 100 μm diameter core wire and 8-12 μm diamond grits
Wire speed	18 m/sec
Feed rate	0.8 mm/min
Reciprocation	500 m forward, 490 m backward

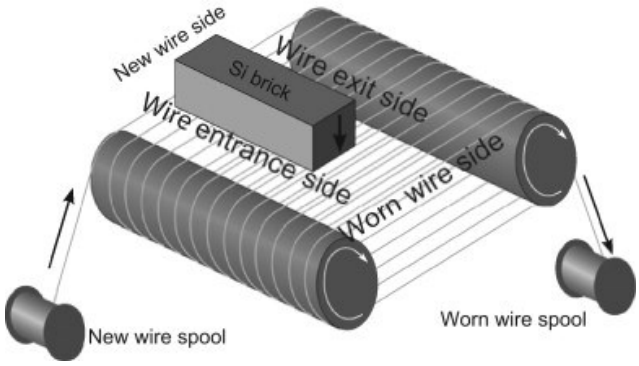

Figure 4.1: Slicing of a silicon brick using fixed abrasive diamond wire sawing [8].

A single continuous wire was used to cut the wafers from a single silicon brick. In the present study, the sliced wafers were divided into groups based on wire wear. The wear condition of the wire was defined using the contact length, which represents the length of

silicon that has interacted with the wire during the slicing process. The contact length depends on the number of times the wire moves forward and back, from the first wafer to the last wafer cut from the ingot. It is also a function of the new wire feed, the distance between the workpiece and roller, ingot length, pitch distance of the wire web, and the number of wafers cut in each forward stroke. In the present study, the cumulative silicon contact length for wafers cut by the new wire was less than 1 km whereas the cumulative silicon contact length for the used wire was approximately 12 km. Representative sections of the new and used wire were extracted for analysis.

Wafers cut by the new and used wire sections were examined in a scanning electron microscope (Hitachi SU8230 SEM) to analyze the surface morphology and material removal characteristics. Raman spectroscopy of the cut wafers was done using a dispersive Raman spectrometer (Thermo Nicolet Almega XR). Areal three-dimensional average surface roughness of the two wafer groups was measured using a laser confocal microscope (Olympus LEXT). Subsurface damage was analyzed in a SEM (FEI NOVA) using focused ion beam (FIB) cross sectioning of the wafer surfaces at selected locations. Wear of the diamond wire was analyzed in a SEM (Zeiss Ultra-60).

4.3 Results and Discussion

4.3.1 Surface Morphology

Representative images of the as-cut wafer surface morphology along with the corresponding Raman spectra are shown in Figure 4.2. It can be seen that wafers cut by the new wire show greater evidence of brittle fracture, which is characterized by frequent chipping and fractured grooves. In contrast, wafers cut by the used wire show more ductile

removal characteristics, which consist of smoother sawing marks with some intermittent chipping, albeit few in number. Diamond wire sawing of silicon is known to be characterized by a mixture of ductile material removal and brittle fracture [10]. Silicon is a brittle material, which, when subjected to compressive stress, undergoes pressure induced phase transformation from crystalline Si-I phase to β-Sn and other metal-like phases, which give rise to ductile cutting [40, 51]. The stress condition varies at each abrasive grit-material interaction point, and hence a *mixture* of ductile cutting and brittle material removal occurs. Based on the results in Figure 4.2, we can hypothesize that the stress conditions for the new wire were such that brittle fracture was more dominant compared to the worn wire case. The corresponding Raman spectra showed a dominant crystalline silicon peak at 520 cm^{-1} and very weak peaks of phase transformed silicon. In comparison, the wafers cut by the used wire showed stronger peaks of phase transformed silicon in addition to the 520 cm^{-1} peak. The Raman spectra support the surface morphology observations that wafers cut by the used wire have more ductile regions compared to wafers cut by the new wire. These observations were found to be repeatable at three different points on each wafer examined.

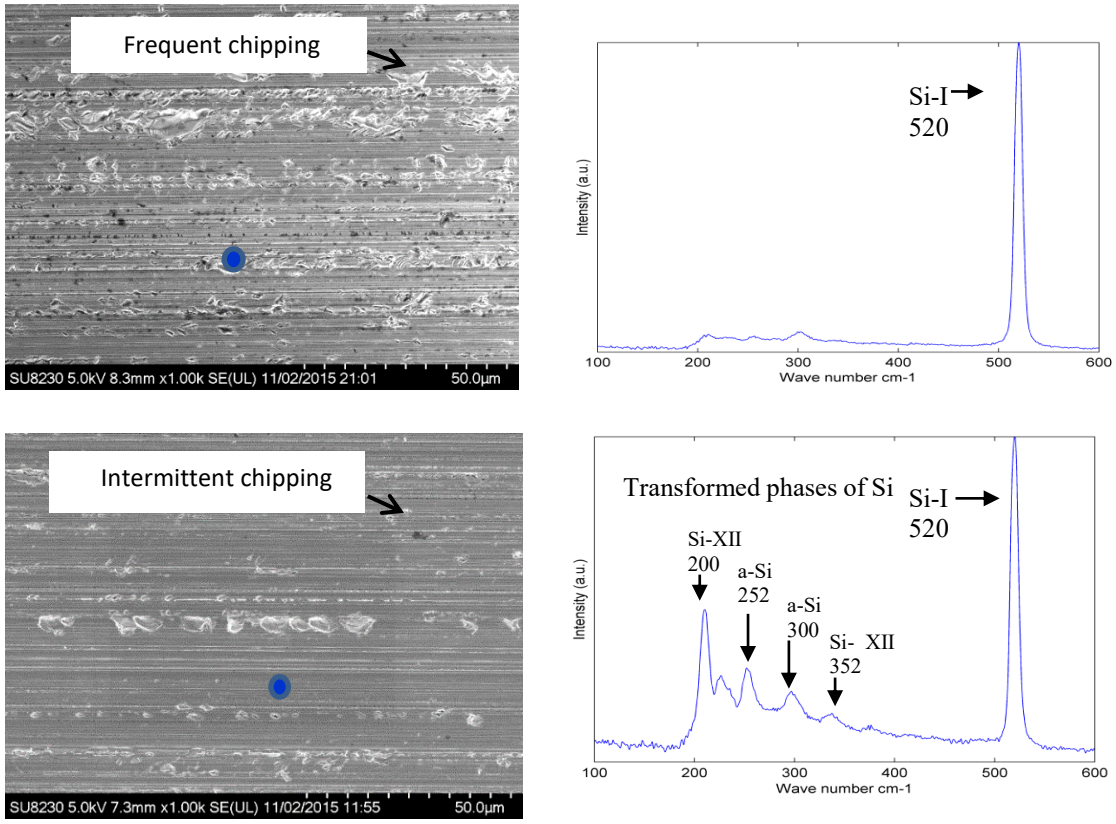

Figure 4.2: Surface morphology and corresponding Raman spectra of wafers cut by new (top) and used (bottom) sections of the diamond wire.

4.3.2 Surface Roughness

Three dimensional (3D) areal surface roughness parameter measurements (S_a) were taken at fifteen locations on the wafer surfaces using a 5 x 3 grid (130 µm X 130 µm evaluation area for each location) and averaged. Results (see box plot in Figure 4.3) show that wafers cut by the new wire have higher average 3D areal surface roughness (0.22 µm) than wafers cut by the used wire (0.16 µm). The middle line in the box shows the median, the upper limit shows the upper quartile (25% of values are higher than the upper quartile), and the lower limit shows the lower quartile, with the ends of the whiskers indicating the

maximum and minimum values [134]. The results agree with the surface morphology observations, which showed that wafers cut by the new wire showed more brittle fracture and chipping, and are therefore expected to have higher roughness than wafers cut by the used wire, which exhibit more ductile behavior. Note that the roughness of wafers cut by the new wire shows more scatter, which is also indicative of random brittle fracture, versus a *tighter* roughness distribution for the wafers cut by the used wire.

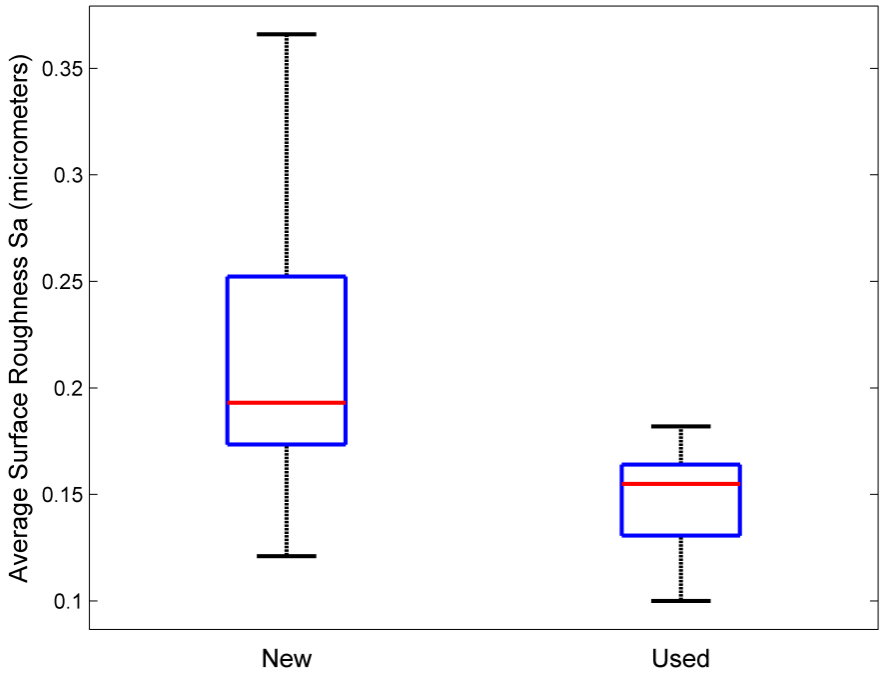

Figure 4.3: Box plot of surface roughness of wafers cut by new and used wire.

4.3.3 Subsurface Damage

Subsurface damage was analysed by cross sectioning the wafers perpendicular to the sawing marks using FIB sections made at 10 locations on the wafer. Figure 4.4 and

Figure 4.5 show representative images of the subsurface damage in wafers cut by the new and used wire sections, respectively. For wafers cut by the new wire, 9 out of 10 locations showed micro-cracks, whereas in wafers cut by the used wire, only 4 out of 10 locations showed subsurface cracks. Counting the number of cracks per unit length, we found wafers cut by the new wire had 0.10 cracks/μm versus 0.05 cracks/μm in wafers cut by the used wire. The subsurface cracks in wafers cut by the new wire (see Figure 4.4 were mostly lateral cracks, with a few median cracks, of 0.6 μm mean depth and 1.5 μm maximum depth. In wafers cut by the used wire (see Figure 4.5), the subsurface damage consisted of mostly median cracks (inclined and perpendicular to the surface), with a mean depth of 0.7 μm and a maximum depth of 2 μm. The box plot Figure 4.6 shows that the mean depth of damage in the two cases are similar, however the scatter is greater in the wafers cut by the used wire compared to the new wire case. A 2-sample t-test of the difference in mean crack depths for the new and used wire cases was found to be statistically insignificant at a 95% confidence level. However, lateral cracks tend to produce shallow chipping of the wafer surface, whereas median cracks make the wafer more prone to fracture under bending. Hence, even though the number of subsurface cracks in the wafer cut by the used wire is lower, the median/inclined crack geometry makes it more likely to fracture during subsequent handling and processing operations.

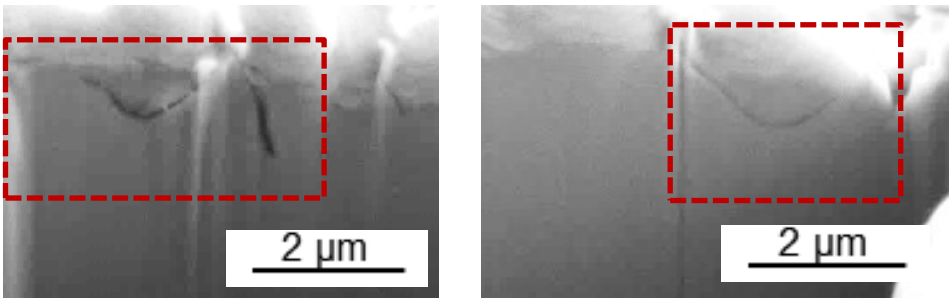

Figure 4.4: Subsurface damage in wafers cut by the new section of diamond wire; shows curved lateral cracks in most locations. The red boxes highlight the cracks.

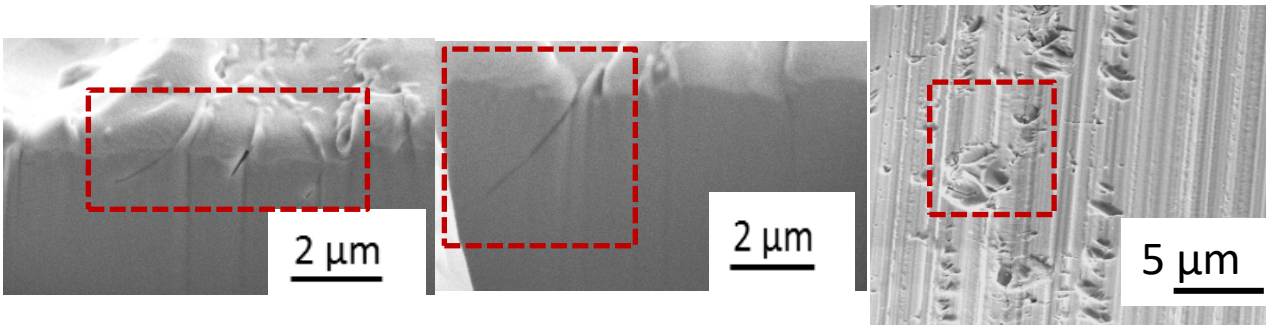

Figure 4.5: Subsurface damage in wafers cut by the used section of diamond wire; shows minimal damage in some locations but inclined median cracks in other locations. The red boxes highlight the cracks. Image of the wafer surface shows indentation type features below which the median cracks were observed.

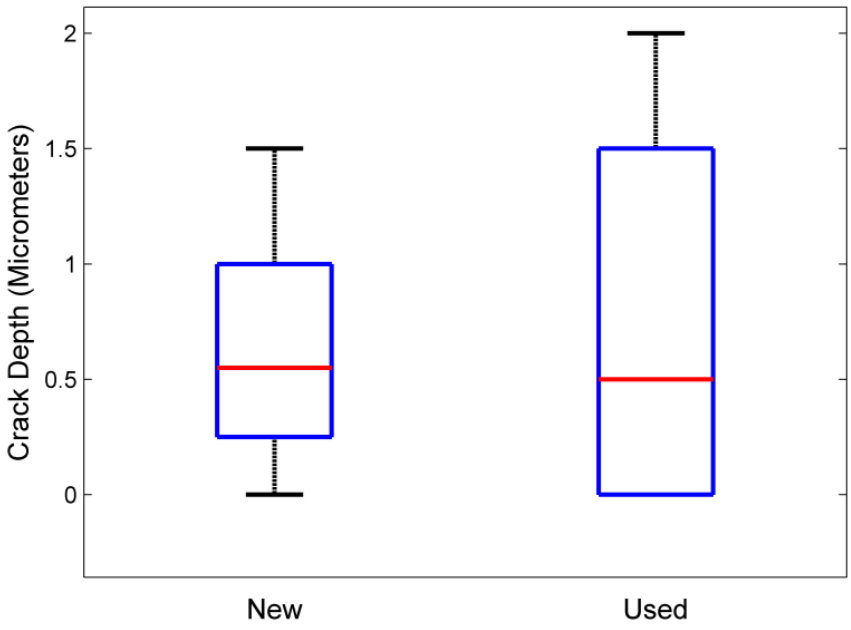

Figure 4.6: Comparison of crack depths in wafers cut by the new and used wire.

4.3.4 Wire Wear

The new and used sections of the diamond wire were imaged in a SEM. Multiple grits (~10) were imaged, but only representative images are shown. Figure 4.7 shows abrasive grit images taken from the new wire section. Figure 4.7(a) shows a grit with some nickel coating still on it, while Figure 4.7(b) shows an exposed grit. The electroplated nickel coating on the abrasives is removed during initial contact with silicon since nickel (Mohs hardness of 4) is softer than silicon (Mohs hardness of 6-7). The exposed grits in the new wire are mostly intact since the new wire section has had *limited contact* with the silicon.

As the diamond wire cuts more silicon, the grits become blunt and round due to wear (see Figure 4.8(a)), and in some cases, due to chipping of the diamond grit (see Figure 4.8(b)). The grit and silicon contact conditions are sometimes extreme due to the small area of contact. Depending on the load acting on the abrasive, there could be rubbing, ploughing, ductile material removal, or brittle fracture of silicon. Ductile material removal can be achieved through a combination of depth of cut, cutting edge radius, which is influenced by wear of the abrasive, and the force acting on the grit [135, 136].

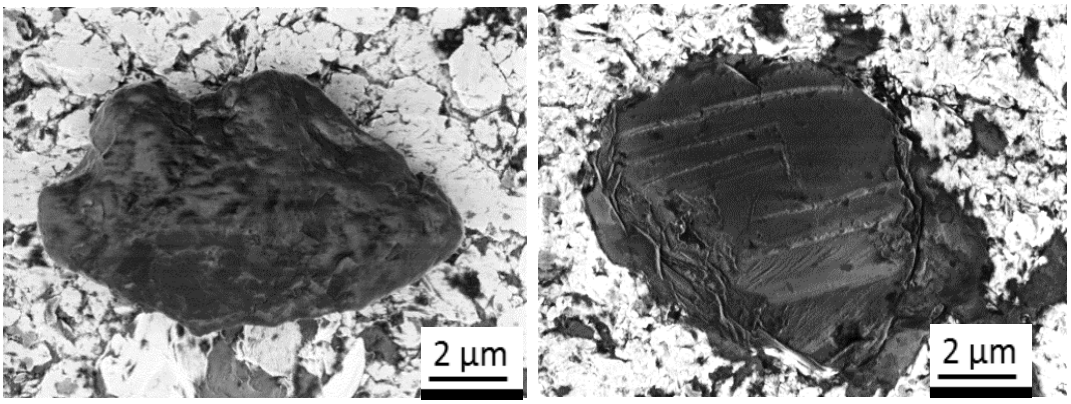

(a) (b)

Figure 4.7: Representative images of the abrasive grit in the new wire section: (a) grit with some nickel coating remaining, and (b) completely exposed grit.

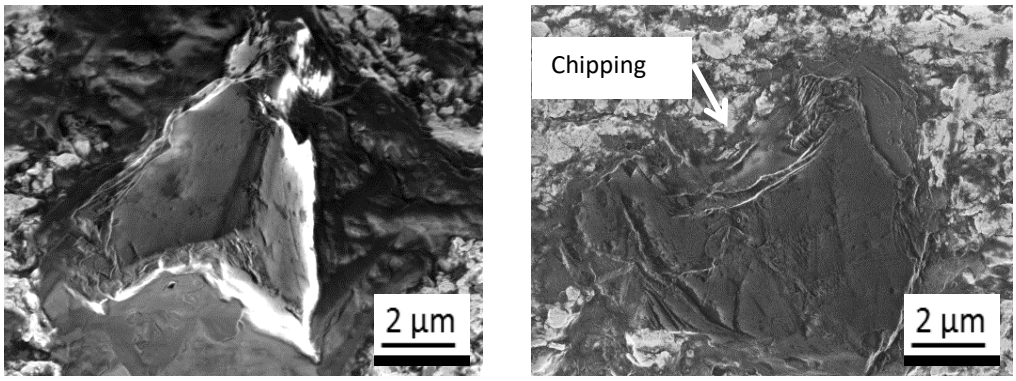

(a) (b)

Figure 4.8: Representative images of abrasive grit in the used wire section: (a) rounding of sharp edges, and (b) chipping and fracture of abrasive.

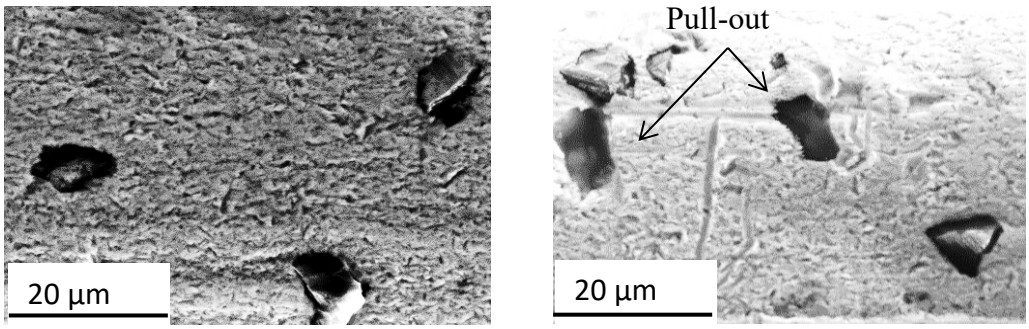

(a) (b)

Figure 4.9: (a) Grits embedded in nickel coating in the new wire, (b) evidence of grit pull-out in the used wire.

The force acting on the grit not only affects the surface and subsurface damage caused in the wafers but also the mechanical integrity of the abrasive. While the new wire shows that diamond grits are still embedded in the nickel coating (see Figure 4.9(a)), a sufficiently high grit force can cause the grit to be dislodged from the nickel binder leading to ‘grit

pull-out', as seen in Figure 4.9(b). We hypothesize that the dislodged abrasives tend to roll around in the cutting channel, and sometimes indent the silicon surface, thereby causing intermittent chipping or the indentation pits seen on the surface of wafers cut by the used wire (see Figure 4.2). Another likely source of the indentations formed on the wafer surface is wire vibration during sawing, which can cause diamond grits still fixed to the wire to indent the silicon surface. The subsurface median cracks observed in the FIB images in the used wire case were found to be in the vicinity of the indentation marks seen on the wafer surface (as shown earlier in Figure 4.5). Median crack systems are known to form in indentation [30, 32, 34], which could potentially explain the wafer fracture strength results presented in the next section.

Note that the FIB cross-sections view a very small volume of material (on the order of tens of μm^3) while the fracture strength experiments employ a larger volume of the silicon (on the order of tens of mm^3). Furthermore, since failure of brittle materials is governed by Weibull's weakest link theory of fracture [137], it is highly probable that the wafer coupons used in the fracture strength tests contain a longer crack than seen in the FIB cross-sectional images. This explains the lower fracture strength of wafers cut by used wire. While it is known that phase transformation of silicon is accompanied by volume expansion [138] and corresponding residual stress generation [51], their effect on fracture strength of silicon needs further investigation.

Figure 4.10 shows the EDS results from a region surrounding a representative grit in the used wire. This shows evidence of silicon debris embedded in the nickel coating. The cutting ability of the wire tends to decrease with increased debris loading of the wire.

This phenomenon is analogous to loading of an abrasive grinding wheel, which tends to lower grinding performance.

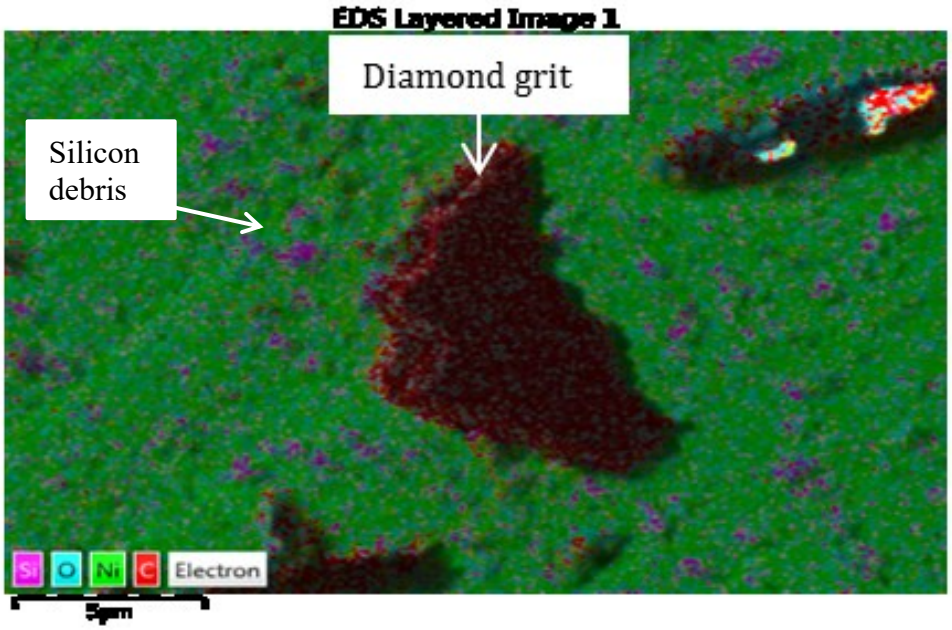

Figure 4.10: EDS spectra showing silicon embedded (pink) in nickel coating (green).

4.3.5 Fracture Strength of Wafers

The fracture strengths of wafers corresponding to the new and used sections of the diamond wire were evaluated using the biaxial flexure method [139]. Circular coupons 35 mm in diameter were laser-cut from the wafers. Care was taken to ensure that there was minimal edge damage due to laser cutting. The biaxial flexure test apparatus consisted of a ring-on-ring fixture with a loading diameter of 9.5 mm and a supporting diameter of 20 mm. Twenty three (23) coupons each were taken from wafers sliced by the new and used wire sections and fractured to obtain the fracture strength data shown in Figure 4.11. It can be seen that the mean fracture strength decreased with wire wear. The difference in the

mean strengths of the coupons cut by the new and used wire sections was statistically significant at a 95% confidence interval. The reduction in the mean fracture strength with wire wear is attributed to the presence of median cracks in the wafers cut by the used wire.

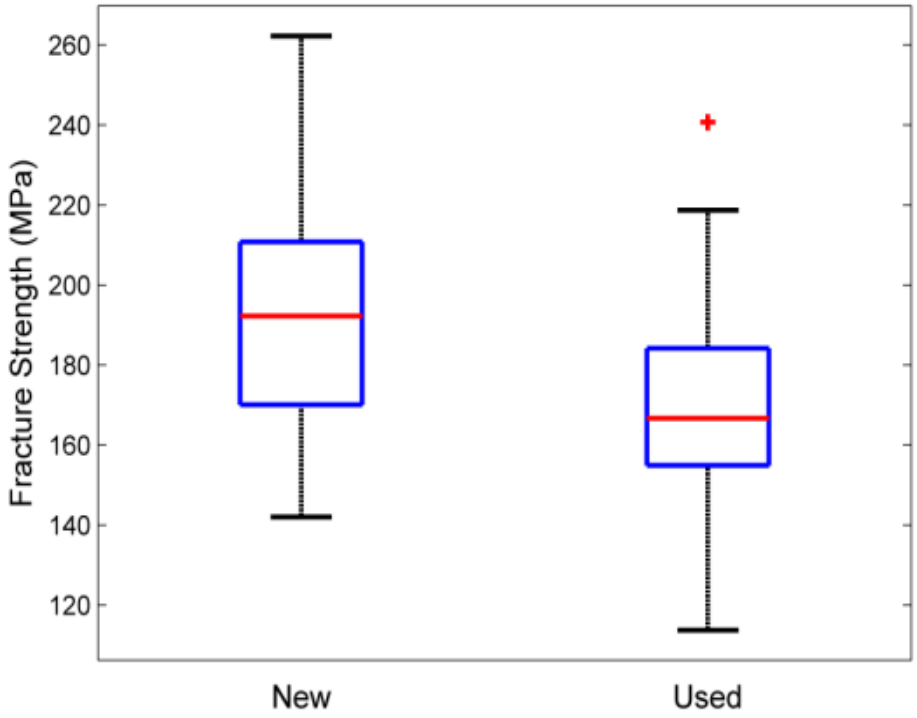

Figure 4.11: Biaxial fracture strength of wafers cut by new and used wire sections.

4.4 Conclusions

The chapter analyzed the effects of fixed abrasive diamond wire wear on the surface morphology, roughness, and subsurface damage of (100) mono-crystalline silicon wafers. With wire wear, the wafer surface morphology changed from mostly brittle fracture, which was characterized by frequent chipping and fractured grooves, to more ductile cutting, which was characterized by relatively smooth grooves with intermittent indentations. The average surface roughness and its scatter decreased with wire wear. Analysis of subsurface

damage showed that wafers cut with the new wire had more subsurface lateral cracks per unit length than wafers cut with the used wire; however wafers cut with the used wire had comparatively more median cracks, which were produced by the occasional indenting action of loose diamond abrasives dislodged from the diamond wire and moving freely in the kerf. With wire wear, the abrasive grits showed rounding and blunting, with some instances of grit fracture and pull-out. The mean fracture strength of the wafers was lower with wire wear and is attributed to the presence of median cracks, which promote failure of the wafer at a lower stress level. The results reported in this chapter provide useful insights into the wear of fixed abrasive diamond wire and its effect on the topographical and mechanical properties of solar silicon wafers.

CHAPTER 5. WEAR OF DIAMOND IN SCRIBING OF MULTI-CRYSTALLINE SILICON

This chapter investigates the wear of diamond in scribing multi-crystalline silicon. A practical challenge in slicing of low-cost multi-crystalline silicon (mc-Si) wafers by the fixed abrasive diamond wire sawing process is increased wire consumption due to greater wear of the diamond compared to slicing of the more expensive mono-crystalline silicon (mono-Si) wafers. In this chapter, we present the results of scribing of mc-Si and mono-Si materials with two conical tip diamond indenters of the same geometry to understand the possible reasons for increased diamond wear in cutting of multi-crystalline silicon. Specifically, the scribing forces and the diamond indenter wear produced in scribing of the two silicon materials are analyzed. The results show that the forces generated in scribing of mc-Si are higher than in scribing of mono-Si. The higher forces in scribing of mc-Si are consistent with the corresponding higher tip radius of curvature (due to wear) of the diamond indenter compared to the tip radius produced in scribing of mono-Si. Scanning electron microscopy and confocal microscopy of the diamond indenters show that wear is primarily due to physical micro fracture and blunting of the diamond. Raman spectroscopy shows evidence of stress-induced phase transformation of the diamond and the formation of compressive residual stress in the diamond. Plausible physical explanations for the wear of diamond during scribing, including the role of material inhomogeneity, are given.

5.1 Introduction

Crystalline silicon solar cells offer an optimum mix of modularity, distributed grid, and lower capital investment compared to other renewable and clean energy sources [1]. However, the cost of energy per kWh from photovoltaic solar cells is still high compared to conventional energy resources. Cost can be reduced by using multi-crystalline silicon (mc-Si) for the silicon wafer substrates, which is cheaper than mono-crystalline silicon (mono-Si) [6, 13, 140]. The reduction in energy conversion efficiency of mc-Si (compared to mono-Si) is offset by the lower substrate cost for many applications [6]. However, there are challenges in manufacturing mc-Si wafers by the state-of-the-art fixed abrasive diamond wire sawing process.

In recent years, industry has transitioned from conventional loose abrasive slurry sawing (LAS) to fixed abrasive diamond wire sawing (DWS) for slicing silicon wafers because of the higher productivity, lower kerf loss, and reduced environmental impact of the DWS process [16, 23]. Material removal in DWS occurs via mechanical interaction of the diamond abrasives (~10 μm in size) bonded to the steel wire by electroplated Ni with the silicon brick [9]. While the use of DWS to slice mono-Si wafers is quite widespread in industry, it is not widely used to slice mc-Si wafers. The primary reason for this is the higher consumption of the more expensive diamond wire when slicing mc-Si than in slicing of mono-Si. It has been reported that more new wire has to be continuously fed into the active cutting zone in diamond wire sawing of mc-Si to ensure cutting effectiveness and to prevent wire breakage and resulting loss of productivity [15]. This suggests that wear of the diamond wire is greater when cutting mc-Si than when cutting mono-Si. This is likely due to the differences in material properties of mono- and mc-Si. Multi-crystalline silicon

is characterized by greater material inhomogeneity compared to the more uniform mono-Si material, and this inhomogeneity is expected to influence the wear behavior of diamond abrasives [13, 70, 71, 141-143].

Prior work on the wear of diamond wire in slicing of mono-crystalline silicon shows that it is characterized by blunting, brittle fracture, and pull-out of diamond grits from the electroplated Nickel coating on the stainless steel wire [9]. During initiation of the cutting process, 'break-in' of the diamond occurs [76]. Limited evidence of graphitization of diamond attributed to the high stresses acting on the diamond wire when slicing mono-Si has been reported [79]. Wear of diamond due to tribologically induced phase transformation has been reported [144]. Wire dynamics and spooling of the wire can also scratch the electroplated nickel coating, which can be prevented by recently developed wire spooling solutions [82]. Based on the wire sawing conditions used, researchers have shown reduction in the diamond density with increase in contact length [77]. Studies of single crystal diamond tool wear in machining (turning) of semiconductor grade mono-Si material show that gradual wear of the single crystal diamond tool occurs in ductile mode cutting while micro-chipping of the diamond occurs in brittle mode cutting [85]. Wear of diamond during die separation of microelectronics MEMS devices has been also reported [83]. The crystallographic orientation of single crystal diamond tools is known to influence the wear of diamond tools, as seen in prior studies of diamond turning [86], and in scratching with diamond tools of specific crystallographic orientations [87]. However, the crystal orientations of diamond grits in a fixed abrasive diamond wire are not controlled, especially since the grits are produced by milling of natural or synthetic diamond. Molecular Dynamics (MD) simulations of scratching of a softer material such as silica have shown

the wear of diamond to be due to the breaking of C-C bonds [88], which is attributed to mechano-chemical mechanisms of wear. Wear of a diamond AFM tip when sliding on softer silicon has been reported [90]. In nanoscale cutting of silicon wafer by diamond turning, XPS analysis of the cut grooves revealed the formation of silicon carbide and diamond-like carbon particles with corresponding scratching and grooving wear of the diamond tool [84]. MD simulations of single point diamond turning of silicon also suggested the formation of silicon carbide [91]. However, Raman spectroscopy of abrasive grits used in the diamond wire sawing of silicon have not shown any evidence of silicon carbide formation [79].

The existing knowledge of diamond wear in scribing and diamond turning of silicon is not adequate to explain the higher wire consumption in fixed abrasive diamond wire sawing of mc-Si compared to sawing of mono-Si. Hence, an investigation of diamond wire wear in scribing of multi-crystalline silicon is needed.

This chapter analyzes the wear of a diamond indenter in scribing of mc-Si through constant depth of cut scribing experiments. For comparison, scribing experiments on mono-Si material are also analyzed. In the next section, the experimental details of the study are presented. This is followed by the results and discussion. The chapter concludes with a summary of the key findings.

5.2 Experimental details

Mono- and mc-Si blocks (25 mm × 10 mm × 10 mm) with mirror polished (0.054 ± 0.015 μm) parallel and flat surfaces were used as substrates in the diamond scribing experiments. Scribing experiments serve as lab-scale models of the actual diamond wire

sawing process, which slices silicon through a mix of ductile and brittle material removal mechanisms [23, 55, 145]. To compare the wear of diamond due to differences in the structure and properties of mono and mc-Si, we used two 120° included angle diamond tipped conical indenters (J&M Diamond Tools) with nominally identical geometries. The cone angles of the indenters used are representative of the actual abrasives in the fixed abrasive diamond wire [141].

All scribes were 20 mm in length and were made under dry ambient conditions at a constant depth of 10 μm and a scribing speed of 100 mm/min (Figure 5.1a). Since the focus of the chapter is on understanding the effect of the material (mc-Si versus mono-Si) on diamond wear, the scribing speed was not varied. The silicon blocks were fixed to a flat aluminum baseplate bolted to a three-component piezoelectric force dynamometer (Kistler 9256C), which was mounted on a computer-controlled X-Y-Z motion platform (Aerotech ANT-4V) (Figure 5.1b). The force dynamometer detected the initial contact of the scriber tip with the silicon surface, and measured the instantaneous X-Y-Z forces produced during scribing.

We inspected the diamond indenters in a confocal microscope (Olympus LEXT), which was used to measure the radius of curvature of the indenter tip at regular intervals during scribing. The diamond indenters were imaged using a scanning electron microscope (Hitachi 8230 SEM). Each indenter was imaged after scribing distances of 0 mm (new), 140 mm, 200 mm, 260 mm, and 320 mm. Care was taken to ensure that the same face of the indenter was used to generate the entire scribe and this same face was inspected. Raman spectroscopy was performed on the diamond tips using a Thermo Fischer Raman spectrometer to detect stress-induced phase transformation and graphitization during the

scribing process. The excitation wavelength of the laser in the Raman spectrometer was 785 nm with a surface penetration of ~0.5-0.6 µm, estimated spot size of 1.6 µm and a spatial resolution of ~1 µm, which is smaller than the radius of curvature of the diamond tips. An objective of 50X was used to collect data, with scans from 736 to 1790 cm^{-1}. The Raman laser's exposure time was 5 seconds, with 5 sample exposures used to average the data for each point investigated.

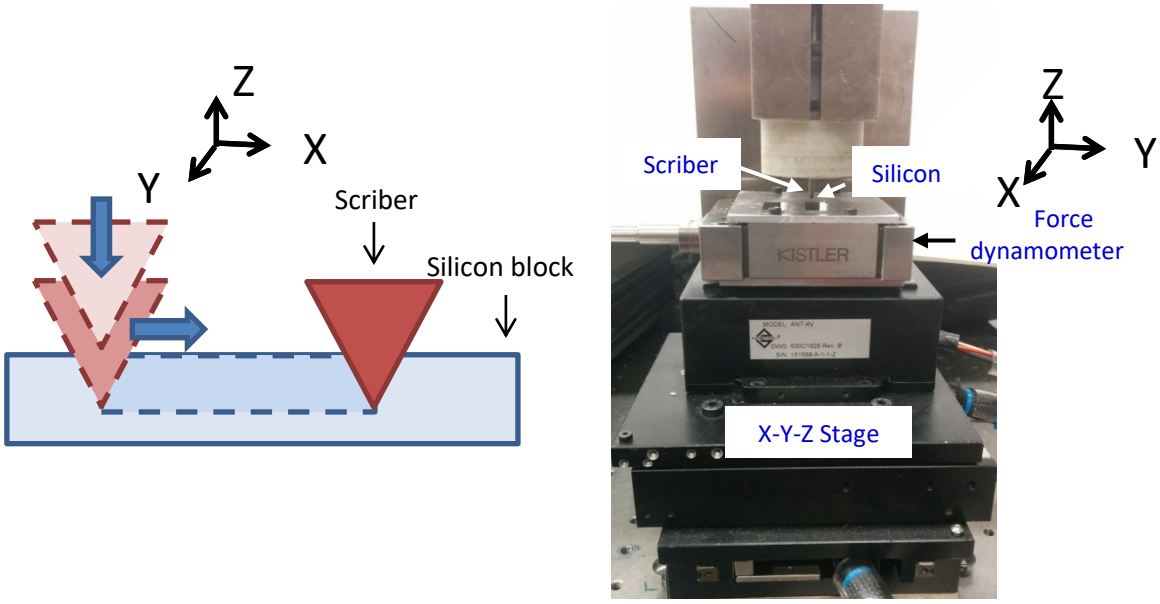

(a) (b)

Figure 5.1: (a) Scribing of silicon by diamond tipped indenter, (b) Scribing setup.

5.3 Results

A comparison of the average resultant force obtained in each scribe produced in the two materials is presented first, followed by analysis of the observed diamond indenter wear behavior.

5.3.1 Comparison of Forces

The average resultant force for mc-Si and mono-Si are shown as a function of the distance scribed in Figure 5.2a. It can be seen that the average resultant force for mc-Si is almost always higher than for mono-Si. Figure 5.2b shows a box plot of the measured resultant force for the two materials. It can be seen that scatter is larger for mc-Si than for mono-Si, which is indicative of the greater inhomogeneity in material properties of mc-Si due to the presence of grain and twin boundaries, and inclusions [13]. The median force for mc-Si is also higher than for mono-Si for the same scribing conditions. The differences in the mean scribing forces are attributed to differences in the material properties of mono and mc-Si [146].

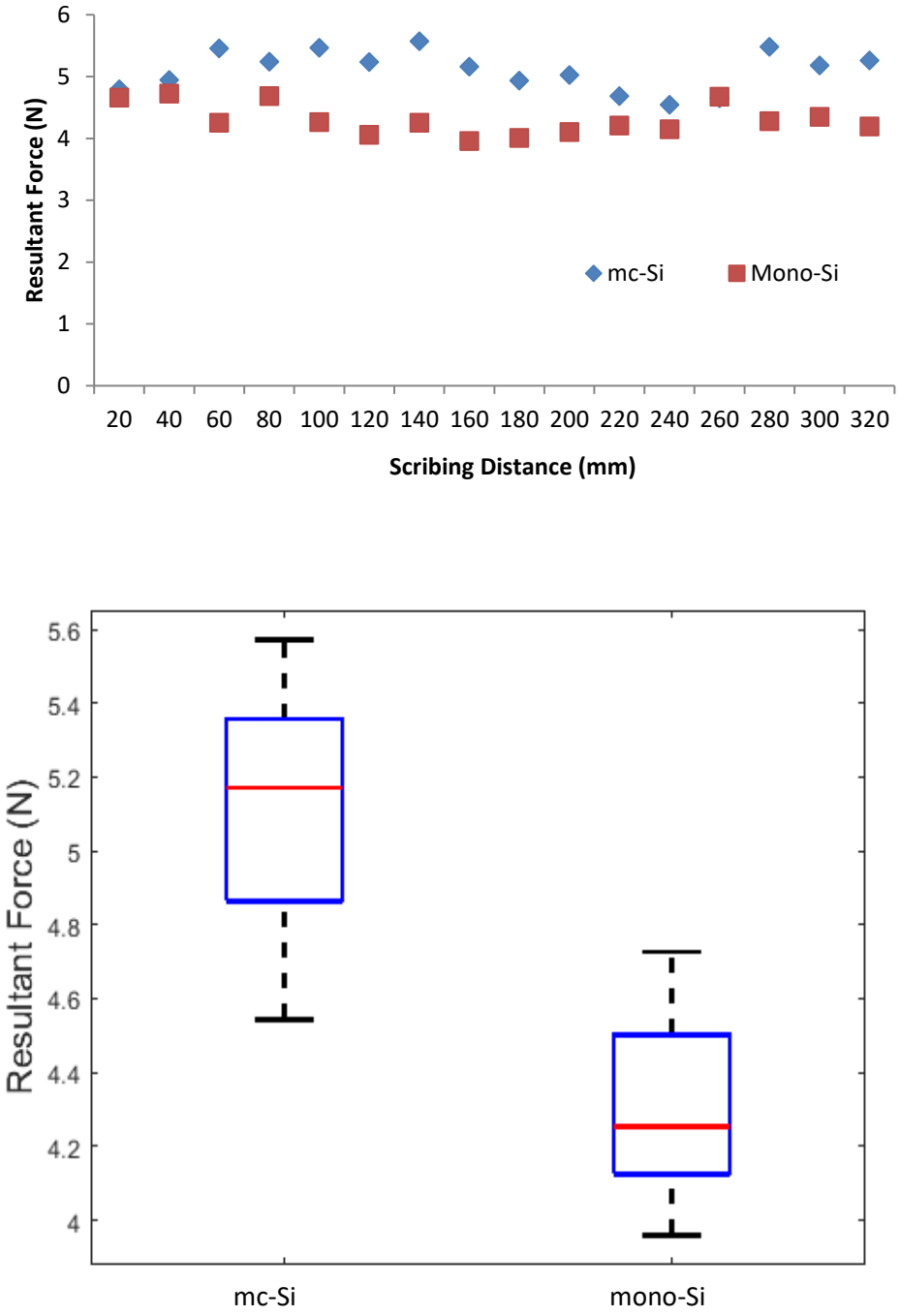

Figure 5.2: (a) Average resultant force for the two materials as a function of scribing distance, (b) Boxplot of the averaged resultant force for the two materials.

5.3.2 Wear of Diamond Indenter

The surface morphologies of the diamond indenters after scribing mc-Si and mono-Si for the specified distances are shown in Figure 5.3. In the following, for convenience, we refer to the indenter used to scribe mc-Si as the "mc-Si tool" and the indenter used to scribe mono-Si as the "mono-Si tool". As can be seen in Figure 5.3b and 3f that after scribing for 140 mm both mc-Si and mono-Si tools show evidence of wear. The mc-Si tool (Figure 5.3b) shows clear evidence of blunting of the tip as well as the formation of a trench produced by micro fracture and located below the tip. The mono-Si tool shows less pronounced tip rounding than the mc-Si tool. Evidence of micro fracture, while present in the mono-Si tool as well, is more scattered. After 200 mm of scribing, the mc-Si tool surface shows growth of the trench, which now extends from the left to the right of the indenter face (Figure 5.3c). The mono-Si tool shows fractured ridges with notches appearing on two sides of the tool as seen in Figure 5.3g. While the increases in tip radii and micro fracture of the scribing surfaces of the two tools are not that pronounced in going from 200 mm to 260 mm of scribing, they are more evident after 320 mm of scribing (see Figure 5.4). Figure 5.4 also shows the different types of diamond fracture evident in the morphologies of the micro fractured surfaces of the diamond tools. Two types of micro morphologies are exhibited by the diamond surfaces - the mc-Si tool shows a typical cleavage fracture with hackly (jagged) fractures and a ridged pattern in the trench, while the fractured surface pattern in the upper part of the mono-Si tool is consistent with the "river pattern" reported by Lawn [147] and Hull [148]. Both tools showed the hackly fracture pattern on the diamond faces contacting the silicon.

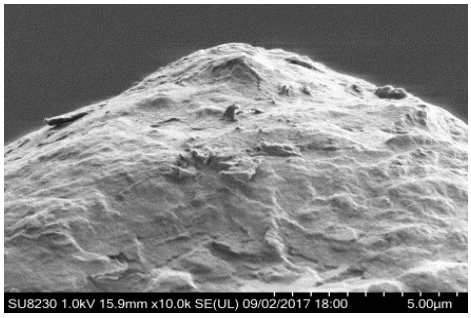

(a) mc-Si: 0 mm

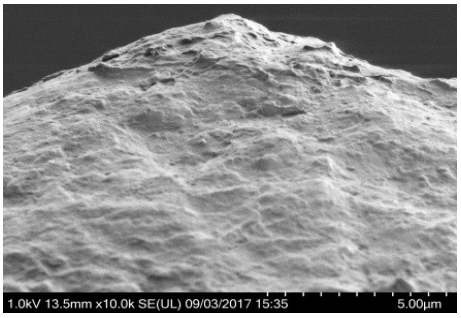

(e) mono-Si: 0 mm

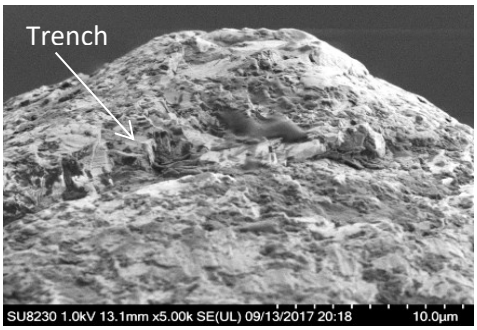

(b) mc-Si: 140 mm

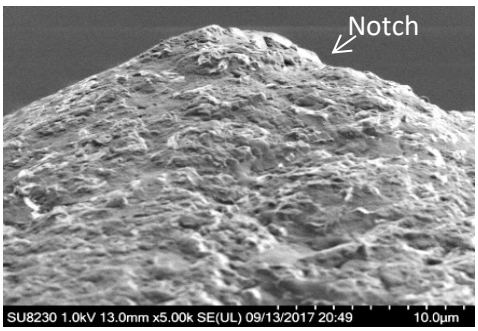

(f) mono-Si: 140 mm

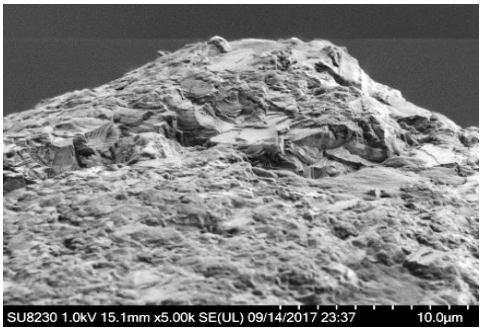

(c) mc-Si: 200 mm

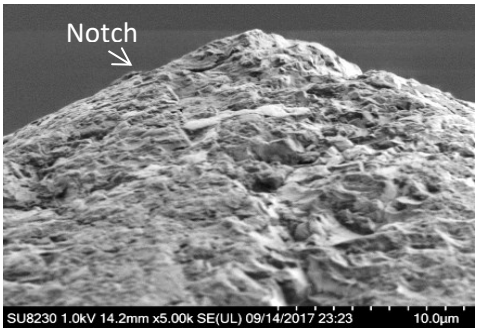

(g) mono-Si: 200 mm

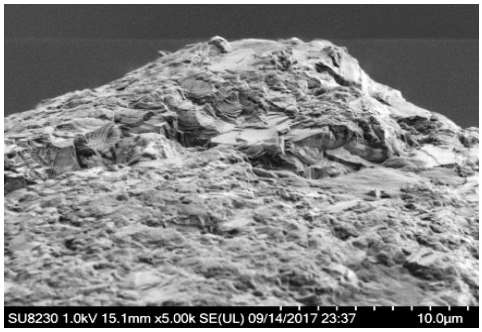

(d) mc-Si: 260 mm

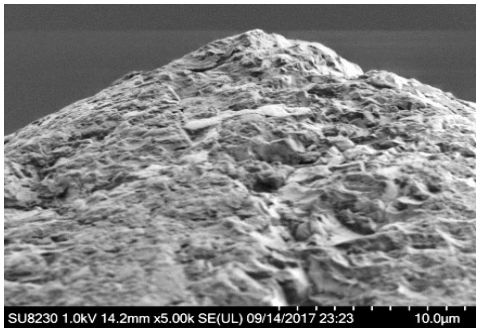

(h) mono-Si: 260 mm

Figure 5.3: Wear progression of the indenters during scribing of mc-Si (a through d) and mono-Si (e through h) as a function of scribing distance.

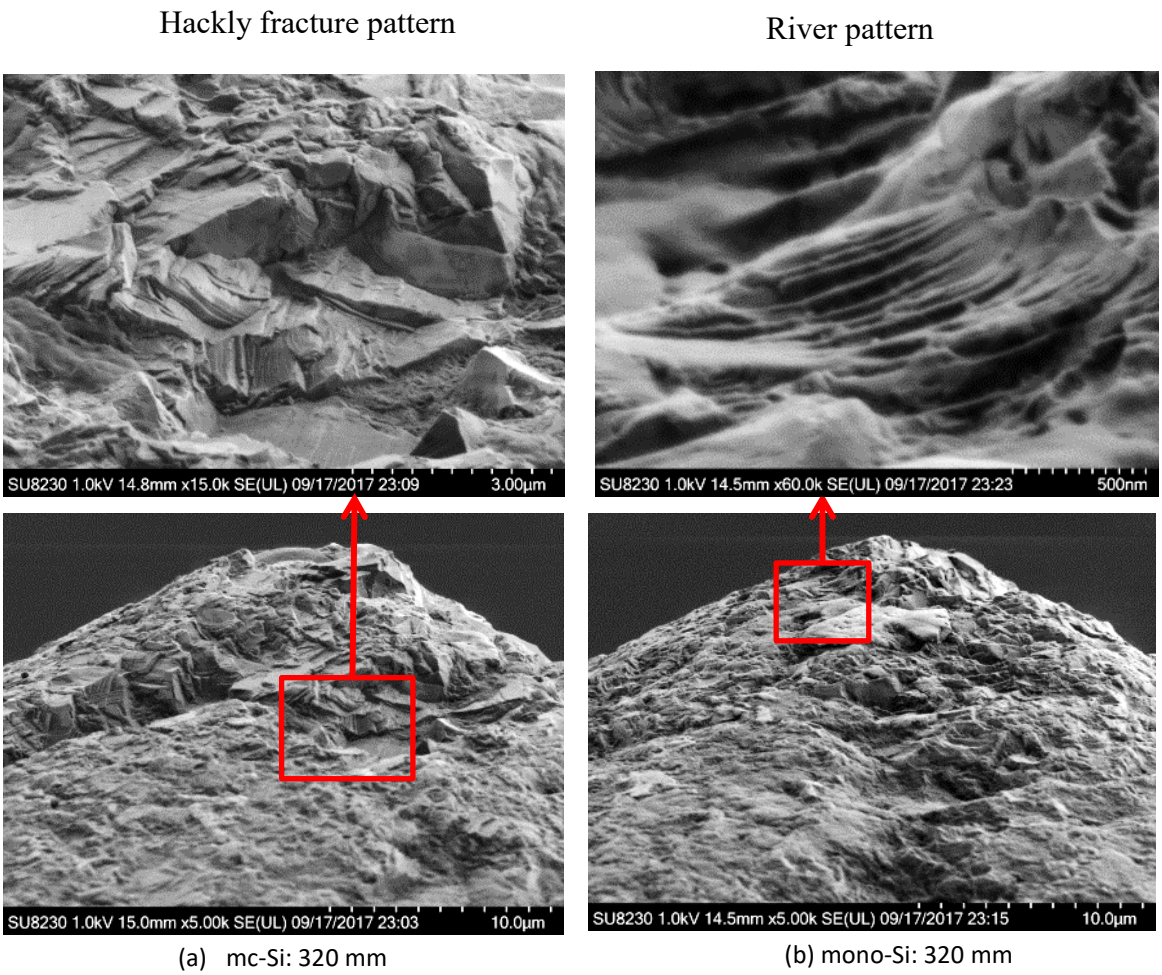

Figure 5.4: Morphologies of micro-fracture patterns in the diamond indenters after scribing (a) mc-Si and (b) mono-Si.

Figure 5.5 shows the change in radius of curvature of the tips of the mc-Si and mono-Si tools as a function of scribing distance. The error bars plotted represent one standard deviation of ten measurements made with the scriber. It is clear from the trend lines in the figure that while the tip radii increase with scribing distance (wear) for both tools, the rate of wear is higher for the mc-Si tool compared to the mono-Si tool. This further confirms the qualitative observations of tip blunting seen in the SEM images of Figure 5.3.

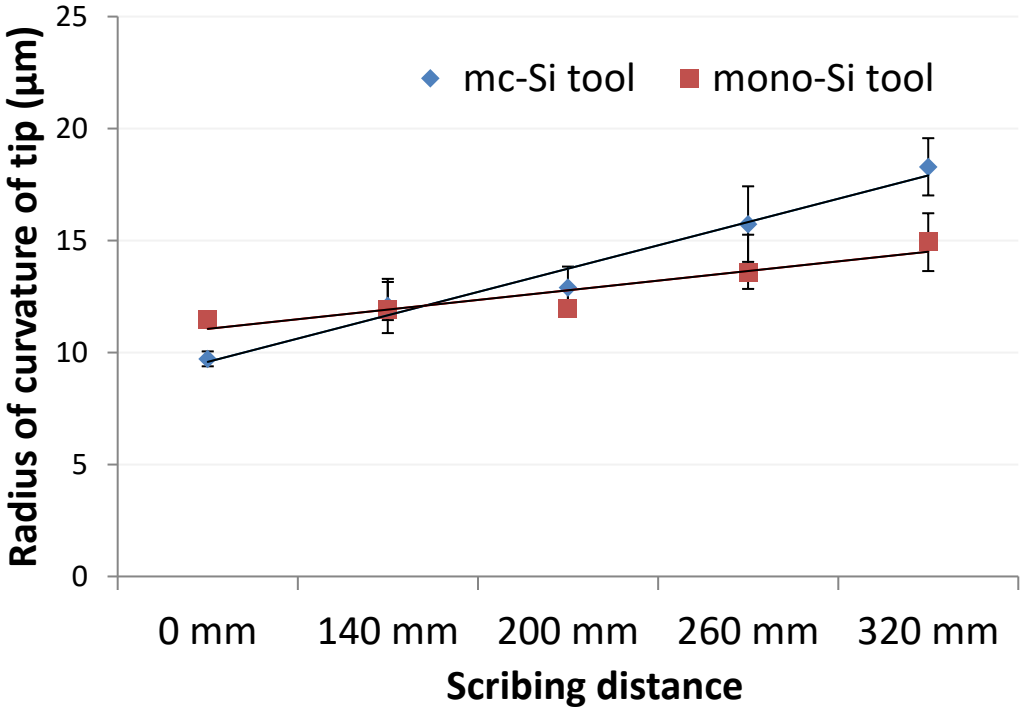

Figure 5.5: Indenter tip radii for mc-Si and mono-Si tools shown as a function of scribing distance. The error bars represent one standard deviation of the tip radius measurements made on the scriber.

5.3.3 Raman Spectra and State of Stress

Raman spectroscopy was used to investigate possible graphitization and any change in the internal stress state of the diamond tools due to scribing. The Raman spectra for both tools before scribing (Figure 5.6) showed the T2g peak of diamond centered at 1332 cm^{-1}. This peak is related to the T2g symmetric vibration of the sp^3 carbon bond [149]. The Raman measurements were repeated at several points on each indenter face prior to

scribing and no evidence of graphite was found in the two tools. Therefore, any peak shift observed after scribing can be attributed to the effect of the scribing process.

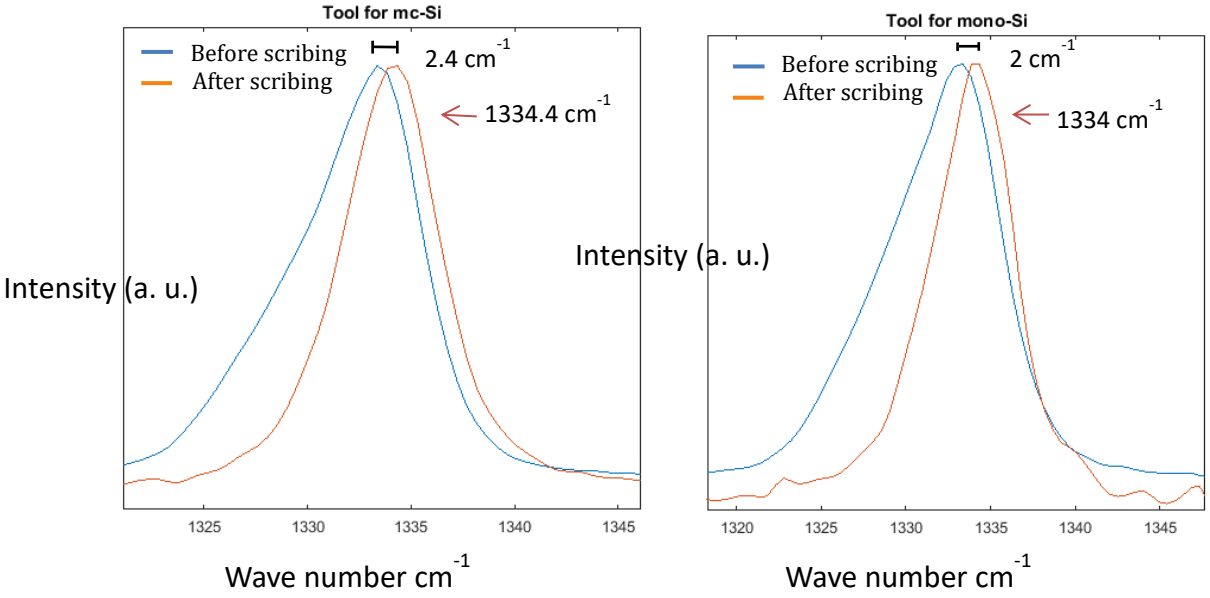

Figure 5.6: Raman spectra for tool after scribing in (a) mc-Si and (b) mono-Si.

After scribing for 320 mm, the diamond peak in the Raman spectra exhibited shifts from the 1332 cm^{-1} peak of diamond [79] to peaks at 1334.4 cm^{-1} for the mc-Si tool and 1334 cm^{-1} for the mono-Si tool. The classic D band peak for graphitic carbon is typically observed around 1350 cm^{-1} depending on the laser power used [150, 151]. The D band in disordered carbon systems is known to be produced by defects in graphite, whereas the G band (around 1580 cm^{-1}) in graphitic materials is due to the E2g Raman active mode for sp^2 hybridized carbon [152]. The D band spectra can be influenced by the surrounding zone of the diamond phase, which is at 1332 cm^{-1}. Any shift in the Raman spectra can be

attributed to the formation of nano-crystalline graphite phase [153], which can form under high stress, as suggested by Yang et al. [79]. Moreover, the peak shift could also be attributed to residual stress introduced in the diamond by the scribing process [154, 155]. For phase transformation to occur, a combination of hydrostatic stress and shear stress is required [154]. Prior research shows that a shear stress of 95 GPa is required for graphitization to occur [156]. Evidently, our experiments did not produce such high shear stresses. However, as suggested by Yang et al. [79], in actual diamond wire sawing repeated interactions of the abrasive with the silicon can create a cumulative effect, giving rise to sufficiently high shear stresses that can cause graphitization.

The Raman spectra for both mc-Si and mono-Si tools showed a positive shift in the diamond T2g peak, which implies compressive residual stresses generated by the scribing process [157]. To quantify the residual stress in the diamond tools, we used Hemley's model [158] given by the following equation, which is valid for non-hydrostatic conditions, where v_d is the peak location (cm^{-1}) and P is the pressure in GPa:

$$v_d = 1332.6 + 1.294P - 0.0062P^2$$

Using the above model, we obtained the residual stress to be 1.087 GPa for mono-Si and 1.400 GPa for mc-Si. We use another model adapted from Gogotsi et al. [154] for calculating the residual stress from the maximum shift of the diamond band (13 cm^{-1}), which corresponds to a compressive residual stress of 8 GPa (1.625 cm^{-1}/GPa). This model yielded residual stresses of 1.18 GPa and 1.47 GPa for mono-Si and mc-Si, respectively. The residual stresses signify that under combined loading of hydrostatic and shear stresses

(during scribing) the diamond indenters undergo phase transformation, which gives rise to the residual stress.

The observed peak shifts suggest compressive residual stresses in the diamond tips due to stress-induced phase transformation. However, the differences in the peak shifts for the mc-Si and the mono-Si diamond tools are small. This is attributed to the relatively short scribing distance used in the experiments reported here. It is expected that with longer scribing distances (on the order of kilometers), the differences in the peak shifts for the two cases will be more pronounced.

5.4 Discussion

Several mechanisms have been hypothesized for diamond wear, with the predominant wear mechanism depending on the cutting conditions. As seen in prior research on ultraprecision diamond turning [84-86], diamond (groove) wear can occur (1) due to mechanical abrasion from hard particles such as inclusions in the multi-crystalline silicon material, (2) due to adhesion at the *high pressure micro-scale contact* between silicon and diamond, and (3) due to diffusion of carbon from the diamond to silicon based on mechano-chemical effects. Mechanisms of mechanical (non-thermal) wear of abrasive bonded grinding wheels include (1) attritious wear (wear flat development) [159], (2) micro-fracture, (3) macro-fracture, and (4) pull-out and loss of abrasives [160, 161]. Our scribing results suggest that wear of the diamond abrasive is primarily by mechanical abrasion resulting in micro-fracture of the diamond. In our experiments, the high localized stresses in the micro-scale contact region cause micro-fracture and chipping of the diamond. Our micro-fracture patterns are similar to those reported by Lawn et al and Hull

et al. [147, 148], and more recently in work on diamond scratching of tantalum-tungsten (Ta12W) high hardness (3 GPa) alloy [87]. For multi-crystalline silicon, the scribing forces are higher due to the grain/twin boundaries and inhomogeneity in the local material properties in comparison to mono-crystalline silicon. Comparing the hardness of silicon (9-12 GPa [121, 162]), to the hardness of silicon carbide (20-30 GPa [163]) and silicon nitride (20-35 GPa [164]), multi-crystalline silicon with impurities is expected to produce higher cutting forces in DWS, as confirmed by our scribing results. Assuming a similar area of contact of the indenters used to scribe mono and mc-Si, diamond wire sawing of mc-Si is expected to be characterized by higher applied stress, which can cause phase transformation and greater wear of the diamond abrasives.

Zong et al.'s XPS measurements on the mono-Si surface produced by ductile mode machining in diamond turning showed evidence of silicon carbide (SiC) [84], which was explained by the diffusion of carbon atoms from diamond to silicon. This experimental observation was also predicted by MD simulations, which yielded sp^3-sp^2 disorder of diamond [91]. However, our XPS measurements did not find any evidence of SiC in either the silicon grooves or on the surface of the diamond indenters, which agrees with the results of prior work [79]. There are two possible reasons for lack of SiC formation in our tests. First, unlike in diamond turning, our scratches are characterized by brittle fracture, which hinders the carbon diffusion mechanism responsible for SiC formation [84]. Second, the tool-workpiece contact length in diamond turning is much larger (~kilometers), and is therefore difficult to replicate in our scratching tests.

It should be noted that under practical diamond wire sawing conditions, which are characterized by higher wire speeds (10-20 m/s), the effect of process dynamics (e.g. wire

vibration) will influence the abrasive-silicon interaction and hence wear of the diamond. Nevertheless, the differences in wire wear due to silicon structure (mc-Si versus mono-Si) observed in the current study are still expected to be observed in the actual wire sawing process.

The higher scribing forces observed in mc-Si are possibly due to the inhomogeneities in the mc-Si material. While prior work has shown the effect of crystal orientation on the scribing of bulk single crystal silicon to be significant [31], the effect of grain orientation on the scribing behavior of a cast mc-Si material containing multiple grains of different orientations, along with other crystal defects such as twin and grain boundaries, dislocations, and inclusions, is not known. Some work on the effect of crystal defects such as dislocation clusters on the intra-granular scribing behavior in quasi-mono and mc-Si wafers has been reported. This work shows that regions of higher dislocation density within a grain are correlated with higher fracture toughness (and higher local fracture strength [70]) and a larger critical depth of cut [69]. These prior findings and the current scribing results suggest that the influence of defect structures such as dislocation clusters dominate the scribing response in the grain interior, thereby masking the influence of crystal orientation differences. Further work is required to confirm this possibility.

The increase in forces in the single grit scribing experiments on mc-Si can be translated to diamond wire sawing, where the increased forces can delaminate or pull-out the diamond grits. Grit loss would lead to the sawing forces being distributed on even fewer grits in the cutting zone in the kerf, leading to even more increased force on grit, and the silicon, thus increased wear of the diamond wire, or worse causing wire breakage and stalling production. Increased force per grit would also lead to deeper micro-cracks in the

sawn wafers [9], which can lower the manufacturing yield of wafers. The wear rate of diamond when cutting multi-crystalline silicon by diamond wire sawing can be reduced by engineering the silicon ingot to lower its impurity and inclusion content and by reducing the number of grain/twin boundaries. This would also improve the electrical properties of the mc-Si solar cells produced using the sliced substrates. Future work will consider these aspects.

5.5 Conclusions

The chapter investigated the wear of diamond in scribing of multi-crystalline silicon with the aim of understanding the underlying reasons for increased wire consumption in diamond wire sawing of multi-crystalline silicon wafers. The results were compared with those obtained in scribing of mono-Si material. The scribing results showed that the scribing forces for mc-Si are higher than for mono-Si, reflecting the influence of localized defects in mc-Si such as grain and twin boundaries, and inclusions. Results showed micro-fracture of the contacting face of the diamond tips, and a higher rate of increase in the radius of curvature of the diamond tip when scribing mc-Si. Although no evidence of graphitization of the diamond indenters was found, the residual stress detected in the diamond indenters suggests some phase transformation took place.

CHAPTER 6. THE CHEMO-MECHANICAL EFFECT OF CUTTING FLUID ON MATERIAL REMOVAL IN DIAMOND SCRIBING OF SILICON

The mechanical integrity of silicon wafers cut by diamond wire sawing depends on the damage (e.g., micro-cracks) caused by the cutting process. The damage type and extent depends on the material removal mode i.e. ductile or brittle. In this chapter, we investigate the effect of cutting fluid on the mode of material removal in diamond scribing of single crystal silicon, which simulates the material removal process in diamond wire sawing of silicon wafers. We conducted scribing experiments with a diamond tipped indenter in the absence (dry) and in the presence of a water-based cutting fluid. We found that the cutting mode is more ductile when scribing in the presence of cutting fluid compared to dry scribing. We explain the experimental observations by the chemo-mechanical effect of the cutting fluid on silicon, which lowers its hardness and promotes ductile mode material removal.

6.1 Introduction

Diamond wire sawing (DWS) is increasingly the preferred process for high volume production of photovoltaic (PV) crystalline silicon wafers [3]. A current challenge faced by the PV industry is the breakage of wafers when processing bare wafers into solar cells. Research suggests that the breakage rates of crystalline silicon photovoltaic wafers are greatly impacted by the surface and subsurface damage produced in the DWS process [9, 165, 166]. Hence, reducing surface and subsurface damage by enhancing ductile mode

material removal of brittle silicon is a goal being pursued by researchers [10, 55]. The cutting mode of silicon is known to be influenced by the sawing process parameters such as wire speed and workpiece feedrate, by the abrasive properties (shape, size, concentration) [141], and by the material properties (mono- vs. multicrystalline silicon). In DWS, a water-based cutting fluid is used primarily as a coolant for cutting the silicon ingot with 8-20 μm average diameter diamond abrasives attached to a high carbon steel wire with nickel coating. In this chapter, we investigate via diamond scribing experiments an unexplored aspect of the role of cutting fluid, namely, the effect of cutting fluid on the mode of material removal (ductile versus brittle) in diamond wire sawing of mono-crystalline silicon (mono-Si).

Material removal in DWS is due to a combination of scratching and indentation processes, with the former process playing a more dominant role. Hence, DWS can be simulated by diamond scribing experiments Figure 6.1(a-b) [55, 141]. In general, the silicon wafer surface is characterized by a mix of ductile and brittle material removal modes [9, 10]. We report here the results of scribing studies performed with a diamond tipped indenter scribing a micro-electronic grade monocrystalline (100) silicon wafer in air (dry scribing) and in the presence of an industrial grade cutting fluid used in the DWS process. The observations are explained in terms of the chemo-mechanical effect of the fluid on the deformation response of silicon.

6.2 Experimental procedure

6.2.1 Scribing Tests

Microelectronic grade double-side polished monocrystalline (100) silicon wafers were diced into small 10 mm x 25 mm coupons, which were used as substrates in the diamond scribing tests. The scribing direction was [110]. Scribing was performed using a conical tipped diamond scriber with a 90° included angle. The scribes were of gradually increasing depth of cut ranging from 0 to 5 μm over a length of 5 mm (Figure 6.1b). We used increasing depth of cut scribes to identify the critical depth of cut for ductile-to-brittle transition, which is defined as the depth of cut at which the mode of material removal transitions from ductile to brittle, and is characterized by the appearance of surface cracks. The diced silicon wafer coupons were fixed to a flat aluminum baseplate bolted to a three-component piezoelectric force dynamometer (Kistler 9256C), which was mounted rigidly on computer-controlled stacked X-Y-Z motion stages (Aerotech ANT-4V) (Figure 6.1c). The dynamometer enabled the detection of initial contact of the scriber with the silicon wafer and was also used to measure the dynamic forces generated in the scribing experiments.

All scribing experiments were performed at room temperature and at a constant scribing speed of 100 mm/min. First, we carried out dry scribing tests. Next, we flooded the top of the wafer sample with water-based cutting fluid a few seconds before scribing (Figure 6.1d). This procedure was repeated for each case: dry and with water-based cutting fluid. We made 3 to 4 scribes for each test condition to ensure repeatability of the results. For the cutting fluid tests, we used a commercial grade DWS coolant (Ambercut DWC-35)

mixed with 97% water by volume (97 ml of water and 3 ml of concentrated cutting fluid). Ambercut DWC-35 is a fixed abrasive wire slicing coolant that is a mixture of synthetic surfactants diluted in water to produce a biodegradable water-based cutting fluid.

6.2.2 Surface Characterization

The critical depth of cut for ductile-to-brittle transition in an increasing depth of cut scribing test was determined through optical confocal microscopy (Olympus LEXT). The scribe morphology was observed in an optical microscope (Leica DVM6). For selected scribes, we obtained higher resolution images using a scanning electron microscope (Hitachi 8230 SEM). Micro-Raman spectroscopy was performed on selected scribes using a Renishaw InVia Raman spectrometer to determine the phase of silicon in the scribed grooves. The wavelength of the laser in the micro-Raman spectrometer was 488 nm with a surface penetration of ~0.5-0.6 μm and a spatial resolution of 1 μm, which is smaller than the width of the scribes.

6.2.3 Zeta Potential Measurements

The zeta potential of the cutting fluid in the presence of silicon was characterized in a Malvern Zetasizer (Nano ZS). This instrument uses solid particles of the monocrystalline silicon wafer ranging in size from 0.6 nm to 6 μm dispersed in the water-based cutting fluid to measure the zeta potential. Monocrystalline silicon wafer coupons diced from the same silicon wafer utilized in the scribing experiments were cleaned using acetone and air-blasted to remove any contamination before crushing them into fine powder using a mortar and pestle. The silicon powder was then dispersed in the water-based cutting fluid. The resulting mixture was sonicated in a water bath for 30 minutes.

The sonicated mixture was not a true suspension since a few silicon particles settled at the bottom of the beaker when the solution was extracted from the sonicator. Therefore, for the zeta potential measurements, the sonicated mixture was sampled from the top to minimize the inclusion of large particles of silicon. The sonicated silicon-fluid mixture was subjected to an applied electric field of 5V in an electrophoresis cell, and the method of electrophoretic light scattering was used to determine the zeta potential.

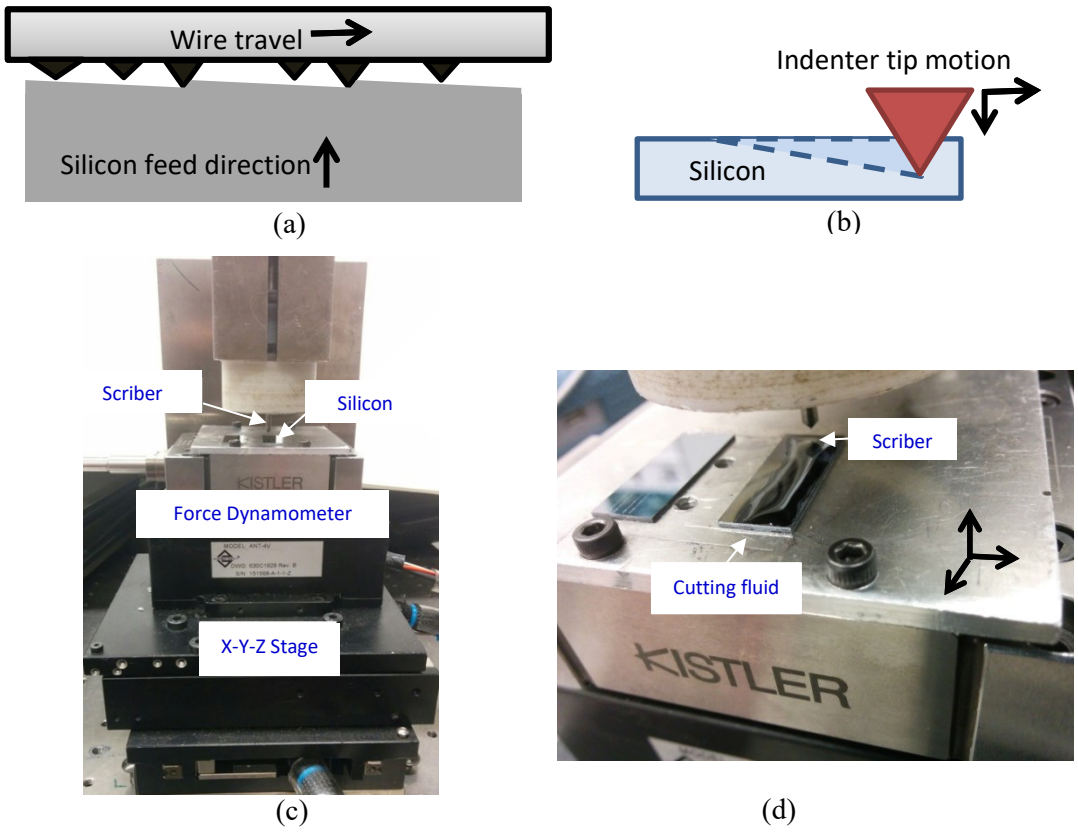

Figure 6.1: (a) Cutting action in diamond wire sawing, (b) scribing of silicon by diamond tipped indenter, (c) scribing setup, (d) cutting fluid on top of sample before scribing.

6.3 Results and Discussion

Figure 6.2a shows a representative optical image of the scribes obtained in dry scribing and in the presence of the cutting fluid. Note that although the X-coordinates of the starting locations of all scribes were the same, the scribe made in the presence of the fluid shows evidence of brittle fracture (dark line) after a longer scribing distance than the dry scribe. Specifically, the average distance to transition from ductile to brittle cutting during dry scribing was 1.27 mm compared to 1.75 mm for scribing with cutting fluid. The average critical depth of cut was greater in the scribes made with cutting fluid compared to the dry scribes (Figure 6.2b). For the same travel distance of approximately 1.50 mm from the start of the scribe, the SEM images (Figure 6.2c and d) showed more ductile deformation of silicon in the presence of the cutting fluid than in dry scribing. Raman spectra of the scribed grooves after ductile-to-brittle transition are shown in Figure 6.3. Even though silicon is a brittle material, it is known to undergo stress-induced phase transformation from Si-I to β-Sn and other phases such as Si-III, Si-XII, and amorphous silicon, depending on the unloading rate [57]. Raman spectra of the dry scribe showed a prominent crystalline Si-I peak around 520 cm^{-1}. In comparison, the scribe made with the cutting fluid showed a Si-III peak (470 cm^{-1}) and broad peaks of amorphous silicon (a-Si) in addition to the Si-I peak, thus indicating evidence of phase transformation and ductile mode material removal. It is therefore evident that the cutting fluid enhances ductile mode deformation of silicon.

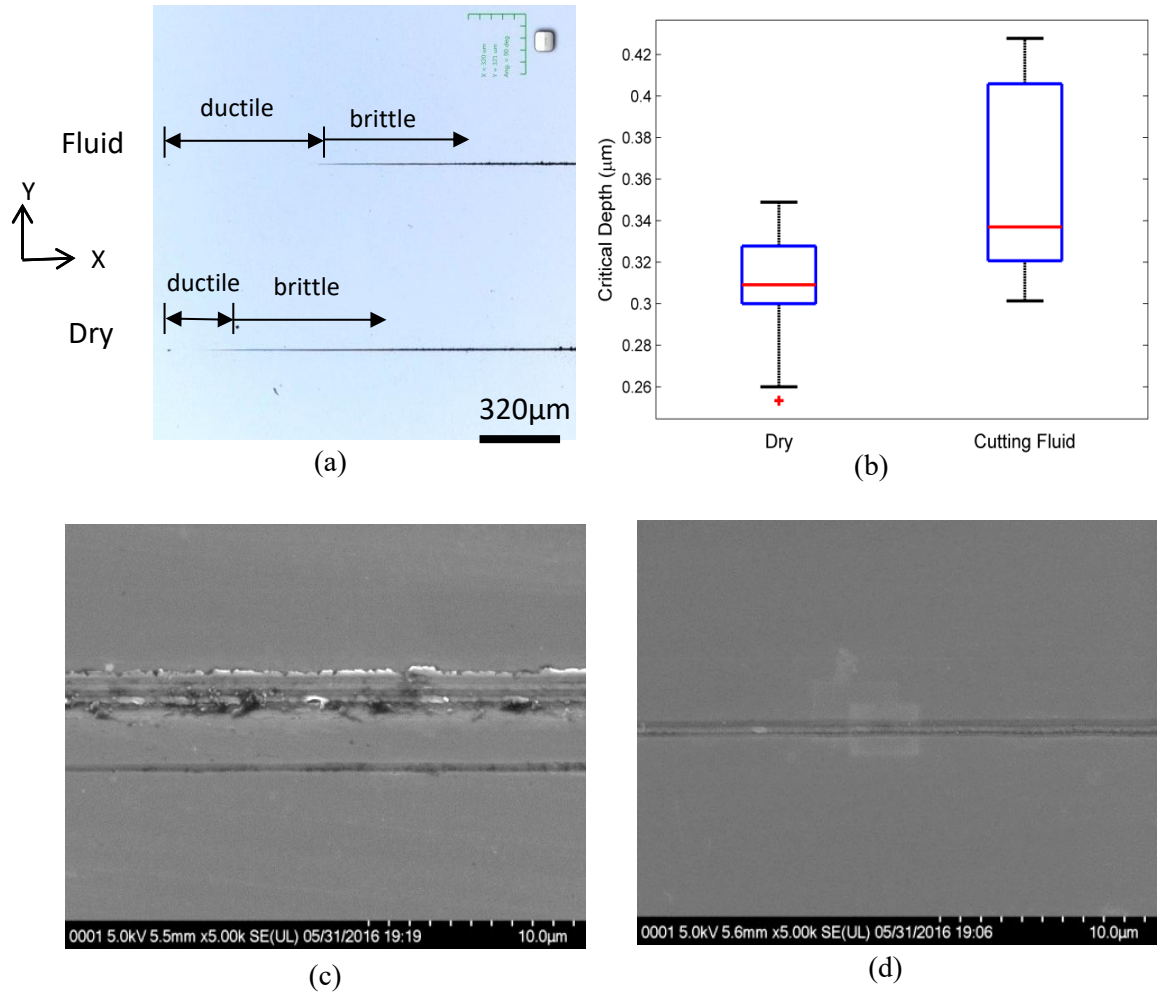

Figure 6.2: (a) Representative scribes obtained in dry scribing and in scribing with water-based cutting fluid, (b) box plot of the critical depths of cut for the dry and cutting fluid cases; SEM images of the scribes after approximately 1.50 mm of travel (c) for dry, and (d) with fluid.

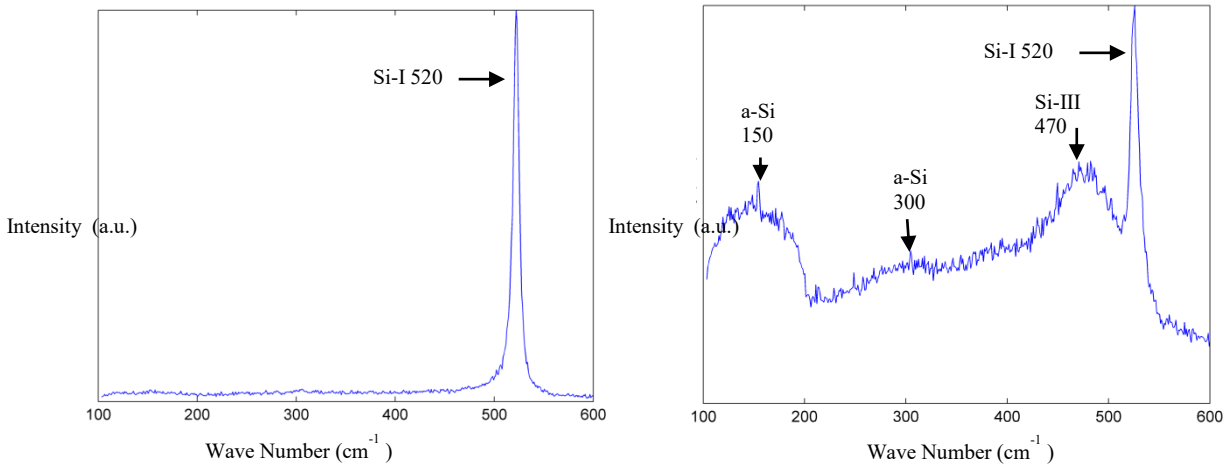

Figure 6.3: Raman spectra of scribes: (a) dry, and (b) cutting fluid. Measurements were made inside the grooves after ductile-to-brittle transition.

Figure 6.4 shows the normal (Z) and the tangential (X) force profiles, plotted against the scribing distance. As expected, the scribing forces are seen to increase with increasing depth of cut. The initial smooth increases in the forces correspond to the ductile portion of the scribes. The transition to brittle material removal is marked by rapidly varying forces. Considering that the rate of increase in the scribing depth is the same for the two cases, scribing with the cutting fluid exhibited brittle fracture after a larger scribing distance, and hence at a higher scribing depth, as seen from the critical depth of cut data shown earlier.

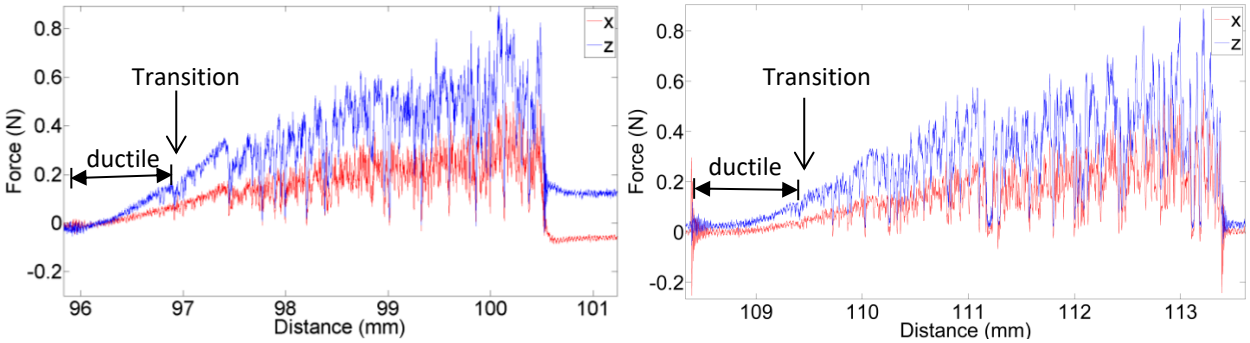

Figure 6.4: Normal (Z) and tangential (X) scribing forces in (a) dry scribing, and (b) scribing with cutting fluid.

Fluids are known to influence the mechanical properties of solids they are in contact with. Prior work investigated the effects of ethanol, acetone, and deionized water in constant-depth scribing of monocrystalline (111) silicon [98-101]. Various theories have been proposed to explain this "chemo-mechanical effect". Research on chemo-mechanical effects dates back to the 1920s when Rebinder's theory of reduction in the hardness of solids due to adsorbed chemical species was proposed [102]. Later, Westwood [103] found the hardness of a solid and the zeta potential of the fluid in contact with the solid to be correlated. Zeta potential is the electrostatic potential between the Stern layer of the double layer at the liquid-solid interface and the bulk solution [105]. Westwood showed that a zero zeta potential corresponds to the maximum hardness of very brittle non-metals [103]. Yost and Williams [105] found that when intrinsic and doped (*n*- and *p*-type) silicon are exposed to NaCl and $Na_4P_2O_7$, the minimum hardness is correlated with the most negative value of

zeta potential. Yost and Williams explained that the change in hardness with zeta potential is due to the surface charges, which affect the near-surface mobility of dislocations. This explanation is based on prior work where charges produced by electronic doping influenced the dislocation velocities [106] and dislocation kink formation [107]. In another study, Westbrook and Gilman [108] reported softening of silicon by 60% during indentation in the presence of a small potential between the silicon surface and the indenter. Therefore, in the following, we use the theory of chemo-mechanical effects to explain our experimental results.

We made zeta potential measurements on single crystal (100) silicon particles dispersed in water (indicative of atmospheric moisture, as our dry scribing tests were performed in ambient conditions), and in the cutting fluid. Figure 6.5 shows the zeta potential for the cutting fluid in contact with silicon is more negative compared to water. Vickers micro-hardness measurements showed a reduction in the hardness of silicon in the presence of the cutting fluid (7.32 ± 0.50 GPa), compared to without the cutting fluid (dry) (8.80 ± 0.47 GPa). The difference in the mean hardness for the two cases is statistically significant within a 95% confidence interval. The zeta potential and hardness results support the theory that the cutting fluid lowers the hardness of silicon, which causes more ductile mode material removal, and hence yields a larger critical depth of cut than dry scribing.

A possible reason to explain the results obtained for scribing under dry conditions versus with cutting fluid could be the differences in the friction coefficient for the two cases. However, the difference in the measured mean coefficients of friction μ (0.41 in dry scribing and 0.39 with cutting fluid) were found to be not statistically significant. Another

possible explanation of the results could be the reduction in normal load acting on the silicon surface due to part of the load being borne by the cutting fluid. However, this explanation is unlikely since the cutting fluid is not confined in the experiments and therefore the pressure buildup in the fluid is likely to be low. Consequently, the observed critical depths of cut and changes in surface hardness are attributed to the chemo-mechanical effect of the cutting fluid.

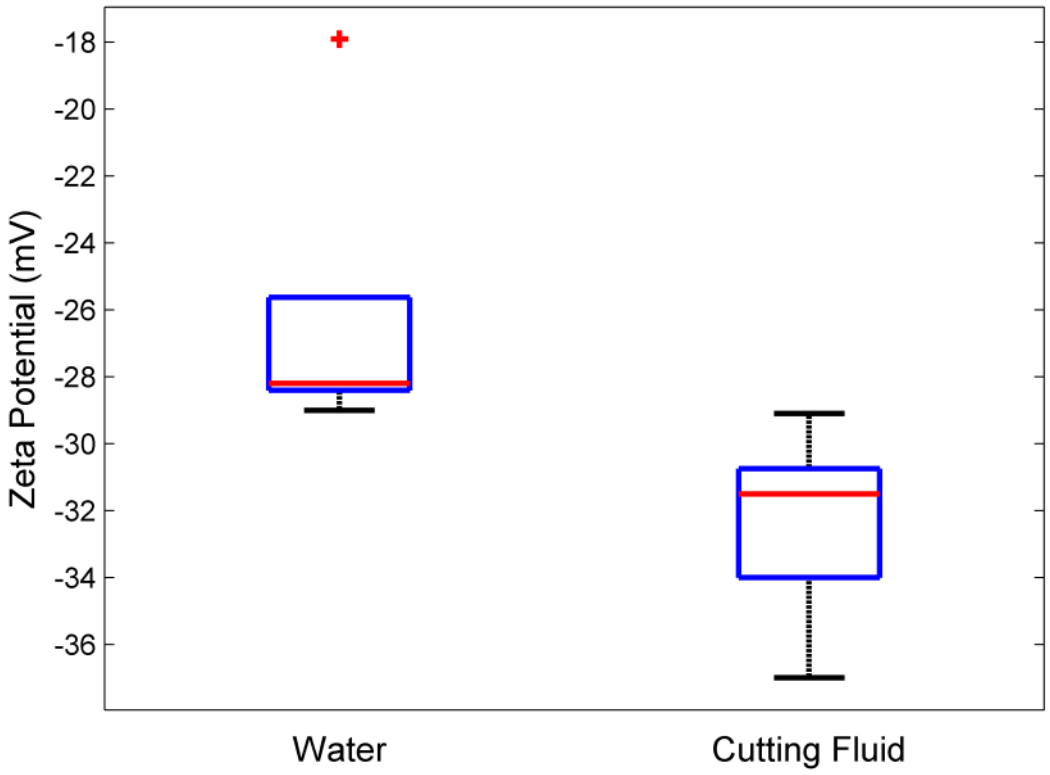

Figure 6.5: Zeta potentials of silicon particles dispersed in water and cutting fluid.

6.4 Summary

In summary, this chapter presented the results of an experimental study of the effects of a water-based industrial grade cutting fluid (Ambercut DWC-35) on the mode of material removal in diamond scribing of single crystal (100) silicon. The scribing process simulates the abrasive-workpiece interaction in diamond wire sawing. We found that the water-based cutting fluid, which is used in the diamond wire sawing process for lubrication and cooling, also promotes ductile mode material removal. We explained the results obtained in our dry scribing experiments and in the cutting fluid experiments using the chemo-mechanical effect theory. The fluid-silicon combination yielded a more negative value of the zeta potential and a corresponding reduction in the hardness of silicon, which caused more ductile material removal. These results suggest that, in addition to their cooling and lubrication properties, cutting fluids also influence the cutting mode in diamond wire sawing of silicon. Nominally, brittle mode removal would be desirable at the bottom of the kerf to maximize material removal rate, while ductile mode removal would be desirable on the sides of the kerf to minimize surface and subsurface damage. This suggests a trade-off in the cutting fluid's role in diamond wire sawing.

CHAPTER 7. CONCLUSIONS AND RECOMMENDATIONS

This chapter summarizes the major contributions and conclusions of this dissertation, and suggests related areas of research for further work.

7.1 Major Contributions

The major contributions of this dissertation are as follows:

- Development of a wire scribing technique for the fundamental understanding of the effect of actual diamond shapes on surface and subsurface damage generation in fixed abrasive wire sawing process.
- Fundamental understanding of the role of grain boundaries, twin boundaries, and material properties (e.g. fracture toughness) on diamond wire sawing of multi-crystalline silicon (mc-Si).
- Understanding of the effect of wear of diamond wire on surface and subsurface damage in sliced monocrystalline silicon (mono-Si) wafers.
- A first understanding of the reasons for increased wear of diamond in cutting of mc-Si.
- Fundamental understanding of the effect of cutting fluid on the material removal mode in diamond wire sawing of mono-Si.

7.2 Major Conclusions

The major conclusions of this dissertation in each of the following topics are:

7.2.1 Effect of Grit Shape and Crystal Structure on Damage in Diamond Wire Scribing of Silicon

A new diamond wire scribing method was designed and implemented on mono and mc-Si to investigate the effect of actual grit shapes present in an industrial grade fixed abrasive diamond wire. The key conclusions are:

- The grit shape significantly affects the scribe morphology. In the brittle cutting regime, the sharper grit produced radial-chevron surface cracks, while the rounder grit produced horseshoe-like surface cracks.
- For a given material (mono or mc-Si), different grit shapes yield different critical depths of cut because of differences in the resulting stress states produced in the material.
- Qualitatively, the same grit shape produced scribes with similar surface morphology in both mono and mc-Si.
- In mc-Si, scribing across the twin and grain boundaries yielded differences in the morphology (specifically, cracking frequency) in the vicinity of the boundaries, but yielded similar morphologies away from the boundaries.
- Away from the twin and grain boundaries, the scribe morphology was more dependent on the grit shape than on crystallographic orientation.
- The subsurface cracks depend on the combination of grit shape and material (mono- or mc-Si).
- In general, the subsurface crack depths produced in mc-Si are larger than in mono-Si due to the presence of more defect sites in mc-Si.

7.2.2 Effect of Wear of the Diamond Wire on Surface Morphology, Roughness and Subsurface Damage of Silicon Wafers

The effects of fixed abrasive diamond wire wear on the surface morphology, roughness, and subsurface damage of (100) mono-crystalline silicon wafers were analyzed by characterizing the silicon wafers and the diamond wires at different levels of wire wear (new vs. used). Scanning electron microscopy (SEM), Raman spectroscopy, confocal microscopy, Focused Ion Beam machining (FIB), and biaxial flexure were used to evaluate the surface morphology, areal surface roughness, and subsurface cracks. The following conclusions are derived from the study:

- Wire wear significantly affects the wafer surface morphology; the wafer surfaces cut by a new wire showed mostly brittle fracture, while the wafer surfaces cut by the used wire showed more ductile cutting.
- The average surface roughness and its scatter decreased with wire wear.
- Wire wear significantly affects subsurface damage. Wafers cut with the new wire had more subsurface lateral cracks per unit length than wafers cut with the used wire; however, wafers cut with the used wire had comparatively more median cracks.
- The worn diamond abrasive grits are characterized by rounding and blunting, with some instances of grit fracture and pull-out.
- The mean fracture strength of the wafers cut by the used wire is lower due to median cracks, which promote failure of the wafer at a lower stress level.

7.2.3 Wear of Diamond in Scribing of Multi-crystalline Silicon

The effect of multi-crystalline silicon on the wear of diamond abrasives was studied by scribing mc-Si with a conical diamond tipped indenter, to understand the possible reasons for increased diamond wear in cutting of multi-crystalline silicon. For comparison, similar experiments were performed on mono-Si material as well. Specifically, the scribing forces and the diamond indenter wear produced in scribing of the two materials were analyzed. The study yielded the following conclusions:

- The scribing forces for mc-Si are higher than for mono-Si, reflecting the influence of localized defects such as grain and twin boundaries, and inclusions in mc-Si.
- The wear of diamond abrasives in scribing of both mono and mc-Si occurs by micro-fracture of the contacting faces of the diamond tips with typical hackly and river-like fracture patterns.
- The rate of increase of the radius of curvature of the diamond tip is higher for scribing mc-Si than for mono-Si.
- The stresses generated in scribing produce residual stresses in the diamond tips, which are attributed to stress-induced phase transformation of diamond. However, no evidence of graphitization of the diamond indenter tips was found.
- The observed compressive residual stresses in the diamond are slightly higher for scribing of mc-Si versus mono-Si.

7.2.4 The Chemo-mechanical Effect of the Cutting Fluid on Material Removal in Diamond Scribing of Silicon

The effect of a water-based cutting fluid used in diamond wire sawing on the mode of material removal in diamond scribing of single crystal silicon was investigated. Scribing experiments were conducted with a diamond tipped indenter in the absence (dry) and in the presence of the cutting fluid. The key conclusions from the study are as follows:

- The critical depth of cut for ductile-to-brittle transition is higher in the presence of the cutting fluid.
- The cutting fluid during scribing promotes brittle-to-ductile phase transformation of silicon.
- The chemo-mechanical effect of the cutting fluid in contact with silicon explains the reduction in hardness and increased ductility of silicon. Specifically, the more negative zeta potential of the cutting fluid creates surface charges that affect the near-surface mobility of dislocations and hence promotes ductile material removal.

7.3 Recommendations for Future Work

The results of the fundamental studies presented in this thesis can be used to optimize the diamond wire sawing process of silicon by reducing the surface and subsurface damage and diamond wear. Potential topics for future research are as follows:

- Develop methods for manufacturing the desired shapes of diamond abrasives and methods for their incorporation into the actual diamond wire to minimize the surface and subsurface damage without compromising productivity.
- Develop methods to engineer the microstructure of mc-Si material to reduce the wear of the diamond wire.
- Investigate the effect of the chemical composition of the cutting fluid to promote ductile mode material removal in diamond wire sawing of silicon.
- Since the actual process in wire sawing involves cutting by a large number of abrasives of different sizes and shapes (and their protrusions), modeling of the DWS process using statistical distributions of the abrasive shapes and sizes can be investigated.
- Investigate the effect of micro-level parameters like abrasive grit shapes, grain/twin boundaries on macro-level responses such as wire vibration using analytical and experimental methods.

REFERENCES

[1] J. Tsao, N. Lewis, and G. Crabtree, "Solar FAQs," *www.sandia.gov,* 2006.

[2] DOE/NREL, "Intitute for Energy Research," *http://instituteforenergyresearch.org/topics/encyclopedia/solar/,* 2016.

[3] ITRPV, "International Technology Roadmap for Photovoltaics " *http://www.itrpv.net/Reports/Downloads/2014/,* 2014.

[4] H. J. Möller, "Basic mechanisms and models of multi-wire sawing," *Advanced Engineering Materials,* vol. 6, no. 7, pp. 501-513, Jul 2004.

[5] C. del Cañizo, G. del Coso, and W. C. Sinke, "Crystalline silicon solar module technology: Towards the 1 € per watt-peak goal," *Progress in Photovoltaics: Research and Applications,* vol. 17, no. 3, pp. 199-209, 2009.

[6] ITRPV, "International Technology Roadmap for Photovoltaics " *http://www.itrpv.net/Reports/Downloads/,* 2017.

[7] Rockwell-Automation, "Wafer slicing equipment," *http://literature.rockwellautomation.com/idc/groups/literature/documents/ap/oem-ap061_-en-p.pdf,* 2009.

[8] A. Bidiville, I. Neulist, K. Wasmer, and C. Ballif, "Effect of debris on the silicon wafering for solar cells," *Solar Energy Materials and Solar Cells,* vol. 95, no. 8, pp. 2490-2496, 2011.

[9] A. Kumar, S. Kaminski, S. N. Melkote, and C. Arcona, "Effect of wear of diamond wire on surface morphology, roughness and subsurface damage of silicon wafers," *Wear,* vol. 364–365, pp. 163-168, 2016.

[10] E. Cai, B. Tang, W. R. Fahrner, and L. Zhou, "Characterization of the surfaces generated by diamond cutting of crystalline silicon," *26th European Photovoltaic Solar Energy Conference and Exhibition,* pp. 1884 - 1886, 2011.

[11] T. G. Bifano, T. A. Dow, and R. O. Scattergood, "Ductile-regime grinding - a new technology for machining brittle materials," (in English), *Journal of Engineering for Industry-Transactions of the ASME,* Article vol. 113, no. 2, pp. 184-189, May 1991.

[12] T. G. Bifano, T. A. Dow, and R. O. Scattergood, "Ductile-regime grinding of brittle materials: experimental results and the development of a model," in *32nd Annual*

Technical Symposium. International Society for Optics and Photonics, 1989, vol. 0966, pp. 108-115.

[13] H. J. Möller, C. Funke, M. Rinio, and S. Scholz, "Multicrystalline silicon for solar cells," (in English), *Thin Solid Films,* Article; Proceedings Paper vol. 487, no. 1-2, pp. 179-187, Sep 2005.

[14] V. Ganapati, S. Schoenfelder, S. Castellanos, S. Oener, R. Koepge, A. Sampson, M. A. Marcus, B. Lai, H. Morhenn, G. Hahn, J. Bagdahn, and T. Buonassisi, "Infrared birefringence imaging of residual stress and bulk defects in multicrystalline silicon," *Journal of Applied Physics,* vol. 108, no. 6, Sep 15 2010, Art. no. 063528.

[15] S. Kaminski and C. Arcona, "Challenges of diamond wire sawing," *Personal communication,* 2016.

[16] A. Kumar and S. N. Melkote, "Diamond Wire Sawing of Solar Silicon Wafers: A Sustainable Manufacturing Alternative to Loose Abrasive Slurry Sawing," *Procedia Manufacturing,* vol. 21, pp. 549-566, 2018.

[17] A. Bidiville, K. Wasmer, J. Michler, P. M. Nasch, M. Van der Meer, and C. Ballif, "Mechanisms of wafer sawing and impact on wafer properties," *Progress in Photovoltaics: Research and Applications,* vol. 18, no. 8, pp. 563-572, 2010.

[18] H. Seigneur, Andrew Rudack, Joseph Walters, Paul Brooker, Kristopher Davis, Winston V., S. R. Schoenfeld, Shreyes Melkote, Steven Danyluk, Thomas Newton, Bhushan Sopori, Stephen, I. T. Preece, Sergei Ostapenko, Atul Gupta, Gunter Erfurt, Bjoern Seipel, Oliver Naumann,, and I. K. F. Genonceau, "Diamond wire sawing for PV – Short and long-term challenges," *Photovoltaics International,* vol. 27, no. 1st Quarter, March, pp. p.27-39, 2015.

[19] C. Yang, H. Wu, S. Melkote, and S. Danyluk, "Comparative analysis of fracture strength of slurry and diamond wire sawn multicrystalline silicon solar wafers," *Advanced Engineering Materials,* vol. 15, no. 5, pp. 358-365, 2013.

[20] B. Meinel, T. Koschwitz, and J. Acker, "Textural development of SiC and diamond wire sawed sc-silicon wafer," *Energy Procedia,* vol. 27, no. 0, pp. 330-336, // 2012.

[21] K. Tomono, H. Furuya, S. Miyamoto, Y. Okamura, M. Sumimoto, Y. Sakata, R. Komatsu, and M. Nakayama, "Investigations on hydrobromination of silicon in the presence of silicon carbide abrasives as a purification route of kerf loss waste," *Separation and Purification Technology,* vol. 103, pp. 109-113, 2013.

[22] K. Tomono, S. Miyamoto, T. Ogawa, H. Furuya, Y. Okamura, M. Yoshimoto, R. Komatsu, and M. Nakayama, "Recycling of kerf loss silicon derived from diamond-wire saw cutting process by chemical approach," *Separation and Purification Technology,* vol. 120, pp. 304-309, 2013.

[23] A. Kumar and S. N. Melkote, "The Chemo-mechanical Effect of Cutting Fluid on Material Removal in Diamond Scribing of Silicon," *Applied Physics Letters* vol. 111, DOI: 10.1063/1.4991536, no. 1, p. 011901, 2017.

[24] N. Duque Ciceri, M. Garetti, and S. Terzi, "Product lifecycle management approach for sustainability," in *Proceedings of the 19th CIRP Design Conference–Competitive Design*, 2009: Cranfield University Press.

[25] M. Garetti and M. Taisch, "Sustainable manufacturing: trends and research challenges," *Production Planning & Control,* vol. 23, no. 2-3, pp. 83-104, 2012.

[26] DMT-Technologies, "Diamond Wire Sawing " *DMT Technologies Meyer Burger,* 2010.

[27] B. R. Lawn and M. V. Swain, "Microfracture beneath point indentations in brittle solids," *Journal of Materials Science,* vol. 10, no. 1, pp. 113-122, 1975.

[28] S. N. Melkote, C. Yang, A. Kumar, and H. Wu, "Wafering of photovoltaic silicon," *International Conference on Precision, Meso, Micro, and Nano Engineering (COPEN),* 2013.

[29] M. V. Swain, "Microfracture about scratches in brittle solids," in *Proceedings of the Royal Society of London A: Mathematical, Physical and Engineering Sciences*, 1979, vol. 366, no. 1727, pp. 575-597: The Royal Society.

[30] A. Misra and I. Finnie, "On the scribing and subsequent fracturing of silicon semiconductor wafers," (in English), *Journal of Materials Science,* vol. 14, no. 11, pp. 2567-2574, 1979/11/01 1979.

[31] H. Leu and R. O. Scattergood, "Sliding contact fracture on glass and silicon," *Journal of Materials Science,* vol. 23, no. 8, pp. 3006-3014, 1988.

[32] B. R. Lawn, A. G. Evans, and D. B. Marshall, "Elastic/plastic indentation damage in ceramics: the median/radial crack system," *Journal of the American Ceramic Society,* vol. 63, no. 9-10, pp. 574-581, 1980.

[33] D. B. Marshall, B. R. Lawn, and A. G. Evans, "Elastic/plastic indentation damage in ceramics: the lateral crack system," *Journal of the American Ceramic Society,* vol. 65, no. 11, pp. 561-566, 1982.

[34] Y. Ahn, T. N. Farris, and S. Chandrasekar, "Sliding microindentation fracture of brittle materials: Role of elastic stress fields," (in English), *Mechanics of Materials,* Article vol. 29, no. 3-4, pp. 143-152, Aug 1998.

[35] X. Jing, S. Maiti, and G. Subhash, "A New Analytical Model for Estimation of Scratch-Induced Damage in Brittle Solids," *Journal of the American Ceramic Society,* vol. 90, no. 3, pp. 885-892, 2007.

[36] B. Lawn and R. Wilshaw, "Indentation fracture: principles and applications," *Journal of Materials Science,* vol. 10, no. 6, pp. 1049-1081, 1975.

[37] O. Borrero-López, T. Vodenitcharova, M. Z. Quadir, and M. Hoffman, "Scratch fracture of polycrystalline silicon wafers," *Journal of the American Ceramic Society,* vol. 98, no. 8, pp. 2587-2594, 2015.

[38] T. Vodenitcharova, O. Borrero-López, and M. Hoffman, "Mechanics prediction of the fracture pattern on scratching wafers of single crystal silicon," *Acta Materialia,* vol. 60, no. 11, pp. 4448-4460, 2012.

[39] O. Borrero-López, T. Vodenitcharova, and M. Hoffman, "Anisotropy effects on the reliability of single-crystal silicon," *Scripta Materialia,* vol. 63, no. 10, pp. 997-1000, 2010.

[40] J. Z. Hu, L. D. Merkle, C. S. Menoni, and I. L. Spain, "Crystal data for high-pressure phases of silicon," *Physical Review B,* vol. 34, no. 7, pp. 4679-4684, Oct 1 1986.

[41] T. Nakasuji, S. Kodera, S. Hara, H. Matsunaga, N. Ikawa, and S. Shimada, "Diamond turning of brittle materials for optical components," *CIRP Annals - Manufacturing Technology,* vol. 39, no. 1, pp. 89-92, 1990.

[42] R. Komanduri, "On material removal mechanisms in finishing of advanced ceramics and glasses," *CIRP Annals - Manufacturing Technology,* vol. 45, no. 1, pp. 509-514, 1996.

[43] J. Yan, M. Yoshino, T. Kuriagawa, T. Shirakashi, K. Syoji, and R. Komanduri, "On the ductile machining of silicon for micro electro-mechanical systems (MEMS), opto-electronic and optical applications," *Materials Science and Engineering: A,* vol. 297, no. 1–2, pp. 230-234, 1/15/ 2001.

[44] M. B. Cai, X. P. Li, and M. Rahman, "Study of the mechanism of nanoscale ductile mode cutting of silicon using molecular dynamics simulation," *International Journal of Machine Tools and Manufacture,* vol. 47, no. 1, pp. 75-80, 1// 2007.

[45] R. Komanduri, N. Chandrasekaran, and L. M. Raff, "Molecular dynamics simulation of the nanometric cutting of silicon," *Philosophical Magazine B-Physics of Condensed Matter Statistical Mechanics Electronic Optical and Magnetic Properties,* vol. 81, no. 12, pp. 1989-2019, Dec 2001.

[46] S. Goel, A. Kovalchenko, A. Stukowski, and G. Cross, "Influence of microstructure on the cutting behaviour of silicon," *Acta Materialia,* vol. 105, pp. 464-478, 2/15/ 2016.

[47] K. Liu, X. P. Li, and S. Y. Liang, "The mechanism of ductile chip formation in cutting of brittle materials," (in English), *International Journal of Advanced Manufacturing Technology,* Article vol. 33, no. 9-10, pp. 875-884, 2007.

[48] J. Yan, T. Asami, H. Harada, and T. Kuriyagawa, "Fundamental investigation of subsurface damage in single crystalline silicon caused by diamond machining," *Precision Engineering-Journal of the International Societies for Precision Engineering and Nanotechnology,* vol. 33, no. 4, pp. 378-386, Oct 2009.

[49] J. J. J. Wang and Y. Y. Liao, "Critical depth of cut and specific cutting energy of a microscribing process for hard and brittle materials," (in English), *Journal of Engineering Materials and Technology-Transactions of the ASME,* Article; Proceedings Paper vol. 130, no. 1, Jan 2008, Art. no. 011002.

[50] T. Shibata, S. Fujii, E. Makino, and M. Ikeda, "Ductile-regime turning mechanism of single-crystal silicon," *Precision Engineering,* vol. 18, no. 2-3, pp. 129-137, Apr-May 1996.

[51] Y. Gogotsi, G. Zhou, S.-S. Ku, and S. Cetinkunt, "Raman microspectroscopy analysis of pressure-induced metallization in scratching of silicon," *Semiconductor science and technology,* vol. 16, no. 5, p. 345, 2001.

[52] A. Kovalchenko and Y. V. Milman, "On the cracks self-healing mechanism at ductile mode cutting of silicon," *Tribology International,* vol. 80, pp. 166-171, 2014.

[53] R. Gassilloud, C. Ballif, P. Gasser, G. Buerki, and J. Michler, "Deformation mechanisms of silicon during nanoscratching," *Physica Status Solidi a-Applications and Materials Science,* vol. 202, no. 15, pp. 2858-2869, Dec 2005.

[54] S. J. Duclos, Y. K. Vohra, and A. L. Ruoff, "Experimental-study of the crystal stability and equation of state of Si to 248 GPa," *Physical Review B,* vol. 41, no. 17, pp. 12021-12028, Jun 1990.

[55] A. Kumar, A. Kovalchenko, V. Pogue, E. Pashchenko, and S. N. Melkote, "Ductile Mode Behavior of Silicon During Scribing by Spherical Abrasive Particles," *Procedia CIRP,* vol. 45, pp. 147-150, // 2016.

[56] A. Kovalchenko, "Studies of the ductile mode of cutting brittle materials (A review)," *Journal of Superhard Materials,* vol. 35, no. 5, pp. 259-276, 2013.

[57] Y. Gogotsi, G. H. Zhou, S. S. Ku, and S. Cetinkunt, "Raman microspectroscopy analysis of pressure-induced metallization in scratching of silicon," *Semiconductor Science and Technology,* vol. 16, no. 5, pp. 345-352, May 2001.

[58] A. Kovalchenko, Y. Gogotsi, V. Domnich, and A. Erdemir, "Phase transformations in silicon under dry and lubricated sliding," *Tribology Transactions,* vol. 45, no. 3, pp. 372-380, 2002.

[59] C. R. Das, H. C. Hsu, S. Dhara, A. K. Bhaduri, B. Raj, L. C. Chen, K. H. Chen, S. K. Albert, A. Ray, and Y. Tzeng, "A complete Raman mapping of phase transitions

in Si under indentation," *Journal of Raman Spectroscopy,* vol. 41, no. 3, pp. 334-339, 2010.

[60] A. Bidiville, K. Wasmer, R. Kraft, and C. Ballif, "Diamond Wire-Sawn Silicon Wafers-From the Lab to the Cell Production," *Proceedings of 24th European Photovoltaic Solar Energy Conference,* pp. 1400-1405, 2009.

[61] D.-H. Choi, J.-R. Lee, N.-R. Kang, T.-J. Je, J.-Y. Kim, and E.-c. Jeon, "Study on ductile mode machining of single-crystal silicon by mechanical machining," *International Journal of Machine Tools and Manufacture,* vol. 113, pp. 1-9, 2017.

[62] M. Budnitzki and M. Kuna, "A thermomechanical constitutive model for phase transformations in silicon under pressure and contact loading conditions," *International Journal of Solids and Structures,* vol. 49, no. 11-12, pp. 1316-1324, Jun 1 2012.

[63] J. Yan, K. Syoji, T. Kuriyagawa, and H. Suzuki, "Ductile regime turning at large tool feed," *Journal of Materials Processing Technology,* vol. 121, no. 2–3, pp. 363-372, 2/28/ 2002.

[64] M. Budnitzki and M. Kuna, "Experimental and numerical investigations on stress induced phase transitions in silicon," *International Journal of Solids and Structures,* vol. 106, pp. 294-304, 2017.

[65] Z. J. Yuan, W. B. Lee, Y. X. Yao, and M. Zhou, "Effect of Crystallographic Orientation on Cutting Forces and Surface Quality in Diamond Cutting of Single Crystal," *CIRP Annals - Manufacturing Technology,* vol. 43, no. 1, pp. 39-42, // 1994.

[66] A. Kumar and S. N. Melkote, "Wear of diamond in scribing of multi-crystalline silicon," *Journal of Applied Physics,* vol. 124, no. 6, p. 065101, 2018.

[67] A. Kumar, R. G. R. Prasath, V. Pogue, K. Skenes, C. Yang, S. N. Melkote, and S. Danyluk, "Effect of Growth Rate and Wafering on Residual Stress of Diamond Wire Sawn Silicon Wafers," *Procedia Manufacturing,* vol. 5, pp. 1382-1393, // 2016.

[68] A. Kumar, Skenes, K., Prasath, R.G.R., Yang, C., Melkote, S.N., Danyluk, S., "Spatial distribution of full-field residual stress and its correlation with fracture strength of thin silicon wafers," *Proceedings of the 28th European Photovoltaic Solar Energy Conference and Exhibition EU PVSEC,* pp. 1474 - 1476, 2013.

[69] H. Wu and S. N. Melkote, "Effect of crystal defects on mechanical properties relevant to cutting of multicrystalline solar silicon," *Materials Science in Semiconductor Processing,* vol. 16, no. 6, pp. 1416-1421, 2013.

[70] A. Kumar, C. Yang, S. N. Melkote, and S. Danyluk, "Relationship between macro and micro-scale mechanical properties of photovoltaic silicon wafers," *Proceedings*

of the 29th European PV Solar Energy Conference and Exhibition, pp. 769 - 772, 2014.

[71] H. Wu, S. N. Melkote, and S. Danyluk, "Effects of carbide and nitride inclusions on diamond scribing of multicrystalline silicon for solar cells," *Precision Engineering,* vol. 37, no. 2, pp. 500-504, 2013.

[72] C. Evans, E. Paul, D. Dornfeld, D. Lucca, G. Byrne, M. Tricard, F. Klocke, O. Dambon, and B. Mullany, "Material removal mechanisms in lapping and polishing," *CIRP Annals-Manufacturing Technology,* vol. 52, no. 2, pp. 611-633, 2003.

[73] W. Wang, Z. X. Liu, W. Zhang, Y. H. Huang, and D. M. Allen, "Abrasive electrochemical multi-wire slicing of solar silicon ingots into wafers," *CIRP Annals - Manufacturing Technology,* vol. 60, no. 1, pp. 255-258, // 2011.

[74] T. Enomoto, Y. Shimazaki, Y. Tani, M. Suzuki, and Y. Kanda, "Development of a resinoid diamond wire containing metal powder for slicing a slicing ingot," *CIRP Annals - Manufacturing Technology,* vol. 48, no. 1, pp. 273-276, // 1999.

[75] Y. Chiba, Y. Tani, T. Enomoto, and H. Sato, "Development of a high-speed manufacturing method for electroplated diamond wire tools," *CIRP Annals - Manufacturing Technology,* vol. 52, no. 1, pp. 281-284, // 2003.

[76] S. Lee, H. Kim, D. Kim, and C. Park, "Investigation on diamond wire break-in and its effects on cutting performance in multi-wire sawing," *The International Journal of Advanced Manufacturing Technology,* journal article pp. 1-8, 2015.

[77] K. Sunder, H. Uhle, S. Knöppel, and O. Anspach, "Prediction of wire wear, wire bow and wafer total thickness variation in the diamond wire wafering process," *Proceedings of the 28th European PV Solar Energy Conference and Exhibition,* pp. 1491 - 1495, 2013.

[78] D. Kim, H. Kim, S. Lee, T. Lee, and H. Jeong, "Characterization of diamond wire-cutting performance for lifetime estimation and process optimization," (in English), *Journal of Mechanical Science and Technology,* Article vol. 30, no. 2, pp. 847-852, Feb 2016.

[79] J. Yang, S. Banerjee, J. Wu, Y. Myung, O. Rezvanian, and P. Banerjee, "Phase and stress evolution in diamond microparticles during diamond-coated wire sawing of Si ingots," *The International Journal of Advanced Manufacturing Technology,* journal article vol. 82, no. 9, pp. 1675-1682, 2016.

[80] X. P. Li, T. He, and M. Rahman, "Tool wear characteristics and their effects on nanoscale ductile mode cutting of silicon wafer," *Wear,* vol. 259, no. 7–12, pp. 1207-1214, 7// 2005.

[81] M. B. Cai, X. P. Li, and M. Rahman, "Study of the mechanism of groove wear of the diamond tool in nanoscale ductile mode cutting of monocrystalline silicon," *Journal of Manufacturing Science and Engineering,* vol. 129, no. 2, pp. 281-286, 2006.

[82] C. H. J. Peguiron, S. Habegger "Reduced-Wear Equipment For Diamond Wire Wafering," *29th European Photovoltaic Solar Energy Conference and Exhibition, Amsterdam, Netherlands,* pp. 386 - 389, 2014.

[83] A. Oliver, T. Wallner, R. Tandon, K. Nieman, and P. Bergstrom, "Diamond scribing and breaking of silicon for MEMS die separation," *Journal of Micromechanics and Microengineering,* vol. 18, no. 7, p. 075026, 2008.

[84] W. Zong, T. Sun, D. Li, K. Cheng, and Y. Liang, "XPS analysis of the groove wearing marks on flank face of diamond tool in nanometric cutting of silicon wafer," *International Journal of Machine Tools and Manufacture,* vol. 48, no. 15, pp. 1678-1687, 2008.

[85] J. Yan, K. Syoji, and J. i. Tamaki, "Some observations on the wear of diamond tools in ultra-precision cutting of single-crystal silicon," *Wear,* vol. 255, no. 7, pp. 1380-1387, 2003.

[86] M. Sharif Uddin, K. H. W. Seah, X. P. Li, M. Rahman, and K. Liu, "Effect of crystallographic orientation on wear of diamond tools for nano-scale ductile cutting of silicon," *Wear,* vol. 257, no. 7–8, pp. 751-759, 10// 2004.

[87] H. Wu, H. Huang, F. Jiang, and X. Xu, "Mechanical wear of different crystallographic orientations for single abrasive diamond scratching on Ta12W," *International Journal of Refractory Metals and Hard Materials,* vol. 54, pp. 260-269, 2016.

[88] A. Peguiron, G. Moras, M. Walter, H. Uetsuka, L. Pastewka, and M. Moseler, "Activation and mechanochemical breaking of C–C bonds initiate wear of diamond (110) surfaces in contact with silica," *Carbon,* vol. 98, pp. 474-483, 2016.

[89] H. Bhaskaran, B. Gotsmann, A. Sebastian, U. Drechsler, M. A. Lantz, M. Despont, P. Jaroenapibal, R. W. Carpick, Y. Chen, and K. Sridharan, "Ultralow nanoscale wear through atom-by-atom attrition in silicon-containing diamond-like carbon," *Nature nanotechnology,* vol. 5, no. 3, p. 181, 2010.

[90] A. G. Khurshudov, K. Kato, and H. Koide, "Wear of the AFM diamond tip sliding against silicon," *Wear,* vol. 203, pp. 22-27, 1997.

[91] S. Goel, X. Luo, and R. L. Reuben, "Wear mechanism of diamond tools against single crystal silicon in single point diamond turning process," *Tribology International,* vol. 57, pp. 272-281, 2013.

[92] C. Jaeggi, DeMeyer, C., Wiedmer, F., Stierli, R., Simoncic, P., Assi, F., and Wasmer, K., "Effect of Wire Lifetime in Diamond Wire Wafering on the Wafer Roughness and Mechanical Strength," *Proceedings of the 27th European PV Solar Energy Conference and Exhibition,* 2012.

[93] A. Bidiville, Wasmer, K., Michler, J., Ballif, C., Van der Meer, M., and Nasch, P. M., "Influence of Abrasive Concentration on the Quality of Wire Sawn Silicon Wafers," *Proceedings of the 23rd European PV Solar Energy Conference and Exhibition,* 2008.

[94] S. Retsch, Hentsch, S., and Möller, H. J., " Influence of Shape and Size Distribution of Abrasive on the Cutting Performance of Multi Wire Sawing and Lapping," *Proceedings of the 27th European PV Solar Energy Conference and Exhibition,* 2012.

[95] B. Hwang, K. Park, H.-B. Kim, K. H. Kim, D.-S. Bae, and Y.-R. Cho, "Effect of tensile properties on the abrasive wear of steel saw wires used for silicon ingot slicing," *Wear,* vol. 290-291, pp. 94-98, 2012.

[96] B. Weber, and Riepe, S, "Challenges of the Multi Wire Sawing Process for Thin Wafers below 120µm Thickness," *27th EUPVSEC,* 2012.

[97] H. Dalaker, Armada, S., Halvorsen, T., Kaminski, S., Moen, M., and Runde, P., "The Evolution of Slurry Grit Properties during Multi Wire Wafering of Silicon Bricks," *Proceedings of the 27th European PV Solar Energy Conference and Exhibition,* 2012.

[98] S. Danyluk and R. Reaves, "Influence of fluids on the abrasion of silicon by diamond," *Wear,* vol. 77, no. 1, pp. 81-87, 1982/03/15 1982.

[99] S.-W. Lee, D.-S. Lim, and S. Danyluk, "The influence of fluids on the microhardness of single crystal silicon," *Journal of Materials Science Letters* vol. 3, no. 7, pp. 651-653, 1984.

[100] S. Danyluk and J. L. Clark, "The wear rate of n-type Si(100)," *Wear,* vol. 103, no. 2, pp. 149-159, 1985/05/15 1985.

[101] D.-S. Lim and S. Danyluk, "Correlation of dynamic friction and the dislocation etch pit density surrounding annealed scratches in (1 1 1) p-type silicon," *Journal of Materials Science,* vol. 23, no. 7, pp. 2607-2612, 1988.

[102] P. Rebinder, "Effect of Changes in Surface Energy on the Embrittlement, Hardness and Other Properties of Crystals," in *Proceedings of the 6th Physics Conference, Moscow*, 1928, p. 29.

[103] A. Westwood, J. Ahearn, and J. Mills, "Developments in the theory and application of chemomechanical effects," *Colloids and Surfaces,* vol. 2, no. 1, pp. 1-35, 1981.

[104] A. R. Westwood, D. L. Goldheim, and R. G. Lye, "Rebinder effects in MgO," *Philosophical Magazine,* vol. 16, no. 141, pp. 505-519, 1967.

[105] G. H. Yost and W. S. Williams, "Chemomechanical effect in doped and intrinsic silicon," *Journal of the American Ceramic Society,* vol. 61, no. 3-4, pp. 139-142, 1978.

[106] J. Patel, L. Testardi, and P. Freeland, "Electronic effects on dislocation velocities in heavily doped silicon," *Physical Review B,* vol. 13, no. 8, p. 3548, 1976.

[107] P. Haasen, "Kink Formation in Charged Dislocation," *Physica Status Solidi A-Applied Research,* vol. 28, no. 1, pp. 145-155, 1975.

[108] J. Westbrook and J. Gilman, "An electromechanical effect in semiconductors," *Journal of Applied Physics,* vol. 33, no. 7, pp. 2360-2369, 1962.

[109] A. Kumar, S. Kaminski, S. N. Melkote, and C. Arcona, "Effect of wear of diamond wire on surface morphology, roughness and subsurface damage of silicon wafers," *Wear,* p. http://dx.doi.org/10.1016/j.wear.2016.07.009, 2016.

[110] H. Wu and S. N. Melkote, "Study of Ductile-to-Brittle Transition in Single Grit Diamond Scribing of Silicon: Application to Wire Sawing of Silicon Wafers," *Journal of Engineering Materials and Technology,* vol. 134, no. 4, p. 041011, 2012.

[111] M. B. Cai, X. P. Li, and M. Rahman, "High-pressure phase transformation as the mechanism of ductile chip formation in nanoscale cutting of silicon wafer," *Proceedings of the Institution of Mechanical Engineers Part B-Journal of Engineering Manufacture,* vol. 221, no. 10, pp. 1511-1519, Oct 2007.

[112] H. Wu and S. N. Melkote, "Effect of crystallographic orientation on ductile scribing of crystalline silicon: Role of phase transformation and slip," *Materials Science and Engineering a-Structural Materials Properties Microstructure and Processing,* vol. 549, pp. 200-205, Jul 15 2012.

[113] B. Bethune, "The surface cracking of glassy polymers under a sliding spherical indenter," (in English), *Journal of Materials Science,* vol. 11, no. 2, pp. 199-205, 1976/02/01 1976.

[114] B. R. Lawn, "Partial cone crack formation in a brittle material loaded with a sliding spherical indenter," (in English), *Proceedings of the Royal Society of London Series a-Mathematical and Physical Sciences,* Article vol. 299, no. 1458, pp. 307-316, 1967.

[115] H. J. Leu and R. O. Scattergood, "Sliding contact fracture on glass and silicon," *Journal of Materials Science,* journal article vol. 23, no. 8, pp. 3006-3014, 1988.

[116] K. Niihara, R. Morena, and D. P. H. Hasselman, "Evaluation of KIc of brittle solids by the indentation method with low crack-to-indent ratios," *Journal of Materials Science Letters,* journal article vol. 1, no. 1, pp. 13-16, 1982.

[117] F. Ebrahimi and L. Kalwani, "Fracture anisotropy in silicon single crystal," *Materials Science and Engineering: A,* vol. 268, no. 1, pp. 116-126, 1999.

[118] R. Cook, "Strength and sharp contact fracture of silicon," *Journal of Materials Science,* vol. 41, no. 3, pp. 841-872, 2006.

[119] K. Sato, T. Yoshioka, T. Ando, M. Shikida, and T. Kawabata, "Tensile testing of silicon film having different crystallographic orientations carried out on a silicon chip," *Sensors and Actuators A: Physical,* vol. 70, no. 1, pp. 148-152, 1998.

[120] T. Ando, X. Li, S. Nakao, T. Kasai, M. Shikida, and K. Sato, "Effect of crystal orientation on fracture strength and fracture toughness of single crystal silicon," in *Micro Electro Mechanical Systems, 2004. 17th IEEE International Conference on.(MEMS)*, 2004, pp. 177-180: IEEE.

[121] C. P. Chen and M. H. Leipold, "Fracture Toughness of Silicon," *American Ceramic Society Bulletin,* vol. 59, no. 4, pp. 469-472, 1980.

[122] B. R. Lawn and A. G. Evans, "A model for crack initiation in elastic/plastic indentation fields," (in English), *Journal of Materials Science,* vol. 12, no. 11, pp. 2195-2199, 1977/11/01 1977.

[123] K. Cheng, X. Luo, R. Ward, and R. Holt, "Modeling and simulation of the tool wear in nanometric cutting," *Wear,* vol. 255, no. 7–12, pp. 1427-1432, 8// 2003.

[124] M. B. Cai, X. P. Li, and M. Rahman, "Characteristics of "dynamic hard particles" in nanoscale ductile mode cutting of monocrystalline silicon with diamond tools in relation to tool groove wear," *Wear,* vol. 263, no. 7–12, pp. 1459-1466, 9/10/ 2007.

[125] R. Komanduri, D. A. Lucca, and Y. Tani, "Technological advances in fine abrasive processes," *CIRP Annals - Manufacturing Technology,* vol. 46, no. 2, pp. 545-596, // 1997.

[126] W. J. Liu, Z. J. Pei, and X. J. Xin, "Finite element analysis for grinding and lapping of wire-sawn silicon wafers," *Journal of Materials Processing Technology,* vol. 129, no. 1–3, pp. 2-9, 10/11/ 2002.

[127] J. Xin, W. Cai, and J. A. Tichy, "A fundamental model proposed for material removal in chemical–mechanical polishing," *Wear,* vol. 268, no. 5–6, pp. 837-844, 2/11/ 2010.

[128] Z. J. Pei and A. Strasbaugh, "Fine grinding of silicon wafers," *International Journal of Machine Tools and Manufacture,* vol. 41, no. 5, pp. 659-672, 4// 2001.

[129] Y. Zhao and L. Chang, "A micro-contact and wear model for chemical–mechanical polishing of silicon wafers," *Wear,* vol. 252, no. 3–4, pp. 220-226, 2// 2002.

[130] A. Chandra, G. Anderson, S. Melkote, W. Gao, H. Haitjema, and K. Wegener, "Role of surfaces and interfaces in solar cell manufacturing," *CIRP Annals - Manufacturing Technology,* vol. 63, no. 2, pp. 797-819, // 2014.

[131] Z. Zhang, B. Wang, R. Kang, B. Zhang, and D. Guo, "Changes in surface layer of silicon wafers from diamond scratching," *CIRP Annals - Manufacturing Technology,* vol. 64, no. 1, pp. 349-352, // 2015.

[132] A. Bidiville, Heiber, J., Wasmer, K., Habegger, S., Assi, F., "Diamond wire wafering: Wafer morphology in comparison to slurry sawn wafers," *Proceedings of 25th European Photovoltaic Solar Energy Conference and Exhibition,* pp. 1673 - 1676, 2010.

[133] C. G. Scott and S. Danyluk, "Examination of silicon wear debris generated in a linear scratch test," *Wear,* vol. 152, no. 1, pp. 183-185, Jan 5 1992.

[134] R. McGill, J. W. Tukey, and W. A. Larsen, "Variations of Box Plots," *The American Staistician,* vol. 32, pp. 12–16, 1978.

[135] H. Tanaka, S. Shimada, and L. Anthony, "Requirements for ductile-mode machining based on deformation analysis of mono-crystalline silicon by molecular dynamics simulation," *CIRP Annals - Manufacturing Technology,* vol. 56, no. 1, pp. 53-56, // 2007.

[136] K. S. Woon and M. Rahman, "Extrusion-like chip formation mechanism and its role in suppressing void nucleation," *CIRP Annals - Manufacturing Technology,* vol. 59, no. 1, pp. 129-132, // 2010.

[137] W. Weibull, *A statistical theory of the strength of materials* (no. 151). Royal Swedish Institute for Engineering Research, Stockholm, Sweden, 1939.

[138] V. Domnich, Y. Gogotsi, and S. Dub, "Effect of phase transformations on the shape of the unloading curve in the nanoindentation of silicon," *Applied Physics Letters,* vol. 76, no. 16, pp. 2214-2216, 2000.

[139] C. Funke, E. Kullig, M. Kuna, and H. J. Möller, "Biaxial fracture test of silicon wafers," *Advanced Engineering Materials,* vol. 6, no. 7, pp. 594-598, 2004.

[140] D. Sarti and R. Einhaus, "Silicon feedstock for the multi-crystalline photovoltaic industry," *Solar energy materials and solar cells,* vol. 72, no. 1-4, pp. 27-40, 2002.

[141] A. Kumar, S. N. Melkote, S. Kaminski, and C. Arcona, "Effect of grit shape and crystal structure on damage in diamond wire scribing of silicon," *Journal of the American Ceramic Society,* vol. 100, no. 4, pp. 1350-1359, 2017.

[142] C. Reimann, M. Trempa, J. Friedrich, and G. Müller, "About the formation and avoidance of C and N related precipitates during directional solidification of multi-crystalline silicon from contaminated feedstock," *Journal of Crystal Growth,* vol. 312, no. 9, pp. 1510-1516, 4/15/ 2010.

[143] K. Skenes, A. Kumar, R. Prasath, and S. Danyluk, "Crystallographic Orientation Identification in Multicrystalline Silicon Wafers Using NIR Transmission Intensity," *Journal of Electronic Materials,* vol. 47, no. 2, pp. 1030-1037, 2018.

[144] X. Zhang, R. Schneider, E. Müller, M. Mee, S. Meier, P. Gumbsch, and D. Gerthsen, "Electron microscopic evidence for a tribologically induced phase transformation as the origin of wear in diamond," *Journal of Applied Physics,* vol. 115, no. 6, p. 063508, 2014.

[145] A. Kumar, S. N. Melkote, S. Kaminski, and C. Arcona, "Effect of Abrasive Grit Shape on Surface Morphology, Subsurface Damage and Fracture Strength of Diamond Wire Sawn Silicon Wafers," *Proceedings of the 32nd European Photovoltaic Solar Energy Conference and Exhibition EU PVSEC,* pp. 1053 - 1056, 2016.

[146] M. A. Hopcroft, W. D. Nix, and T. W. Kenny, "What is the Young's Modulus of Silicon?," *Journal of Microelectromechanical Systems,* vol. 19, no. 2, pp. 229-238, 2010.

[147] B. Lawn, *Fracture of brittle solids*. Cambridge university press, 1993.

[148] D. Hull, *Fractography: observing, measuring and interpreting fracture surface topography*. Cambridge University Press, 1999.

[149] J. Robertson, "Diamond-like amorphous carbon," *Materials Science and Engineering: R: Reports,* vol. 37, no. 4, pp. 129-281, 2002.

[150] F. Tuinstra and J. L. Koenig, "Raman spectrum of graphite," *The Journal of Chemical Physics,* vol. 53, no. 3, pp. 1126-1130, 1970.

[151] M. Matthews, M. Pimenta, G. Dresselhaus, M. Dresselhaus, and M. Endo, "Origin of dispersive effects of the Raman D band in carbon materials," *Physical Review B,* vol. 59, no. 10, p. R6585, 1999.

[152] M. Pimenta, G. Dresselhaus, M. S. Dresselhaus, L. Cancado, A. Jorio, and R. Saito, "Studying disorder in graphite-based systems by Raman spectroscopy," *Physical chemistry chemical physics,* vol. 9, no. 11, pp. 1276-1290, 2007.

[153] L. G. Cançado, A. Jorio, E. Martins Ferreira, F. Stavale, C. Achete, R. Capaz, M. Moutinho, A. Lombardo, T. Kulmala, and A. Ferrari, "Quantifying defects in graphene via Raman spectroscopy at different excitation energies," *Nano letters,* vol. 11, no. 8, pp. 3190-3196, 2011.

[154] Y. G. Gogotsi, A. Kailer, and K. G. Nickel, "Pressure-induced phase transformations in diamond," *Journal of Applied Physics,* vol. 84, no. 3, pp. 1299-1304, 1998.

[155] S. K. Sharma, H. Mao, P. Bell, and J. Xu, "Measurement of stress in diamond anvils with micro-Raman spectroscopy," *Journal of Raman Spectroscopy,* vol. 16, no. 5, pp. 350-352, 1985.

[156] H. Chacham and L. Kleinman, "Instabilities in diamond under high shear stress," *Physical review letters,* vol. 85, no. 23, p. 4904, 2000.

[157] I. De Wolf, "Micro-Raman spectroscopy to study local mechanical stress in silicon integrated circuits," *Semiconductor Science and Technology,* vol. 11, no. 2, p. 139, 1996.

[158] J.-a. Xu, H.-k. Mao, and R. J. Hemley, "The gem anvil cell: high-pressure behaviour of diamond and related materials," *Journal of Physics: Condensed Matter,* vol. 14, no. 44, p. 11549, 2002.

[159] S. Malkin and N. H. Cook, "The wear of grinding wheels: part 1—attritious wear," *Journal of Engineering for Industry,* vol. 93, no. 4, pp. 1120-1128, 1971.

[160] G. Lal and M. Shaw, "Wear of single abrasive grains in fine grinding," in *Proc. Int. Grinding Conf*, 1972, vol. 107.

[161] S. Malkin and C. Guo, *Grinding technology: theory and application of machining with abrasives*. Industrial Press Inc., 2008.

[162] L. Vandeperre, F. Giuliani, S. Lloyd, and W. Clegg, "The hardness of silicon and germanium," *Acta Materialia,* vol. 55, no. 18, pp. 6307-6315, 2007.

[163] P. T. Shaffer, "Effect of crystal orientation on hardness of silicon carbide," *Journal of the American Ceramic Society,* vol. 47, no. 9, pp. 466-466, 1964.

[164] A. Zerr, M. Kempf, M. Schwarz, E. Kroke, M. Göken, and R. Riedel, "Elastic moduli and hardness of cubic silicon nitride," *Journal of the American Ceramic Society,* vol. 85, no. 1, pp. 86-90, 2002.

[165] A. Kumar, "Methods and Materials for Smart Manufacturing: Additive Manufacturing, Internet of Things, Flexible Sensors and Soft Robotics," *Manufacturing Letters,* vol. 15, pp. 122-125, 2018.

[166] R. Buchwald, K. Fröhlich, S. Würzner, T. Lehmann, K. Sunder, and H. J. Möller, "Analysis of the Sub-surface Damage of mc- and cz-Si Wafers Sawn with Diamond-plated Wire," *Energy Procedia,* vol. 38, no. 0, pp. 901-909, 2013.